The Treatment of Carwash Wastewater Using a Combined Process of Chemical Coagulation and Electrochemical Oxidation

by

Chad Eric Steenberg

A thesis submitted in fulfilment of the requirements for the degree

Master of Engineering: Chemical Engineering

in the

Faculty of Engineering and the Built Environment

at the

Cape Peninsula University of Technology

Supervisor: **Dr Mujahid Aziz**

June 2021

Declaration

I, Chad Eric Steenberg hereby declare that the contents of this dissertation/thesis represent my unaided work and that the dissertation/thesis has not previously been submitted for academic examination towards any qualification. Furthermore, it represents my own opinions and not necessarily those of the Cape Peninsula University of Technology

Signed: *Chad Eric Steenberg* Date: *June 2021*

Abstract

Carwashes are found in every city across the world, whether informal or formal stations, a large amount of water is required to effectively clean a car to the owner's satisfaction. Typically, 150 to 600 L of water is required per car, depending on the size of the vehicle. This in turn generates complex wastewater which contains high levels of pollutants which is discharged into water sources. This creates serious environmental concerns that have a devasting effect on aquatic life. Therefore an effective, low-cost solution is required for the remediation of carwash wastewater (CWW) for re-use application. This would reduce operational cost and conserve fresh water. Due to the high concentration of organic matter and suspended solids in the wastewater, it is necessary to pre-treat the CWW prior to sequential electrochemical oxidation treatment. Conventional treatment processes are not capable of treating contaminants and pollutants in CWW to sufficient concentrations, and hence advanced treatment processes are necessary.

In this study, a lab-scale integrated treatment process was used to treat carwash wastewater to reduce high levels of pollutants such as COD, FOG, anionic surfactants, and turbidity. The integrated treatment process used, consisted of a chemical coagulation (CC) pre-treatment and an electrochemical oxidation (EO) process.

Polyaluminium chloride (PAC) was selected as the coagulant in the chemical coagulation process, where experimental runs were conducted in a batch reactor. The effect of PAC dosage was examined. The efficiency of the pollutant removal was measured through COD, anionic surfactants, FOG's, and turbidity, which were found to be 68.44, 19.88, 97.93 and 95.70%, respectively. This was achieved at experimental condition where the PAC concentration was 100 mg/L. The PAC sludge samples generated after the CC process were characterized with Fourier transform infrared (FTIR) spectroscopy. The analyses showed the presence of alcohols, phenols and alkanes which is strongly associated with pollutants and heavy metal ions.

The electrochemical oxidation process with Ti/IrO_2 -Ta_2O_5 electrodes was applied to treat the wastewater effluent from the electrocoagulation process. The experimental runs were also carried out in a batch reactor, at a constant temperature of 60°C with a working volume of 1 L. The highest COD removal percentage of 97.13 was achieved at a pH of 2, current density 10 mA/cm^2, and supporting electrolyte (NaCl) concentration of 0.055 M. The highest anionic

surfactant removal percentage of 99.22 was achieved at experimental conditions at pH 7, current density 10 mA/cm^2, and supporting electrolyte (NaCl) concentration of 0.1 M.

The electrochemical oxidation experiments were characterized by a Box-Behnken design (BBD). Polynomial quadratic models were successfully developed for the removal of COD and anionic surfactants. They were identified as the major pollutants in this study. Their removal was found to be significant.

It was observed that the integrated CC-EO treatment system was able to reduce COD, FOG, anionic surfactants, and turbidity levels by 97.13%, 100%, 98.49%, and 99.41%, respectively. This concludes that the treated CCW effluent complies with the industrial effluent discharge standards for disposal or recycling.

Research Output

Kasongo G; **Steenberg C**; Morris B; Kapenda G; Jacobs N & Aziz M*; 2019; Surface grafting of polyvinyl alcohol (PVA) cross-linked with glutaraldehyde (GA) to improve resistance to fouling of aromatic polyamide thin-film composite reverse osmosis membranes using municipal membrane bioreactor effluent, IWA*: Water Practice, and Technology*, 14 (3), 614-626 [ISSN 1751-321X / DOI.org/10.2166/wpt.2019.047]

Steenberg C & Aziz M; 2020. Removal of Anionic Surfactant and COD from Car Wash wastewater using an integrated process: Chemical Coagulation and Electrochemical Oxidation with IrO_2-Ta_2O_5/Ti anodes. *Environmental Processes an International Journal.* Submitted XX January 2021 [Paper ID.: XX-XX-XX]

Acknowledgements

I thank God for giving me the strength to succeed with this project, for protecting me, and blessing me with my family and friends.

This research project was undertaken within the Chemical Engineering Department at the Cape Peninsula University of Technology between January 2018 and November 2020.

I want to express my gratitude to the following people for their contributions towards the completion of this thesis:

My Supervisor, Dr Mujahid Aziz, for his incomparable supervision, persistent guidance, motivation, encouragement and technical expertise in the field of this research. I am thankful for his sustained academic, moral and fatherly assistance throughout my academic journey.

The technical and administrative staff in the Chemical Engineering Department Mrs Hannelene Small, Mrs Elizma Alberts and Mr Alwyn Bester, always willing to assist.

The Environmental Engineering Research Group (*EnvERG*) in the Department of Chemical Engineering.

All my family members, brothers, aunts and uncles, and friends for their moral support, prayers and encouragement.

My parents, for their continued moral and financial support and for those who have passed on.

Dedication

To my parents and role models, Mr Christopher and Mrs Belinda Steenberg, for their endless love, support, encouragement and inspiration. This achievement would not be possible without you. I am forever grateful for your presence in my life

Thank You, Mommy and Daddy!

Table of Contents

Contents

List of Tables

List of Figures

List of Photographs

List of Acronyms

BOD:	Biological Oxygen Demand
BDD:	Boron Doped Diamond
BBD:	Box-Behnken Design
CWW:	Carwash Wastewater
COD:	Chemical Oxygen Demand
DSA:	Dimensionally Stable Anodes
EC:	Electrical Conductivity
EO:	Electrochemical Oxidation
FOG:	Fats, Oils, & Grease
ICE:	Instantaneous Current Efficiency
MMO:	Mixed Metal Oxides
M:	Molarity
PAC:	Polyaluminium Chloride
rpm:	Revolutions per minute
TDS:	Total Dissolved Solids
TSS:	Total Suspended Solids

List of Symbols

Symbol	Definition	Unit
I	Applied Current	A
cm^2	Area	Squared centimeter
COD_t	COD at time T	g/L
mA/cm^2	Current Density	mA/cm^2
VR	Electrolyte Volume	Litre
F	Faraday's Constant	C/mol
COD_o	Initial COD	g/L
g	Mass	gram
Vm	Mean cell voltage	Voltage
E	Mean energy consumption	kWh/m^3
mA	Milli-ampere	mA
M	Molarity	Mol/L
Δt	Reaction time	seconds
T	Temperature	Celsius/Kelvin
R	Universal Gas Constant	J/mol.K
L	Volume	Litre
m^3	Volume	Cubic metre
V	Volume of solution	L

Chapter 1:

Introduction

Chapter 1: Introduction

1.1 Background

Globally the availability of water is an extreme concern. The current reliability on freshwater supplies will continue to increase with increasing population growth and climate change (Gosling & Arnell, 2016). According to Gönder et al. (2017), the amount of wastewater generated per car is estimated between 150 and 600 L depending on the type of car-washing station and the size of the vehicle.

According to Tian et al. (2017), water reclamation and reuse is becoming a promising approach to mitigate the global water resource risks. Greywater can be classified as the used water from baths, showers, and washing machines as well as dishwater from kitchens. Approximately, between 50 and 80% of the wastewater from a household accounts for greywater and the reuse of greywater is a possible solution to conserve freshwater supplies. Raw greywater can be used for the flushing of toilets, however treated greywater is more acceptable for users. The use of greywater has the potential to reduce freshwater consumption by 25 – 30% (Ren et al., 2019). Mohammadi et al. (2017) states that carwash wastewater is part of this category as well.

The carwash process is divided into three stages: the application of a degreasing agent, the addition of acid and alkaline cleaners, and in the final stage a coat is provided to the surface to protect it from any abrasion. Carwash wastewater contains oil and grease, detergents, various heavy metals, organic and sulphur compounds, degreasers, and many phosphorous and nitrogen compounds (Juárez et al., 2015; Panizza & Cerisola, 2010b; Kiran et al., 2015).

Technologies that have been employed to treat carwash wastewater include membrane processes, membrane bioreactors, flocculation, flotation, filtration, adsorption, chemical coagulation and electrochemical processes (Gönder et al., 2017). Due to the contaminants in carwash wastewater, surfactants, free oil, grease, sand-dust, salts, and hydraulic fluid, it may be harmful to human health and aquatic life if disposed of untreated (Gönder et al., 2017; Kiran et al., 2015; Panizza & Cerisola, 2010a). According to Bhatti et al. (2011), the reuse of carwash wastewater is extremely important for environmental protection, due to the amount of water used, as well as the complexity of the quality of water due to the pollutants in them.

Sarmadi et al. (2020) reviewed various treatment technologies specifically for the treatment of carwash wastewater and their study concluded that combined treatment methods are the most attractive option in remediation of carwash wastewater, therefore, an integrated coagulation and electrochemical oxidation process was investigated in this study for the treatment of carwash wastewater to meet safe discharge and re-use standards.

1.2 Problem Statement

The discharge of wastewater and its re-use is governed by the South African National Water Act, 1998 (Act No. 36 of 1998). Currently, carwash wastewater (CWW) does not comply with the effluent requirements for discharge and irrigation re-use application. Therefore, research studies are being investigated to effectively improve the quality of carwash wastewater to reduce the hazardous effects it has on the environment. Effective treatment of carwash wastewater may result in the re-use of the treated water; thus, conservation of fresh water will be achieved.

1.3 Research Questions

1.3.1 Can coagulation-flocculation followed with electrochemical oxidation treat carwash wastewater to meet the required wastewater discharge standards?

1.3.2 How will initial pH, current density and NaCl concentration affect the pollutant removal rate during electrochemical oxidation of CWW?

1.4 Aim and Objectives

The aim of this study is to improve the quality of carwash wastewater (CWW) with an integrated chemical coagulation (CC) and electrochemical oxidation (EO) process to meet safe discharge and re-use standards.

The specific objectives were:

1.4.1. Investigate the different poly-aluminum chloride (PAC) concentrations as pre-treatment on the removal of pollutants such as turbidity, anionic surfactants, COD and FOG, during a batch chemical coagulation process.

1.4.2. Study the effect of initial pH, current density and electrolyte (NaCl) concentration on the removal efficiency of turbidity, anionic surfactants, COD and FOG during a batch electrochemical oxidation (EO) process.

1.5 Significance of the study

The effective treatment of carwash wastewater may result in compliance with wastewater discharge standards. Protecting the environment as well as reducing freshwater usage through reuse and recycling of water in the production process.

1.6 Delineation

During this study, the removal of anionic surfactants, chemical oxygen demand and fats, oils and grease from carwash wastewater were attempted through an integrated treatment process.

This process consists of two consecutive steps:

1. Chemical Coagulation
2. Electrochemical Oxidation

Chemical coagulation occurred using polyaluminium chloride, while electrochemical oxidation occurred using Ti/IrO_2-Ta_2O_5 electrodes.

All other variables are delineated.

1.7 Structure of the thesis

Chapter 1: Introduction

This chapter presents an introduction and background information about the evaluation of the performance of the integrated treatment process in the removal of anionic surfactants, chemical oxygen demand and fats, oils & grease from carwash wastewater effluents. Thereafter follows the problem statement, aim, objectives and delineation.

Chapter 2: Literature Review

This chapter presents a comprehensive literature review in which chemical coagulation and electrochemical oxidation is discussed and compared to other industrial effluent treatment technologies. The choice of a wastewater treatment technology is determined from the characteristics of wastewater.

Chapter 3: Methodology

This chapter describes procedures, equipment, and chemicals that were used in this study. It also shows the chemical analysis techniques used as well as the design of experiments using the Design-Expert software package.

Chapter 4: Results & Discussion

This chapter displays all the results from the experimental runs completed. The graphs are discussed with the intention to optimise the chemical coagulation and electrochemical oxidation processes.

Chapter 5: Optimization using Response Surface Methodology (RSM)

This chapter shows the optimization of the electrochemical oxidation removal process using RSM. This includes the development of the multilevel factorial design, central composite design, and Box Behnken design predictive models. The best fitted models were optimized to identify the optimum operating conditions for COD and anionic surfactant removal in carwash wastewater effluent, by evaluation and verification using Design Expert software.

Chapter 6: Conclusion & Recommendation

This chapter follows on the significances of the results and concludes the thesis based on the findings and outputs. Recommendations are presented based on the understanding from the research and its findings.

Chapter 2:

Literature Review

Chapter 2: Literature Review

2.1 Introduction

This chapter presents the characteristics of carwash wastewater, previously used technologies and the re-use standards according to the City of Cape Town. However, the focus on this chapter will be on the sequential chemical coagulation (CC) and electrochemical oxidation (EO) treatment processes for carwash wastewater. The coagulant that this chapter focuses on is polyaluminium chloride. The anodic material for the electrochemical process is a mix metal oxide (MMO), IrO_2-Ta_2O_5/Ti. The mechanisms of this MMO material are discussed in detail, as well as factors that govern the EO process.

2.2 Global Water Crisis

According to Hanjra & Qureshi (2010), the demand for freshwater required by the entire world population is constantly increasing and it has tripled in the last 70 years. Currently, there are a half billion people in the world who live in water-scarce conditions, and this will increase to 3 billion by the year 2025.

Jury & Vaux (2007), and Hanjra & Qureshi (2010), stated that the main factor causing the increase in the demand for water usage is population growth. Other factors which create a negative impact on water scarcity include the following: (i) increasing costs of developing new water sources; (ii) land degradation in irrigated areas; (iii) groundwater depletion; (iv) water pollution and (v) ecosystem degradation (Hanjra & Qureshi, 2010).

Gude (2017), concurred with other authors and added that the depletion of water sources included the increase in the standard of living as well as the important effect of climate change. He also stated that 30% of the population lacks the mandatory water sources for basic sanitation requirements. Figure 2-1 illustrates the water scarcity worldwide, resulting in physical and economic absence.

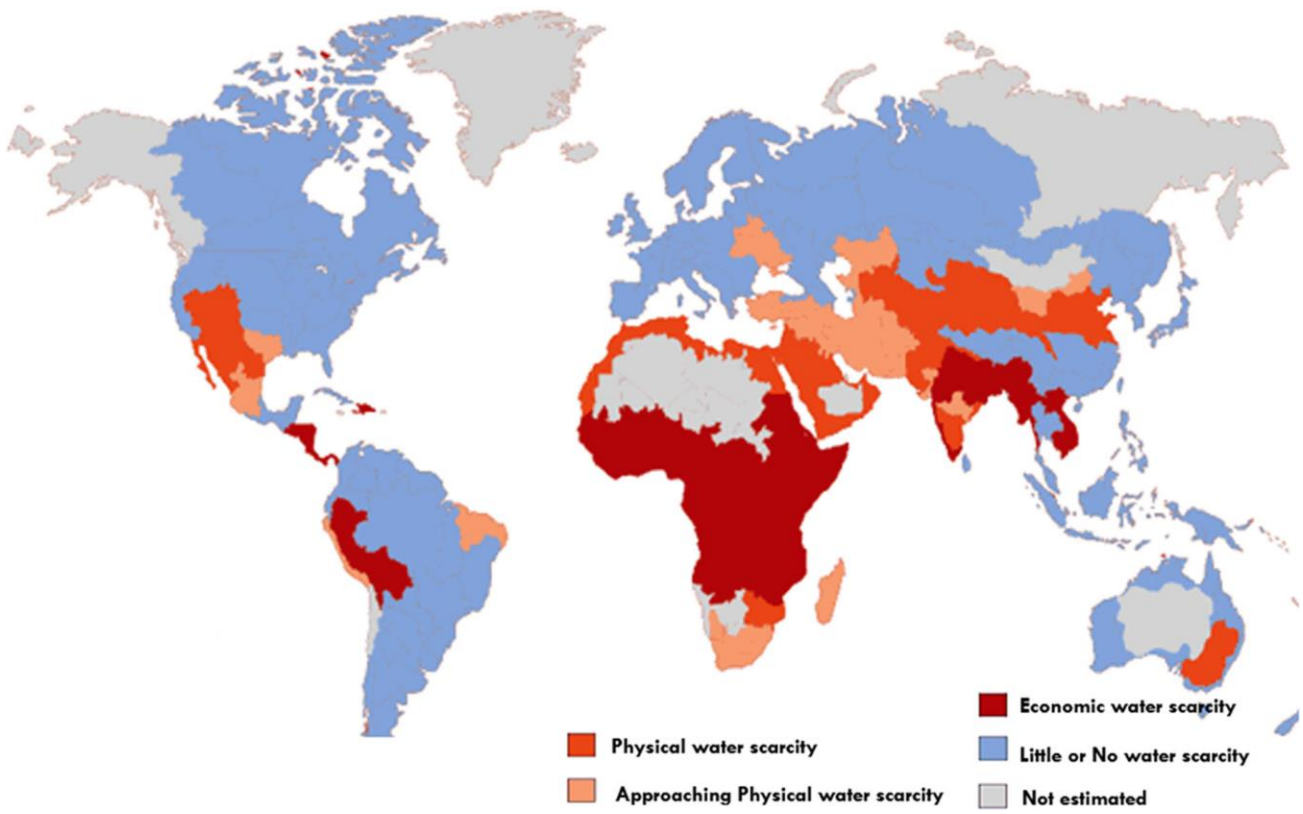

Figure 2- 1: Global Water Scarcity (Gude, 2017)

Larsen et al. (2016) states that emerging solutions to water challenges includes new concepts for stormwater drainage, increased water productivity, on-site treatment of wastewater, source separation of human waste, and institutional and organizational reforms.

2.3 National Water Act, 1998 (Act 36 of 1998) (The Act)

Schedule: Engaging in a controlled activity, identified as such in section 37(1)(a): Irrigation of any land with waste or water containing waste generated through any industrial activity or by a water work

Irrigation with Wastewater

A person who –

a. owns or lawfully occupies property registered in the Deeds Office as at the date of this notice.
b. lawfully occupies or uses land that is not registered or surveyed; or
c. lawfully has access to land on which the use of water takes place.

may on that property or land –

I. irrigate up to 2000 cubic meters of domestic and biodegradable industrial wastewater on any given day as set out in Table 2-1:

Table 2- 1: Wastewater limit values applicable to the irrigation of any land or property up to 2000 cubic metres (Department of Water Affairs-South Africa, 2013)

Variables	Limits
pH	Not less than 5.5 or more than 9.5
Electrical Conductivity	Does not exceed 70 milli Siemens above intake to a maximum of 150 milli Siemens per meter (mS/m)
Suspended Solids	Does not exceed 25 mg/l
Chloride as Free Chlorine	Does not exceed 0.25 mg/l
Fluoride	Does not exceed 1 mg/l
Soap	Does not exceed 2.5 mg/l
Oil and Grease	Does not exceed 2.5 mg/l
Chemical Oxygen Demand	Does not exceed 75 mg/l
Feacel coliforms	Does exceed 1000 per 100 ml
Ammonia as Nitrogen	Does not exceed 3 mg/l
Nitrate/Nitrite as Nitrogen	Does not exceed 15 mg/l
Orthophosphate as phosphorous	Does not exceed 10 mg/l

2.4 Carwash Wastewater

Bazrafshan et al. (2012) stated that the wastewater produced from carwash industries is potentially harmful to human and aquatic life if it is disposed of without treatment into water bodies. According to Panizza & Cerisola (2010), the composition of carwash water is quite complex. It contains detergents, oils, grease, gasoline residues, metals, organic matter, and suspended solids, which can include dust, sand, and salt. The problem with the disposal of carwash wastewater into the stormwater system is that there are no treatment measures in place, leading to the pollution of lakes, rivers, and oceans (Bhatti et al., 2011). In Table 2-2, the raw CWW characteristics can be seen by various authors.

Table 2- 2: Raw Carwash Wastewater characteristics

Parameter	(Panizza & Cerisola, 2010a)	(Bazrafshan et al., 2012)	(Juárez et al., 2015)	(Lau et al., 2013)	(Zaneti et al., 2011)	(Asha et al., 2016)	(Baddor et al., 2014)
COD (mg/L)	572	924.17	1295	738	241	245	403
BOD (mg/L)	178	266.31	150	-	133	52	100
Conductivity (ms/cm)	1.6	7.08	796	-	0.633	1.536	-
Oil and Grease (mg/L)	-	-	368.82	-	6	190	35
Anionic Surfactant (mg/L)	95.5	34.17	68.33	-	11.7	-	32
Turbidity (NTU)	-	132.2	898	68.9	89	195	-
TSS (mg/L)	-	291.35	-	-	68	260	49
pH	6.4	7.65	7.3	-	7.7	7.86	7
TDS (mg/L)	-	-	-	89.5	502	1020	1200

According to Kumar & Chauhan (2018), the impact of untreated carwash wastewater on the environment can cause excessive growth of nuisance plants in water bodies, as the water contains phosphates, which are nutrients for plants. The oil and grease present in the water is harmful to living organisms and the methylene blue active substances (detergents) are destructive to aquatic life. It damages fish mucus membranes and grills and thus leads to fish losing their natural oils. This causes the interruption of transferring oxygen for fish to survive. Table 2-2 summarizes the characteristics of raw carwash wastewater from different studies that applied remedial processes.

2.5 Carwash Wastewater Treatment: Previous Studies

2.5.1 Electrocoagulation

A study was conducted by Gönder et al. (2017), to treat carwash wastewater with electrocoagulation using iron and aluminum electrodes. The authors mentioned that the pH of the water is a very important parameter, and the optimum conditions were 8 and 6 for Fe and Al electrodes, respectively. They also stated that the main operating parameter for the investigated process was current density. The best suited current density for the electrodes were 1 and 3 mA/cm^2 for aluminum and iron, respectively. The electrode which performed the best under the same conditions was aluminum as it removed 89% COD, 30-69% oil and grease, and 73 to 90% chloride. This was achieved in the most efficient operational time of 30 minutes.

The treatment of carwash wastewater by electrocoagulation was investigated by Priya & Jeyanthi (2019), for the removal of COD and oil and grease. The spacing between the electrodes, current density, reaction time, and pH of the wastewater were factors taken into consideration when the experiments were conducted. With regards to the anode material, four materials were considered, namely, aluminum, iron, copper, and antinomy. Copper was found to be the best-suited anode, with aluminum as the cathode. The conditions which yielded the most favourable results were 5 cm electrode spacing, 25 A/cm^2 current density, a reaction time of 40 minutes, and a pH of 6. At these conditions, the removal efficiencies of COD, oil and grease, and turbidity were found to be 95.1, 92,5 & 99%, respectively.

2.5.2 Chemical Coagulation

Mohamed et al. (2014) treated carwash wastewater by using a coagulation/flocculation process. The authors compared commercial and natural coagulants to determine which was more effective. The commercial coagulants used in their study were aluminum sulphate (alum) and ferrous sulphate. The natural coagulants used were Moringa Oleifera and Strychnos Potatorum. When the authors investigated turbidity removal it was found that Strychnos Potatorum had the highest turbidity removal of 95%. Mohamed et al. (2014) stated that the commercial coagulant, alum, had the highest COD removal of 80%, with the ferrous sulphate producing the second-highest COD removal rate. Phosphorous removal was investigated as well, and it was found that the commercial coagulants performed better in this regard.

A three-part treatment process was investigated by Bhatti et al. (2011), which included aeration, coagulation, and chemical oxidation to treat carwash wastewater (CWW). The aeration process focused on removing the oil, 96.3% of it was removed within 90 minutes. The second process used alum as a coagulant. COD and turbidity were reduced to 92.35 and 96%, respectively, at the optimum dosage of 80 mg/L. Hydrogen peroxide was used as an oxidant in the final process and the overall COD removal was 94.43%. The dissolved oxygen increased from 0 mg/L to 4.2 mg/L.

2.5.3 Membrane Technology

A combined process of chemical coagulation and a membrane bioreactor treatment was investigated to treat carwash wastewater by Alicia et al (2016). The two coagulants used in this study were alum and PAC. It was found that in terms of turbidity, the PAC had the highest removal efficiency of 99.6% and the alum removed 99.5%. The COD removal was 65.25% when the PAC was used as the coagulant. Thereafter, the MBR process was employed and the COD removal was found to be 99.2%. The total organic carbon (TOC) removal after the entire treatment process was completed was an impressive 97.3% while the removal of ammonia and nitrite in the MBR process was found to be 41% and 49.2%, respectively (Alicia et al., 2016).

Carwash wastewater was treated using two ultrafiltration membranes and one nanofiltration membrane by Lau et al. (2013), to compare the individual effectiveness. The three different membranes were NF270, PES30, and PVDF100. It was found that the membrane which displayed the most stable flux was the NF270, while the PES30 showed close to equivalent results. However, in terms of turbidity, all three membranes showed satisfactory performance as they removed 92% of turbidity at least but the NF270 outperformed the others as it reached a turbidity removal of 98%. Lau et al. (2013) states that the NF270 membrane had the highest COD removal of up to 91.5%, while the ultrafiltration membrane's highest COD removal was just above 80%. At the end of the treatment process, the membranes underwent physical backflushing and the only membrane which showed promising results was the NF270 membrane as it nearly recovered 90% of the membrane flux while the two ultrafiltration membranes performed poorly in this regard (Lau et al., 2013).

2.5.4 Adsorption

Nadzirah et al. (2015) prepared activated carbon by chemical activation using sugarcane bagasse and it was used to treat real carwash wastewater. The variables investigated in the study were the effect of activation time, the temperature of carbonization, and impregnation percentage. The parameters used to determine the optimal conditions were COD, alkalinity, and oil and grease removal. Nadzirah et al. (2015) found that the optimal conditions were 20% impregnation of H_3PO_4 and 500˚C of carbonization for a period of two hours. These conditions yielded COD, alkalinity, and oil & grease removal efficiencies of 52.08, 59.09, and 40.64%, respectively.

2.5.5 Electrochemical Oxidation

A comparative study using electrochemical oxidation to treat carwash wastewater was conducted by Panizza & Cerisola (2010) to compare a lead oxide anode with a boron-doped diamond (BDD) anode. With regards to the lead dioxide anode when analyzing the COD removal, it was found that it was nearly completely removed after 10 hours, however, shortly after the start of the process a plateau was achieved then after some time it slowly decreased again. The current used was 3 A, and at 25˚C, the COD removal was 97%, and at 40˚C it was 99%. According to Panizza & Cerisola (2010), when the BDD anode was used it was extremely effective as complete mineralization was obtained at all applied currents, and there was no plateau observed compared to when the lead dioxide anode was used. The energy consumption for the EO processes was 770 kWh m^{-3} and 375 kWh m^{-3} for lead dioxide and BDD, respectively. Panizza & Cerisola (2010) stated that even though the BDD is extremely effective at COD reduction, the energy consumption is extremely high, therefore, it must be employed as a coupled process.

Electrocoagulation and electrochemical oxidation were employed by Panizza et al. (2010), to treat carwash wastewater and the anodes for the processes were iron and BDD. According to Panizza et al. (2010), the reason for combining the two processes was due to EC being ineffective by itself to remove most of the contaminants and EO consumes too much energy to operate alone, therefore, the optimal conditions of the combined process were 6 minutes for EC and an hour and a half for EO. Panizza et al. (2010) states that the coupled process removed 97% COD and the energy consumption was 12 kWh m^{-3} compared to 375 kWh m^{-3} which is the consumption when electrochemical oxidation is used alone to arrive at the same result.

Electrocoagulation and electrooxidation were performed by Juárez et al. (2015), using iron and aluminum for the EC process and BDD for the EO process. In the EC process, the preferred electrode was the aluminum one as the iron electrode imparted the colour, this process was effective in removing organics but when EO was introduced it showed promising results. It was found that the best initial pH to use for EC was 7 and for the EO process, it was 8. The EC process was used for 60 minutes and the EO was used for 120 minutes. The combined process removed 100% of oils, 96% of COD, and 93% of BOD. The treated water met the standards for reuse in the car wash water. A tabulated summary was comprised by Moazzem et al. (2018) on the conventional treatment technologies for carwash wastewater. The table can be found below:

Table 2- 3: Conventional treatment technologies for Car wash wastewater (Moazzem et al., 2018)

Technology Applied	Influent Concentration	Effluent Concentration	Removal Efficiency
Coagulation-flocculation and ozonation	COD:443 mg/L Turbidity:1000 NTU	COD:141 mg/L Turbidity:3.73 NTU	COD: 67% Turbidity: 99.6%
Flocculation-flotation, sand filtration and ozonation	BOD: 397 mg/L COD: 683 mg/L	BOD: 60 mg/L COD: 96 mg/L	BOD: 85% COD: 86%
Commercial coagulants and natural coagulants	Turbidity: 180.3 NTU	Turbidity: 12.4 NTU	Turbidity: 93% (30 mg/L Strychnos Potatorum)
Coagulation, flocculation, sand filtration, oxidation, sand filtration, and activated carbon filtration	COD: 1430 ppm	COD: 184 ppm	COD: 87.13%
Flocculation-column-flotation (FCF)-sand filtration (FCF-S) FCF-sand filtration-chlorination (FCF-SC)	BOD: 81 mg/L COD: 213 mg/L Turbidity:160 NTU	BOD: 38.5 mg/L COD: 96 mg/L Turbidity:13 NTU	BOD: 53% COD: 55% Turbidity:92%
Aeration, coagulation (alum) and hydrogen peroxide used as an oxidant	COD: 1019 mg/L Turbidity: 772 NTU	COD: 80 mg/L Turbidity: 33 NTU	COD: 93% Turbidity: 94%
Electrocoagulation and electrochemical oxidation	Not available	Not available	97% COD removed in 100 min of treatment

2.6 Coagulation and Flocculation

In wastewater treatment there are several processes which can be applied to improve the quality of the wastewater. The coagulation-flocculation process is quite a significant part of wastewater treatment due to its simplicity and cost-effectiveness (Ebeling et al., 2003). This process can be coupled with other wastewater treatment processes to enhance the quality by incorporating both processes at their respective optimal conditions and according to Ebeling et al. (2003), it can be applied as either a pre or post-treatment step.

The reason for applying the coagulation-flocculation process in wastewater treatment is to condition impurities in the wastewater, as well as removing colour from the wastewater. There are two mechanisms that occur when the coagulant is added, the first being coagulation, and shortly thereafter flocculation occurs (Environmental Protection Agency, 2002).

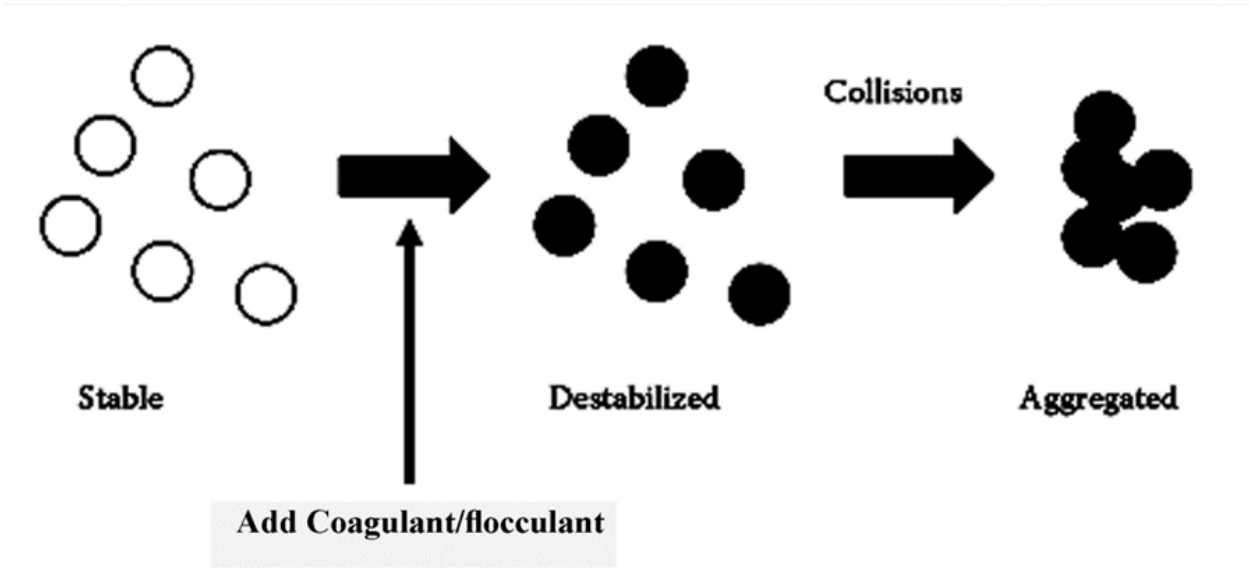

Figure 2- 2: Principle of Coagulation (Asha et al., 2016)

According to Sahu & Chaudhari (2013), the coagulation step of the process is defined as the addition of a positively charged ion of a metal salt or catalytic polyelectrolyte which yields the destabilization of the particles present in the wastewater. This also results in charge neutralization. To go into slightly more detail, Sincero & Sincero (2003) state that in the water there are atoms that are agglomerated together, and because the agglomerated atoms are so small they are suspended in the wastewater. These agglomerated atoms are referred to as colloids. Since the colloids are suspended in the wastewater, they can be referred to as stable and this is due to mutual repulsions of the colloids in

the wastewater. The reasons for adding the coagulant is to destabilize the mutual repulsions, which then allow the colloids to attach themselves together in the coagulation process. The colloids are the cause of the wastewater to be high in terms of turbidity and colour (Sincero & Sincero, 2003). The mechanism of the coagulation process can be found in the Figure 2-2.

The second part of the two-step process is referred to as flocculation and according to Zaleschi et al. (2012), it is described as after the colloidal particles are destabilized they begin to form micro-floccules, which results in the agglomeration of them to form larger particles which are in suspension. Bratby (1980) states that during the flocculation process there are two sub-divided processes that occur referred to as perikinetic flocculation, followed by orthokinetic flocculation. According to Bratby (1980), the perikinetic step is caused due to thermal agitation, which is referred to as Brownian movement and this is a naturally random process that occurs. This step starts to take place immediately after the coagulation is complete by the destabilization of the particles. The duration of this step only lasts a few seconds due to the limiting floc size beyond which the Brownian motion has little or no effect.

As mentioned above the second step is referred to as orthokinetic flocculation. This step is induced by the velocity gradients in the liquid (Bratby, 1980). The velocity gradients which occur in this step are due to movement of the liquid and this occurs in three possible ways; passage around baffles or mechanical agitation within a flocculation reactor; the tortuous path through interstices of a granular filer bed where floes are sufficiently formed; by sedimentation within a settling basin and so on. The purpose of the velocity gradients in the wastewater is to set up relative velocities between particles which results in more opportunity for them to come in contact.

2.6.1 Poly-aluminum Chloride

The proposed coagulant to be used in this study is Poly-aluminum chloride (PAC). According to Alicia et al. (2016), when comparing the performance of PAC and alum in terms of turbidity removal, it was found that alum removed 99.5% and PAC removed 99.6%. Another parameter Alicia et al. (2016) looked at by using PAC as the coagulant was the COD removal, and the authors found that PAC managed to remove 65.25%. Banchon et al. (2017) compared two coagulants, PAC and ferric chloride, and it was reported that they both removed almost 100% of turbidity. A 5% PAC solution was used as the coagulant as well as a 15% ferric chloride solution.

The table 2-4 summarizes the use of the PAC coagulant and the removal efficiencies achieved.

Table 2- 4: Summary of car wash wastewater treatments with PAC

Coagulant with/without additional treatment	Wastewater	Removal Efficiency	Reference
Poly-aluminum chloride	Car wash	Turbidity:95.6% COD:65.25%	(Alicia et al., 2016)
Poly-aluminum chloride with bio adsorption	Car wash	Turbidity:100% COD:95.96 % Oil & Grease:99.96% BOD:95%	(Banchon et al., 2017)
Poly-aluminum chloride	Car wash	COD:85.4%% TSS:74% BOD:74.49%	(Bazrafshan et al., 2012)
Poly-aluminum chloride & potassium permanganate, Ultrafiltration and activated carbon	Car wash	Final percentages not given but the treatment of the wastewater resulted in it being acceptable for re-use. COD: 33.4 mg/L BOD:4.8 mg/L LAS:0.06 mg/L Oil:0.95 mg/L	(Tang et al., 2007)

The authors state that it is quite remarkable that with the 5% PAC it was able to remove colloidal contamination and because of it being so low in percentage this means that there will be savings in chemical and remediation costs (Banchon et al., 2017). The reason why PAC was preferred as a coagulant in that study was due to the wide pH range the PAC coagulant could be used for. Bazrafshan et al. (2012) conducted a study to treat carwash wastewater with a combined process of coagulation and electrocoagulation. The coagulant used in the study was poly-aluminum chloride and it was found that at the highest dose of PAC at 100 mg/L, the COD removal was 85.36%, BOD removal was 74.49% and the TSS removal was 74%. Tang et al. (2007) performed a study on carwash wastewater by incorporating coagulation, ultrafiltration, and adsorption. In the coagulation part of the study Tang et al. (2007) compared four coagulants, PAC, iron chloride hexahydrate, polyferric sulphate, and polyacrylamide (PA). It was found that PAC, iron chloride and PA had identical turbidity removal rates, but PAC was chosen for the study due to its low cost when compared to the other coagulants and an additional reason for the preference of PAC to the iron chloride hexahydrate is that it doesn't produce an extra reddish-brown color in the treated water. In the coagulation process, a coagulant aid was added to assist the PAC and the name of it is potassium permanganate. Tang et al. (2007) found that when the aid was applied compared to when it wasn’t, the minimum difference was 5 NTU in terms of turbidity, thus the coagulant aid improves the flocculating effect on turbidity removal.

2.6.2 Chemistry of Poly-aluminum Chlorides

PAC coagulants are characterized by their degree of neutralization (r), or basicity. The expressions can be seen as follows (Pernitsky & Edzwald, 2003):

$$r = [OH^-] / [AL_T], \qquad \text{(Eq. 2-1)}$$

where $[OH^-]$ base added during production

$$\text{basicity} = (r / 3) \times 100\ \% \qquad \text{(Eq. 2-2)}$$

r can typically vary between 0 – 3, which corresponds to the basicity range of 0 to 100%. Commercial PAC coagulants possess a basicity ranging between 15 – 85%. The alkalinity consumption of the coagulant is affected by the basicity. The basicity affects the relative prevalence of the monomeric and polymeric species as well. According to Bottero et al. (1980), the higher the basicity the greater the fraction of polymeric species, which typically reaches a maximum r of 2.1, corresponding to a basicity of 70%.

When r is equal to a value of 3, precipitation of amorphous $Al(OH)_{3(am)}$ is predicted according to the following stoichiometry (Pernitsky & Edzwald, 2003):

$$Al^{3+} + 3OH^- \rightarrow Al(OH)_{3am} \qquad \text{(Eq. 2-3)}$$

A tridecameric Al_{13} species with the formula $Al_{13}O_4(OH)_{24}(H2O)^{7+}{}_{12}$ has been shown to be the dominant polymeric species in partially neutralized Al solutions (Pernitsky & Edzwald, 2003).

Wei et al. (2015) states that coagulation using hydrolyzing coagulants has been studied thoroughly, but the behavior of pre-hydrolyzed coagulants (such as PAC), especially the mechanisms at various coagulant dosages and pH values of raw water, has not been systematically investigated and is not very well understood.

At present the coagulation mechanisms for PAC is confined to adsorption charge neutralization because of the high positive chargers of Al_{13}, $Al_{13}O_4(OH)_{24}(H_2O)^{7+}{}_{12}$ and Al_{30}, $Al_{30}O_8(OH)_{56}(H_2O)^{18+}{}_{24}$ (Wei et al., 2015).

2.7 Sludge Characterization – FTIR Analysis

Fourier transform infrared (FTIR) spectroscopy is employed to identify all types of organic and various inorganic materials, quantitative determination of species in complex mixtures, determine the molecular composition of surface species, the differentiation of structural and geometrical isomers, and determining molecular orientation in polymers & solutions. Applications of FTIR in materials science range from determining key functional groups in organic polymers and paints to use in the food and beverage industry, determining sugar and carbonation content, and industrial monitoring of stack gas emissions (Kaufmann, 2012).

Authors have also reported that FTIR was used to determine key functional groups in African catfish mucus (Oluwole et al., 2020), coagulant sludge (Lal & Garg, 2017), sawdust (Wahab et al., 2010), and sludge generated from electrocoagulation (Gönder et al., 2017).

Table 2-5 shows the frequency ranges of some common organic functional groups, where m = medium, s = strong, vbr = very broad, vs = very strong, and w = weak (Kaufmann, 2012).

Table 2- 5: Characteristic Frequency ranges of Some Common Organic Functional Groups (Kaufmann, 2012)

Range (cm^{-1})	Relative Intensity	Functional Group	Species
3700 - 3250	s	-OH	Alcohols, phenols
3520 - 3320	m-s	$-NH_2$	Primary/aromatic amines, amides
3360 - 3340	m	$-NH_2$	Primary amides
3320 - 3250	m	-OH	Oximes
3300 - 3250	m-s	≡CH	Acetylenes
3300 - 3280	s	-NH	Secondary amides
3200 - 3180	s	$-NH_2$	Primary amides
3100 - 2400	vbr	-OH	Carboxylic acids

3100 - 3000	m	=CH	Aromatic, unsaturated
2990 - 2850	m-s	$-CH_3$, $-CH_2$	Aliphatics
2750 - 2650	w-m	-CHO	Aldehydes
2285 - 2250	s	-N=C=O	Isocyanates
2260 - 2200	m-s	-C≡N	Nitriles
1870 - 1790	vs	-C=O	Anhydrides
1780 - 1760	s	-C=O	Lactones
1750 - 1740	vs	-C=O	Esters
1740 -1720	s	-C=O	Aldehydes
1720 - 1700	s	-C=O	Ketones
1710 - 1690	s	-C=O	Carboxylic acids
1670 - 1650	vs	-C=O	Primary amides
1550 - 1490	s	$-NO_2$	Aromatic nitro
1400 - 1310	s	$-COO^-$	Carboxylic acids
1000 - 950	s	$-CH=CH_2$	Vinyl
980 - 960	vs	-CH=CH-	Trans alkenes
950 - 900	vs	$-CH=CH_2$	Vinyl

I. FTIR Principle

The type of instrument which determines the absorption spectrum for a compound is known as a spectrophotometer. Fourier transform spectrophotometer provides the IR spectrum at a much faster rate in comparison to a traditional spectrophotometer. Figure 2-3 illustrates the FTIR procedure (Mohamed et al., 2017).

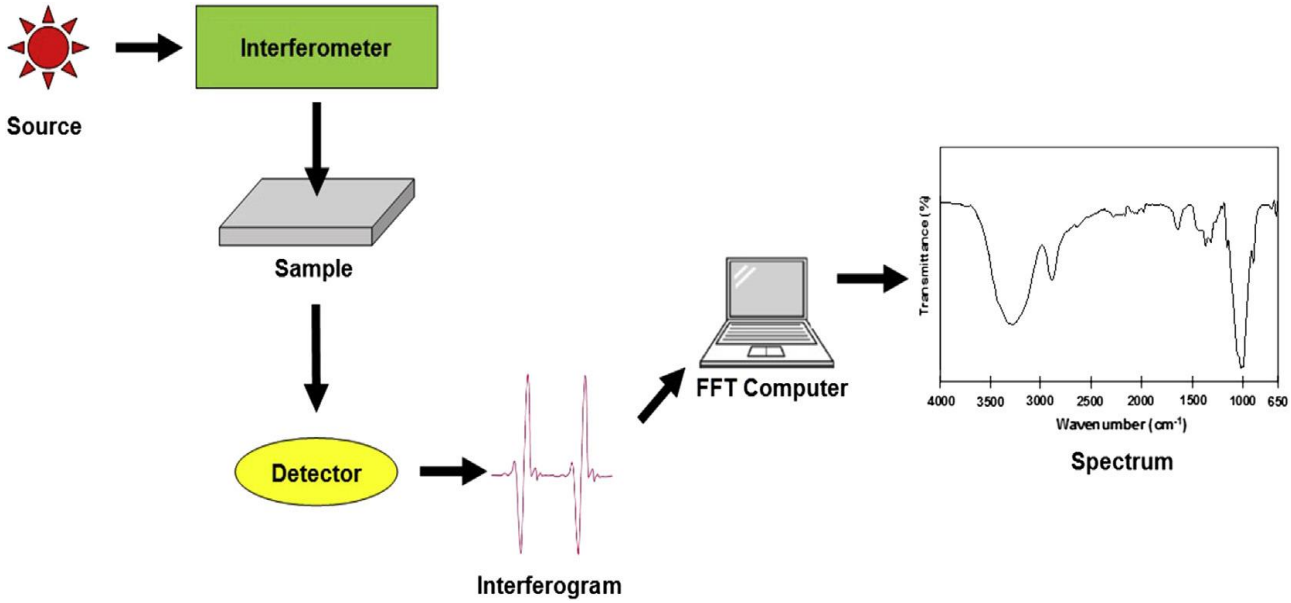

Figure 2- 3: Components of FTIR analysis (Mohamed et al., 2017)

The Fourier transform spectrophotometer produces a beam of IR irradiation; it is emitted from a glowing black-body source. The beam then travels through an interferometer where the spectral encoding occurs. The recombination of beams with different path lengths in the interferometer produces constructive and destructive interference which is referred to as an interferogram. At this point the beam enters the sample compartment. The sample absorbs specific frequencies of energy, which are individually characteristic of the sample from the interferogram. The detector then measures the special interferogram signal in energy versus time for all frequencies simultaneously. While this takes place, a beam is superimposed to provide a background for the instrument operation. At the last stage of the process the desirable spectrum is obtained after the interferogram automatically subtracts the spectrum of the background from the sample spectrum by Fourier transformation computer software (Mohamed et al., 2017).

2.8 Electrochemical Oxidation

Urtiaga & Ortiz (2009) states that the treatment process known as electrochemical oxidation is an environmentally friendly treatment method that can completely mineralize non-biodegradable organic matter as well as eliminate nitrogen species. Research is still being investigated to this day to minimize the high energy requirement of the electro-oxidation process. According to Urtiaga & Ortiz (2009), Radjenovic & Sedlak (2015), and Feng et al. (2016), there are two mechanisms through which oxidation can take place, either through direct anodic oxidation or indirect oxidation. It must be noted that it is possible for both mechanisms to take place simultaneously (Urtiaga & Ortiz, 2009).

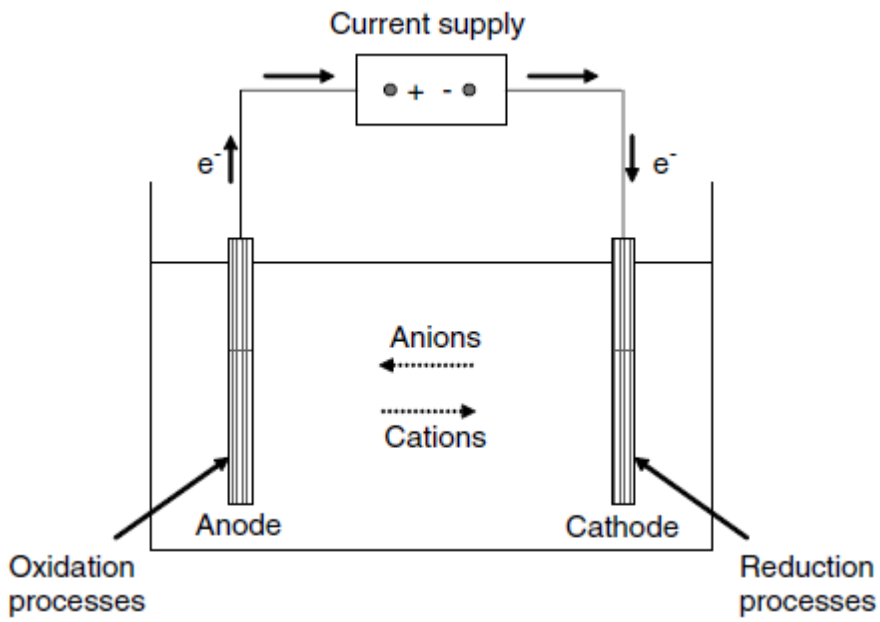

Figure 2- 4: Conceptual diagram of an electrochemical reactor (Urtiaga & Ortiz, 2009)

2.8.1 Direct Oxidation

Feng et al. (2016) states that during direct anodic oxidation the pollutants present in the wastewater are eliminated after adsorption on the anode surface and this occurs only through the mediation of the electrons. No other substances play a role in the destruction of the pollutants. The drawback of this type of oxidation is that it could lead to electrode fouling because of the polymeric layers being formed on the surface of the electrode and this then leads to very poor chemical decontamination.

The reaction mechanism which govern direct oxidation is as follows (Martínez-Huitle & Panizza, 2018):

$$M + H_2O \rightarrow M(^{\bullet}OH) + H^+ + e^- \quad \text{(Eq. 2-4)}$$

$$R + M(^{\bullet}OH) \rightarrow M + CO_2 + H_2O \quad \text{(Eq. 2-5)}$$

Where M is the metal surface and R is the organic species. The efficiency of the electrochemical oxidation process is affected by two factors, the operating conditions and the nature of the electrode material. Anodes which possess low oxygen evolution over-potential (IrO_2, RuO_2, Pt) are considered to display "active" characteristics, which favours the partial and selective oxidation of pollutants, however, anodes with high oxygen evolution over-potential (SnO_2, PbO_2, BDD) displays "non-active" behavior and are thus ideal electrodes for the complete EO of organic material to CO_2 in wastewater treatment (Martínez-Huitle & Panizza, 2018).

Figure 2-5 shows the over-potential of some anodes.

Electrode	Oxidation potential (V)	Over-potential of O_2 evolution (V)	Adsorption enthalpy of M-OH	Oxidation power of anode
RuO_2–TiO_2 (DSA–Cl_2)	1.4–1.7	0.18	Chemisorption of OH radical	
IrO_2–Ta_2O_5 (DSA–O_2)	1.5–1.8	0.25		
Ti/Pt	1.7–1.9	0.3		
Ti/PbO_2	1.8–2.0	0.5		
Ti/SnO_2–Sb_2O_5	1.9–2.2	0.7		
p-Si/BDD	2.2–2.6	1.3	Physisorption of OH radical	

Figure 2- 5: Oxidation Power of Various Anodic Material (Comninellis et al., 2008)

2.8.2 Indirect Oxidation

According to Urtiaga & Ortiz (2009), when indirect oxidation takes place a strong oxidizing agent is formed through electro-generation and this occurs at the surface of the anode and once this occurs it then destroys the pollutants present in the bulk solution. Chlorine is one of the most common electrochemical oxidants and it is formed on the surface of the anode after oxidation of chlorine takes place (Urtiaga & Ortiz, 2009). Active chlorine is most widely employed for wastewater treatment. It occurs as gaseous chlorine, hypochlorous acid or hypochlorite ions. It is produced during the electrochemical oxidation process from chlorides present or added to the solution (Martínez-Huitle & Panizza, 2018). It has been reported by Urtiaga & Ortiz (2009) that a few other common oxidants which can be produced electrochemically are hydrogen peroxide, peroxodisulfutic acid, and ozone.

The reactions of active chlorine is as follows (Martínez-Huitle & Panizza, 2018):

$$2Cl^- \rightarrow Cl_2 + 2e^- \qquad \text{(Eq. 2-5)}$$

$$Cl_2 + H_2O \rightarrow HOCl + H^+ + Cl^- \qquad \text{(Eq. 2-6)}$$

$$HOCl \rightarrow H^+ + OCl^- \qquad \text{(Eq. 2-7)}$$

Figure 2-6 shows a schematic diagram of the two types of oxidation which can occur.

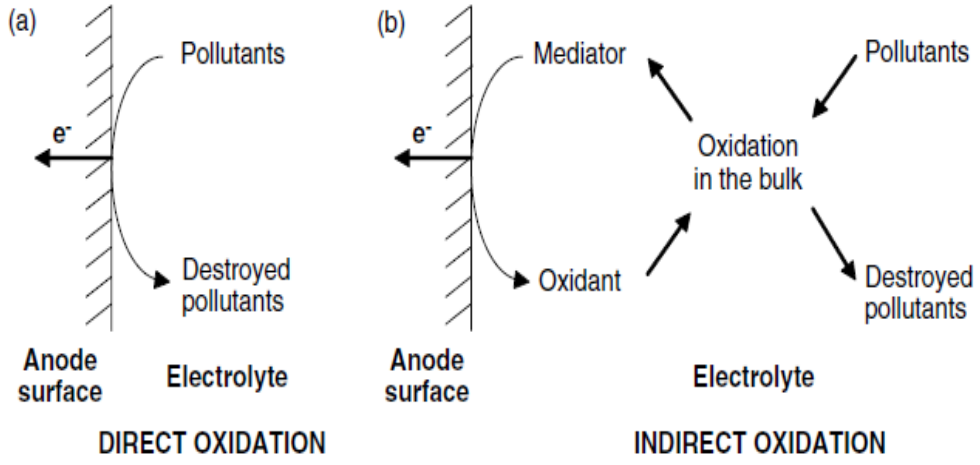

Figure 2- 6: Schemes for (a) direct and (b) indirect electrolytic treatment of pollutants (Urtiaga & Ortiz, 2009)

2.8.3 Advantages and Disadvantages of Electrochemical Processes

Electrochemical oxidation has many advantages for the prevention and treatment of various pollution problems. One of the key advantages of implementing EO is its environmental friendliness, as it makes use of a 'clean reagent', the electron. Therefore, minimal addition of chemicals is required for the process to operate. Other advantages of using EO is it's robustness, versatility, and easy operation (Urtiaga & Ortiz, 2009).

The main disadvantages of using electrochemical oxidation are its high operating cost caused by the high energy consumption. Another factor to consider is that for the process to be effective, the effluent being treated would need to be conductive, if not the addition of an appropriate electrolyte would be necessary. Fouling of electrodes could occur as the pollutants are deposited on the surface of the electrode (Urtiaga & Ortiz, 2009).

Muddemann et al. (2019) tabulated the advantages and disadvantages of various anode materials for electrochemical systems. This can be seen in table 2-6.

Table 2- 6: Anode Material for Electrochemical Systems (Muddemann et al., 2019)

Anode Material	Advantages	Disadvantages	Comparison to other Electrodes
Ti	Stable	Passive, expensive	
Pt	High chemical stability, low overvoltage for oxygen evolution, high proportion of direct oxidation	Expensive	Low efficiency in anodic oxidation of organic compounds
PbO_2	Cost-effective, high current yield, efficient in EO, high overvoltage for oxygen evolution, simple production	Susceptible to corrosion, hazardous to health and the environment due to Pb^{2+} ions	-
SnO_2	Increased current yield of ozone, mostly chemically and electrochemically inert	-	Lower degradation rates compared to BDD

DSA (Dimensionally stable anode)	Enable indirect oxidation, high current yield, increased overvoltage for oxygen evolution, commercially available, reasonably priced.	Not long-term stable, insufficient electrochemical stability	-
BDD (Boron Doped Diamond)	Largest potential window in an aqueous electrolyte, very high chemical and electrochemical stability, high overvoltage for oxygen evolution, high current yield of hydroxyl radicals, corrosion-resistant, good conductivity	Very expensive	Increased activity

2.8.4 Electrochemical Oxidation Operating Conditions

Current density is of the variables which is modified often when performing electrochemical oxidation operations. This is due to it controlling the reaction rate in the electrochemical process. It is important to note that an increase in current density does not necessarily mean the oxidation efficiency/oxidation rate will increase proportionally. For a given anodic material, the effect of current density on the removal efficiency of pollutants is dependent on the nature of the effluent being treated (Urtiaga & Ortiz, 2009).

The effect of temperature on the removal efficiency of the electrochemical oxidation process has not been investigated thoroughly in literature, however in direct oxidation processes it is noted that there is no significant effect of adjusting temperature. In mediated oxidation processes where, inorganic reagents (active chlorine, peroxydisulfate) are being electrochemically generated, an increase in removal efficiency has been reported (Urtiaga & Ortiz, 2009).

The effect of pH on the electrochemical process is mostly seen in indirect oxidation processes. It must be noted that reviewing previous publications does not allow a concise conclusion to be drawn on whether increasing/decreasing the pH increases the removal efficiency of pollutants in electrochemical oxidation of wastewaters. In wastewaters where chloride mediated reactions are taking place, the pH value might influence the oxidation rate as it determines the primary active chloro species present. At low pH values (less than 3.3) the primary species is Cl_2, while at higher pH values it diffuses away from the anode to react and form HClO (pH < 7.5) and ClO^- (pH > 7.5). The strongest oxidant among the three is chlorine, while HClO follows second, therefore, strong acidic conditions are preferred for optimal removal efficiencies for the electrochemical oxidation treatment of wastewater containing chlorine (Urtiaga & Ortiz, 2009).

The material of the electrode used in the oxidation process is extremely important as it affects the selectivity and the efficiency of the electro-oxidation process, the electrode should possess the following properties (Urtiaga & Ortiz, 2009):

a. High physical and chemical stability.
b. High electrical conductivity.
c. Catalytic activity and selectivity.
d. The materials which are low cost and very durable are desired.

2.8.5 Measurement of Process Efficiency

For determining the removal efficiencies for turbidity, FOG, COD, and anionic surfactant the following expressions were used (Gilpavas et al., 2018):

$$Turbidity\ \%\ removal = \frac{T_i - T_t}{T_i}\ x\ 100 \qquad (Eq. 2-8)$$

Where: T_i and T_t are the initial turbidity value (NTU) and the turbidity at time t, respectively.

$$FOG\ \%\ removal = \frac{FOG_i - FOG_t}{FOG_i}\ x\ 100 \qquad (Eq.\ 2-9)$$

Where: FOG_i and FOG_t are the initial FOG value (mg/L) and the FOG at time t, respectively.

$$COD\ \%\ removal = \frac{COD_i - COD_t}{COD_i}\ x\ 100 \qquad (Eq.\ 2-10)$$

Where: COD_i and COD_t are the initial COD value (mg/L) and the COD at time t, respectively.

$$Anionic\ surfactant\ \%\ removal = \frac{AS_i - AS_t}{AS_i}\ x\ 100 \qquad (Eq.\ 2-11)$$

Where: AS_i and AS_t are the initial anionic surfactant value (mg/L) and the anionic surfactant at time t, respectively.

The instantaneous current efficiency (ICE) (%) was evaluated from the expression shown in equation 2-12 (da Costa et al., 2016):

$$\%ICE = FV\left(\frac{[COD]_0 - [COD]_t}{8I\Delta t}\right) x\ 100 \qquad (Eq.\ 2-12)$$

Where: COD_0 and COD_t are the initial and final COD values ($g.O_2/L$), F the Faraday constant (96,487 C/mol), V the volume treated (dm^3), I the applied current (A), 8 is the oxygen equivalent mass ($g\ eq.^{-1}$) and Δt is the time in seconds.

The specific energy consumption (E_c, in kWh m^{-3}) was obtained as follows (Panizza & Cerisola, 2010a):

$$E_c = \frac{U_{cell}.I.t}{V.3600} \qquad (Eq. 2-13)$$

Where: U_{cell} is the average cell voltage (V), I the applied current (A), t is the electrolysis time (s), and V is the volume of the treated solution (dm^3).

2.8.6 Titanium Electrode

Myburgh et al. (2019) states that the mixed oxides of IrO_2-Ta_2O_5 on a titanium substrate show high electrical conductivity, are electrochemically active anodes and are well known for their longevity, therefore, they are used in many industrial applications, including wastewater treatment. The authors conducted a study to treat biodiesel wastewater using an integrated process which included electrochemical oxidation using IrO_2-Ta_2O_5 anodes, and adsorption using chitosan. Optimal electrochemical oxidation removal efficiencies were found to be 86%, 88%, and 85% for COD, BOD, and FOG, respectively.

da Costa et al. (2016) conducted a study evaluating two anodes, Ti/Pt and Ti/IrO_2-Ta_2O_5 to treat fuel station effluent at different supporting electrolytes (K_2SO_4 and NaCl). The authors discovered that Ti/Pt performed better when using K_2SO_4 as the supporting electrolyte, while Ti/IrO_2-Ta_2O_5 performed better when NaCl was used. The Ti/IrO_2-Ta_2O_5 anode achieved a maximum 52.1% COD reduction and 94% TOG (total oil & grease) reduction when NaCl was used as the supporting electrolyte.

Wang et al. (2020) used Ti/IrO_2-Ta_2O_5 as an anode to treat polluted river water and found that the optimal electrochemical conditions were 10 mA/cm^2 for current density, 8 cm for anode diameter, 2 mg/L for electrolyte concentration, and the electrolysis time was between 30 and 40 minutes. At these conditions NH_3-N and COD removal efficiencies were found to be 95.28% and 33.62%, respectively. The authors also investigated the pollutant removal mechanism of Ti/IrO_2-Ta_2O_5 and they found that the direct oxidation of the pollutants was often accompanied by indirect oxidation in actual operation. The authors concluded by stating that the Ti/IrO_2-Ta_2O_5 electrode treatment of polluted river water is an attractive environmental-friendly technology.

2.8.7 Electrochemical Oxidation Applications in Wastewater Treatment

Table 2- 7: Electrochemical Oxidation applications in Wastewater Treatment

Electrode	Wastewater	Reduction	Reference
Boron Doped Diamond	Carwash	COD by 82% Colour by 81% Methylene blue active substances by 81% BOD by 73% Chlorides by 72%	(Juárez et al., 2015)
Combined EC & EO EO Electrode: BDD	Car Wash	Complete COD removal Electrolysis time: 100 minutes	(Panizza & Cerisola, 2010b)
Combined EC & EO EO Electrode: BDD	Industrial	The combined process eliminates COD, BOD, colour, turbidity, and coliforms in 120 minutes	(Linares-Hernández et al., 2010)
Combined EC & EO: EO Electrode: Graphite and $RuO_2/IrO_2/TaO_2$ coated titanium	Synthetic Textile	Removal of Cl ions and COD were high with graphite electrode. Minimal decrease with the $RuO_2/IrO_2/TaO_2$ coated titanium electrode	(Raju et al., 2008)
Boron Doped Diamond	Industrial wastewater sludge	Sludge volatile solids were degraded 23% and total COD 27%	(Barrios et al., 2015)
Ti/RuO_2	Real Textile WW	COD removal was 80% Color removed 97.25%	(Kaur et al., 2017)
IrO_2-Ta_2O_5/Ti	Petroleum Produced Water (fresh, brine and saline)	COD removal for fresh:88% COD removal for brine:100 % COD removal for saline:50%	(da Silva et al., 2013)

2.8.8 The Addition of an Electrolyte

The electrochemical oxidation of oxalic acid was performed by Scialdone et al. (2009), comparing two anodic materials, boron doped diamond (BDD) and IrO_2-Ta_2O_5 (DSA-O_2). The experiments were conducted in the absence and presence of NaCl to see what effect the salt has on the performance of the electrochemical process. It was found that the presence of NaCl resulted in higher current efficiency when the DSA electrode was used compared to the absence of NaCl, however, the opposite was found with regards to the BDD electrode. It showed higher current efficiency in the absence of NaCl. At lower pH levels the chlorine evolution reaction is favored (Czarnetzki & Janssen, 1992; Scialdone et al., 2009). This also results in the formation of other species, such as hypochlorite and hypochlorous acid, that can be further oxidized at the surface of the anode to form chlorate. Due to this, the DSA electrode was found to produce the most favourable results at a pH of 2, with 10 g/L of NaCl resulting in 99% conversion and above 70% current efficiency and BDD resulting in 93 and 65% respectively for those same conditions for the incineration of oxalic acid.

Zambrano & Min (2019) conducted a study for the electrochemical oxidation of phenols using a Pt/Ti anode and compared two electrolytes, NaCl and Na_2SO_4. The current density for the electrochemical oxidation was fixed at 9.6 mA/cm^2 and the analysis to determine the most effective electrolyte included the removal of phenol, COD and other factors which were considered as energy consumption and current efficiency. It was found that COD and phenol removal occurred much faster when NaCl was used compared to the Na_2SO_4 electrolyte, Zambrano & Min (2019) suggest the possible reason for this was due to the formation of chloride-oxychloride radicals. The COD and phenol removal rates were 9.5 and 1.5 faster, respectively, when NaCl was used compared to Na_2SO_4. For 96% of COD removal, the energy consumption when NaCl was used was 0.17 per kWh dm^{-3} compared to 0.25 per kWh dm^{-3} when Na_2SO_4 was used. This indicates NaCl produced the most favourable results.

Fajardo et al. (2017) treated phenolic wastewaters using electrochemical oxidation with the addition of NaCl as the supporting electrolyte in the study. The authors results confirmed the use of NaCl instead of Na_2SO_4 yielded more desirable results as in the case of NaCl the removal of total phenol content (TPh) and COD was found to be 100 and 64.4% respectively, compared to when Na_2SO_4 was used yielding removal efficiencies of 30.4 and 6.8% for TPh and COD, respectively.

2.9 Sequential Treatment Process

Sarmadi et al. (2020) conducted a thorough review of carwash wastewater treatment technologies. The authors concluded that integrated processes appear to be a more appealing approach for the remediation of carwash wastewater.

The integrated process for the treatment of carwash wastewater in this study incorporates chemical coagulation and electrochemical oxidation.

Gilpavas et al. (2018) conducted a study of the treatment of industrial textile wastewater using a sequential chemical coagulation and electrochemical oxidation treatment process. Aluminum sulfate was used as the chemical coagulant in the process while BBD was the anodic material for the EO process. They reported achieving removal efficiencies of 100% of colour, 93.5% of COD, and 75% of TOC using the integrated process at optimal conditions.

Torres et al. (2019) reported after treating real textile wastewater using aluminum sulfate as a coagulant and a DSA for the electrochemical oxidation treatment, that TOC removal was found to be 20% for coagulation and an optimum of 82% for EO after 180 minutes of electrolysis time.

The proposed treatment process has never been investigated in conjunction with one another for carwash wastewater, therefore, this study proposes chemical coagulation and electrochemical oxidation for carwash wastewater following the promising results by Gilpavas et al. (2018), and Torres et al. (2019).

2.10 Design of Experiments

2.10.1 Introduction

Design of experiments (DOE) involves the planning and executing of a set of experimental runs to determine the effects of the variables on the respective system. The data gathered from the experiments is then separated into variation generated by the system and uncertainties/errors which always exist in empirical data. At this point a statistically validated model is obtained, which gives insight on the effects of experimental variables on the direction and magnitude of the specific measured response. The experimental runs which are generated are performed in a manner that maximizes the amount of obtainable information from a limited number of experimental runs. When a satisfactory predictive model has been determined, it can be used to predict future observations within the initial design range of the respective system. Design of experiments is a useful tool not only for research, but also developing and optimizing a broad range of engineering systems (Mäkelä, 2017).

Design of experiments was first introduced in the early 20th century in the agricultural sector. Robert A. Fischer, along with scientific consultants and mathematicians proposed methods which included randomization and replication of experiments. In subsequent years, improvements were made on their methods which are still implemented today, namely fractional plans and analysis of variance (ANOVA), factor plans, and elimination plans. Response Surface Methodology (RSM) was introduced into the design of experiments approach during the second half of the 20th century (Jacyna et al., 2019).

Figure 2-7 shows common designs in two dimensions.

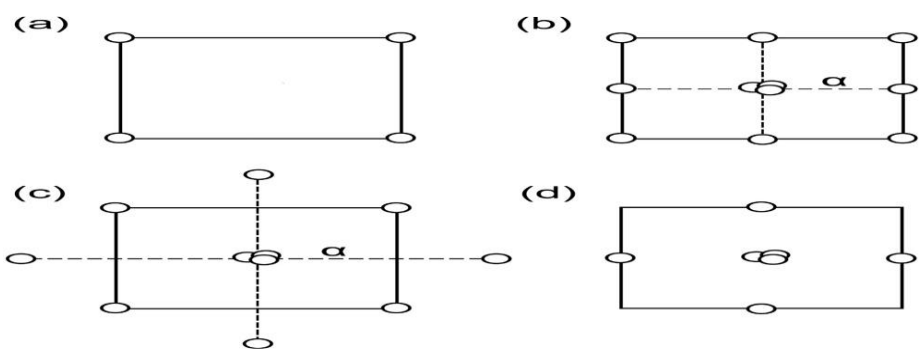

Figure 2- 7: Common Designs: a (Factorial Design), b (central composite design with coded star point distance α = 1), c (central composite design with α > 1), d (Box Behnken Design) (Mäkelä, 2017)

2.10.2 One Factor at a time

The one-factor-at-a-time experimental approach is one of the oldest and simplest methods for design of experiments. It involves setting variables to a constant level and the effect of each variable is investigated by varying one specific variable at a time. It is an inefficient approach and may possibly produce inaccurate results as the effects of varying one factor compared to changing multiple factors at a time is significantly different from each other (Yu et al., 2018).

According to Wahid & Nadir (2013), one-factor-at-a-time may result in obtaining false optimal conditions, as it consists mainly of trial and error. Design of experiments on the other hand identifies factors which causes a change in the response and thus a mathematical expression can be developed to predicted responses based on various conditions. Design of experiments is, therefore, useful to research as it allows for the investigation of many variables with the least number of experimental runs.

Figure 2-8 shows three-factor two level design with a one-factor-at-a-time of equivalent precision. The two-level factorial proposes 8 experimental runs, while the one-factor-at-a-time provides 16 runs, therefore, it can be concluded that the factorial design is much more efficient than the one-factor-at-a-time and its efficiency advantage only becomes more notable as the number of factors increases (Othmer, 2007).

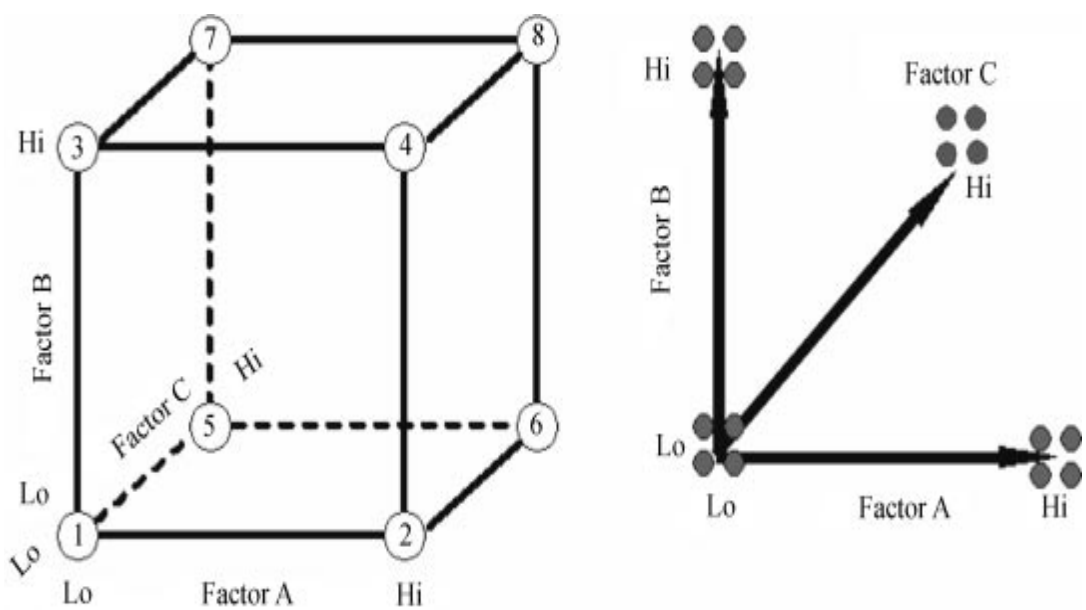

Figure 2- 8: Comparison of Factorial Design vs One-Factor-at-a-Time (Othmer, 2007)

2.10.3 Factorial Design

Factorial designs are considered a classical approach for experimental designs, and it has been vastly used to conduct scientific experiments. It is based on combining multiple factors to investigate their interactions simultaneously while minimizing the degree of biasness in the conducted experiments (Yu et al., 2018).

Factorial design can include one, two, three and more factors in the experimental design. When only one factor is being considered, it is often referred to as simple comparative experiments, ANOVA is typically used for analysis in these types of factorial designs (Durakovic, 2018).

Full factorial designs are said to orthogonal, well-balanced designs which allows an evaluation of main and interacting factors, however, this typically produces many design points. The expression can be seen in equation 2-14 (Yu et al., 2018):

$$n = m^k \qquad \text{(Eq. 2-14)}$$

where n is the total number of samples, k is the number of factors, and m represents the number of levels of each factor.

In most experimental designs where full factorial designs are being implemented, two levels would be considered. This results in a 2^K design and as the expression suggests, the number of experimental runs increases exponentially with the addition of factors, which makes it extremely expensive to conduct experiments of this nature. Three-level factorial designs are usually more suitable for research as they can produce second-order polynomial models to predict the behavior of the independent variables, however, it is more complicated than the two-level counterpart and the complications become more complex as the number of factors increases. When factors of two or more levels are considered, the required experimental runs can reach a very large number even when minimal factors are considered. It is, therefore, preferred to perform two-level factorial designs as a screening tool to determine important factors, which are then investigated in greater detail using factorial designs containing higher factor levels (Yu et al., 2018).

2.10.4 Response Surface Methodology

Response Surface Methodology (RSM) is a useful tool for experimental research in terms of design, optimization, and analysis of any given process. It is compiled of mathematical and statistical methods which provide details of interaction and quadratic effects of the process variables involved in the process, which are not revealed by conventional one-factor-at-a-time optimization methodologies. Figure 2-9 illustrates the highlights of Response Surface Methodology (Manojkumar et al., 2020; Gaitonde et al., 2017).

Figure 2- 9: RSM Highlights (Manojkumar et al., 2020)

There are two main categories in which RSM is divided into, namely Central Composite Design (CDD) and Box-Behnken Design (BBD). CCD is used to study process variables at five levels (+α, +1, 0, -1, α), while BBD is used at three levels (-1, 0, +1). In most cases a second-order polynomial equation is developed to describe the relation between the variables and the responses. The general expression can be seen in equation 2-15 (Manojkumar et al., 2020).

$$Y = \beta_0 + \sum_{i=1}^{n} \beta_i x_i + \sum_{i=1}^{n} \beta_{ii} x_i^2 + \sum_{i<j}^{n} \sum \beta_{ij} x_i x_j + € \qquad (Eq.\ 2-15)$$

Where Y is the response, β_0 is constant, β_i is the linear effect coefficient for the ith factor, β_{ii} is the quadratic effect coefficient for the ith factor and β_{ij} is the interaction effect coefficient for ith and jth factors and € is random error. The least-squares method is used to fit the model with the experimental data (Manojkumar et al., 2020).

I. Central Composite Design

Central Composite Design is a statistical tool which is employed to fit empirical models to the experimental data obtained from the respective experimental design. CCD is appropriate for fitting second order polynomial equations for optimizing a variety of research problems. There are three groups of design points under CCD as follows (Asghar et al., 2014):

a) Two level factorial design (2k), consisting of possible combinations + 1 and - 1 levels of factors.
b) 2k axial points fixed axially from a distance α from the centre point to generate quadratic terms.
c) Centre points which represent replicate terms that gives useful insight of the experimental error

Taking those three factors into consideration, the number of experimental runs for CCD is determine by the following expression:

$$N = k^2 + 2k + n \qquad \text{(Eq. 2-16)}$$

Where N represents the total number of experiments, k is the number of factors in the process and n is the number of replicates. CCD under RSM is typically performed using either Design Expert or Minitab software (Asghar et al., 2014).

Alpha is an important term to calculate in CCD as it could possibly determine the location of axial points in the experimental domain. The design could either be orthogonal, face centered, or rotatable, determined by the alpha value. An alpha value of 1 is desirable as it ensures the position of axial point within the factorial portion region. The calculation is as follows (Asghar et al., 2014):

$$\alpha = (2^k)^{0.25} \qquad \text{(Eq. 2-17)}$$

Experimental results obtained are analyzed using the second-order polynomial expression denoted in equation 2-15.

II. Box-Behnken Design

Box-Behnken Designs (BBD) are composed of rotatable second-order designs which are based on three-level incomplete factorial designs. The graphical representation of the BBD is displayed in figure 2-10 (Ferreira et al., 2007):

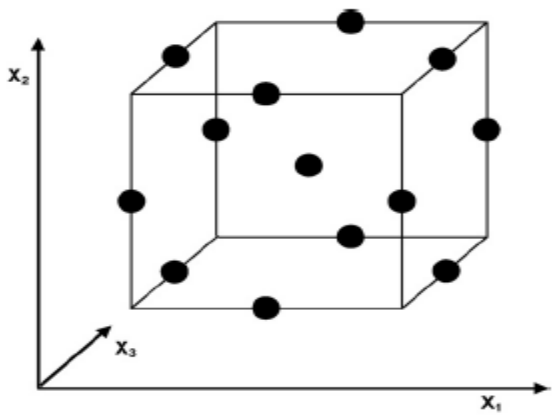

Figure 2- 10: BBD Cube (Ferreira et al., 2007)

The number of experimental runs (N) required for the development of the BBD is expressed as:

$$N = 2k\,(k - 1) + C_0 \qquad \text{(Eq. 2-18)}$$

Where k is the number of factors and C_0 is the number of centre points.

Experimental results obtained are analyzed using the second-order polynomial expression denoted in equation 2-15.

Ferreira et al. (2007) compared the efficiency between BBD, CCD, Doehlert matrix, and three-level full factorial design. They reported that the BBD and the Doehlert matrix is slightly more efficient than the CCD but significantly more efficient when compared to the three-level full factorial design. They also found by using their efficiency comparative method that the three-level full factorial designs are quite costly when the factor is greater than 2. Table 2-8 shows their findings.

Table 2- 8: Comparison Efficiency between CCD, DM, and BBD (Ferreira et al., 2007)

Factors (k)	Number of coefficients (p)	Number of experiments (f)			Efficiency % (p/f)		
		CCD	DM	BBD	CCD	DM	BBD
2	6	9	7	-	67	86	-
3	10	15	13	13	67	77	77
4	15	25	21	25	60	71	60
5	21	43	31	41	49	68	61
6	28	77	43	61	36	65	46
7	36	143	57	85	25	63	42
8	35	273	73	113	16	62	40

2.10.5 Evaluation of the Design Model

A. Predicted vs Actual

Figure 2-11 shows a typical Predicted vs Actual graph, according to Kusuma & Mahfud (2016), the predicted values are in good agreement with the experimental values in this graph.

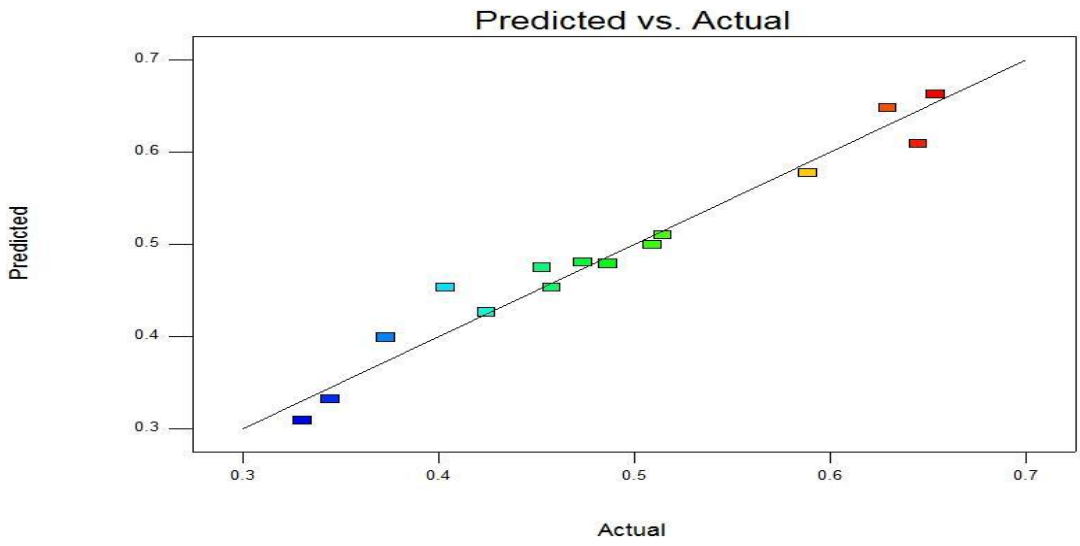

Figure 2- 11: Predicted vs Actual (Kusuma & Mahfud, 2016)

B. Residual vs Predicted

A plot of residuals vs predicted is shown in figure 2-12. Montgomery (2013) states that if the model is correct, the residuals shouldn't have any type of structure and no obvious pattern should be observed. This is apparent in figure 2-12.

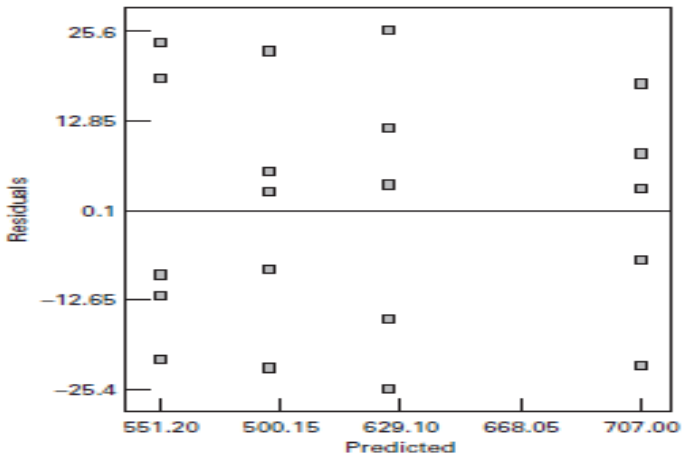

Figure 2- 12: Residuals vs Predicted (Montgomery, 2013)

C. Normal Probability vs Residuals

According to Montgomery (2013), if the underlying error distribution is normal, the plot of normal % probability vs residuals will resemble a straight-line. This is illustrated in figure 2-13. He states that in general moderate departure from normality is of little concern. Plots that indicate considerably thinner/thicker tails are of more concern than skewed distribution.

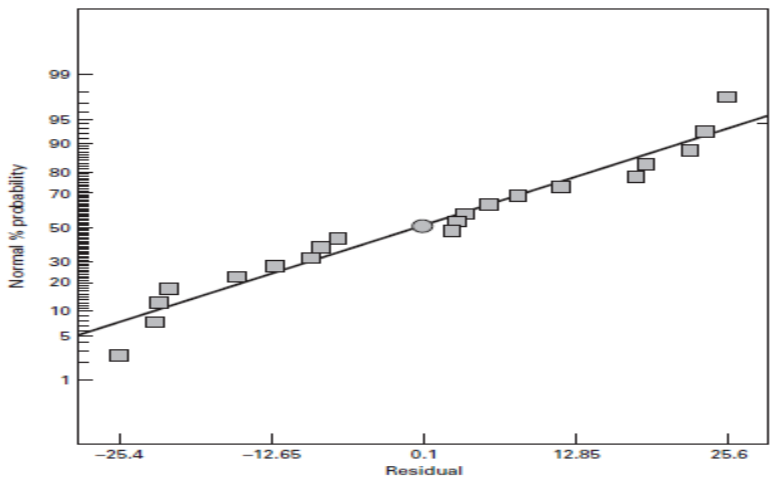

Figure 2- 13: Normal % Probability vs Residuals (Montgomery, 2013)

D. Perturbation

The Perturbation plot shows a comparison between all factors at a selected point in the specific design space. A typical plot is shown in figure 2-14 (Kusuma & Mahfud, 2016).

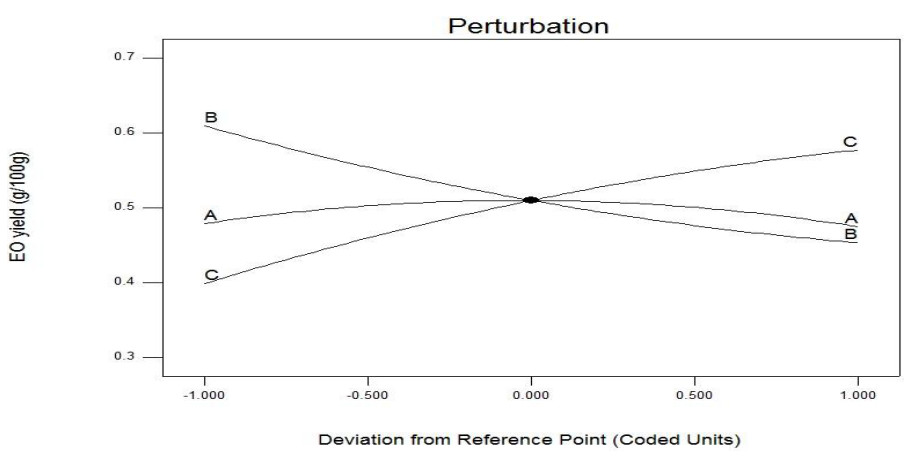

Figure 2- 14: Perturbation Graph (Kusuma & Mahfud, 2016)

E. Contour Plot and 3D

Figures 2-15, 2-16, and 2-17, respectively, show 3D response surface graphs and contour plots for stationary points with a maximum response, minimum response, and a saddle point. Contour plots are critical in analyzing a response surface, the characterization of the shape of the surface is illustrated as well as the location of the optimum point (Montgomery, 2013).

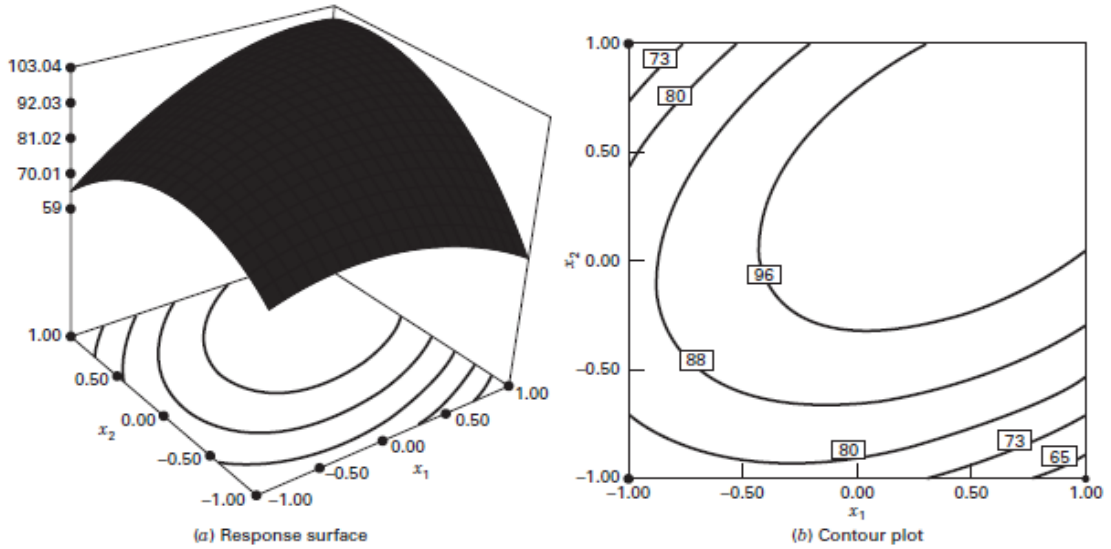

Figure 2- 15: Response Surface and contour illustrating a Maximum (Montgomery, 2013)

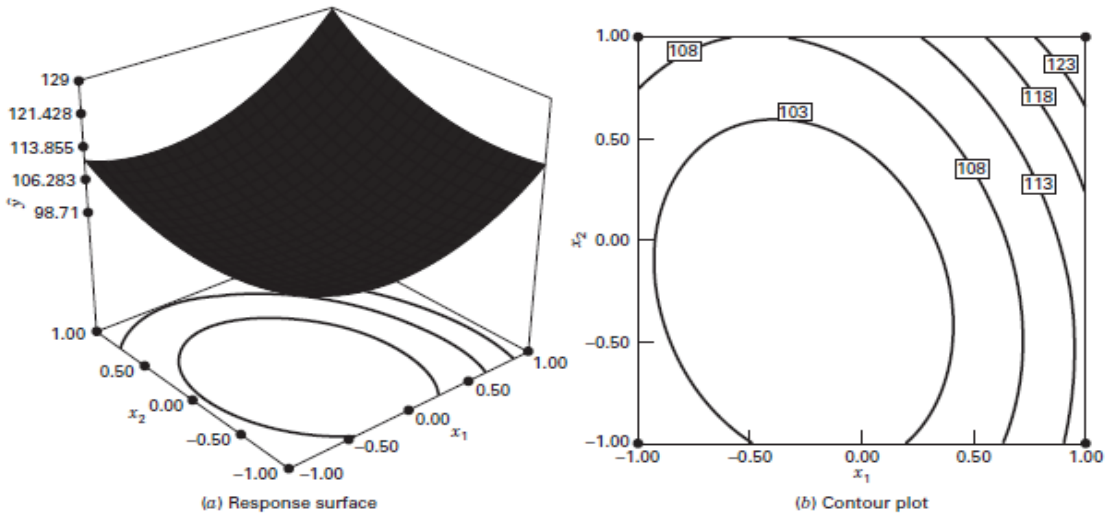

Figure 2- 16: Response Surface and Contour illustrating a Minimum (Montgomery, 2013)

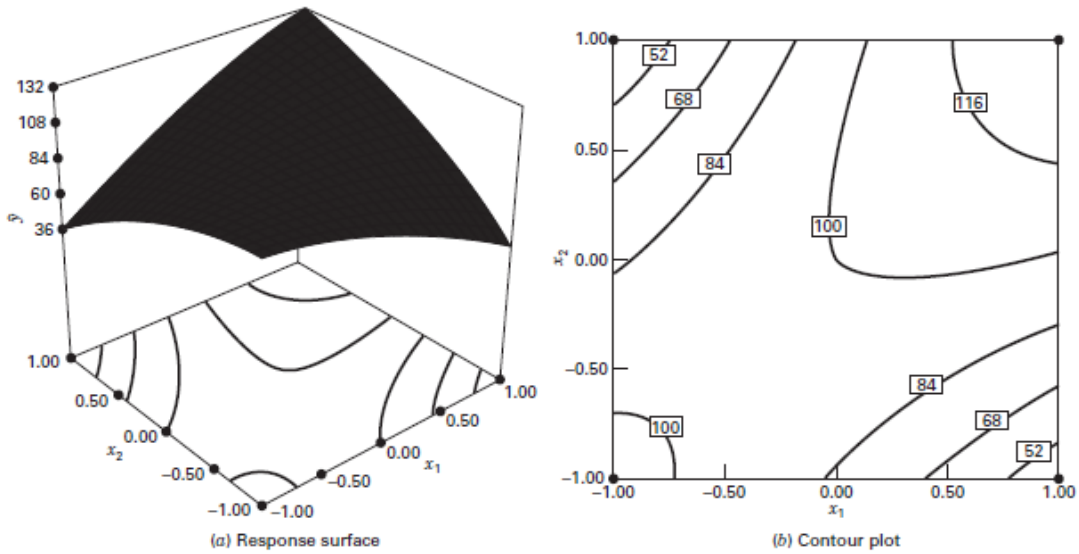

Figure 2- 17: Response Surface and Contour illustrating Saddle Point (Montgomery, 2013)

Chapter 3:
Research Methodology

Chapter 3: Research Methodology

3.1 Introduction

This chapter is composed of all the equipment, materials, experimental conditions as well as the experimental procedures for the various runs being investigated, including pre-treatment and secondary treatment for the integrated process. The instruments used for analytical procedures are described.

3.2 Research Design

The research approach taken for this study was a quantitative design, specifically experimental research. This study consists of two parts. The first part focuses on identifying the most suitable dosage of poly aluminum chloride (PAC) for the coagulation process. The second part consists of using the identified PAC dosage as a pre-treatment for the electrochemical oxidation (EO) process, where three variables were investigated.

3.3 Sample Collection

Carwash wastewater (CWW) was collected from a local car dealership in the City of Cape Town (CoCT), Western Cape region. The name of the specific dealership is not disclosed as it forms part of the agreement between the company and this research study. The wastewater was collected in one batch (enough for all experiments) to try and keep the composition of the water as uniform as possible for the experiments conducted. Once collected, it was transported and stored in a refrigerator at 4˚C. All experiments were conducted in the Environmental Engineering Research Laboratory 1.18 in the Chemical Engineering building.

3.4 Carwash Wastewater Treatment Processes

3.4.1 Chemical Coagulation

Treatment Process

The dosages which were investigated during the chemical coagulation process can be seen in Table 3-1.

Table 3- 1: Coagulant Dosages

	PAC Dosages(mg/L)		
Experimental Run	60	80	100
Duplication	60	80	100

The chemical coagulation process, aimed to reduce the organic pollutants from CWW, was performed by adding a specific concentration to the carwash wastewater followed by rapid mixing (500 rpm) for 10 minutes and then 20 minutes of slow mixing (100 rpm). The solution was left to settle for 1 hour, thereafter a filtration unit was employed to remove the settled solids. This solution was then the influent for the electrochemical oxidation process. Three different concentrations were investigated, 60, 80, and 100 mg/L of PAC, respectively. All coagulation experiments were performed at room temperature. Figure 3-1 below is an illustration of the coagulation process followed by how the initial and settled solution looks, respectively.

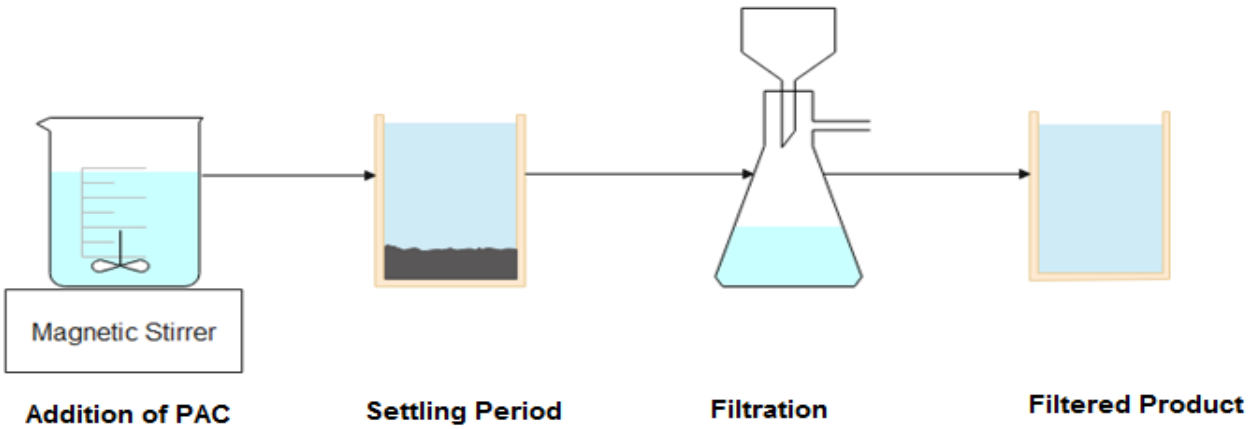

Figure 3- 1: Schematic Diagram of Coagulation Process

The initial step of the coagulation process of the carwash wastewater can be seen in photograph 3-1, while photograph 3-2 shows the settling stage.

Photograph 3- 1: Initial Carwash Wastewater in Coagulation process

Photograph 3- 2: Settling Period after Coagulation

3.4.2 Electrochemical Oxidation

Treatment Process

The influent for the electrochemical oxidation process was the treated coagulated carwash wastewater. It was transferred into a 1 L glass reactor. Two commercial IrO_2-Ta_2O_5/Ti electrodes (NMT electrodes, South Africa) were used, and the working anode surface area was 200 cm^2. The distance between the electrodes were kept at approximately 10 mm. The glass reactor was kept in a water-bath maintaining a constant temperature of 60˚C. All experimental runs for electrochemical oxidation were 24 hours and was stored in a 1 L Schott bottle thereafter in a refrigerator at 4˚C. The process is represented by Photograph 3-3 and Figure 3-2 as seen below.

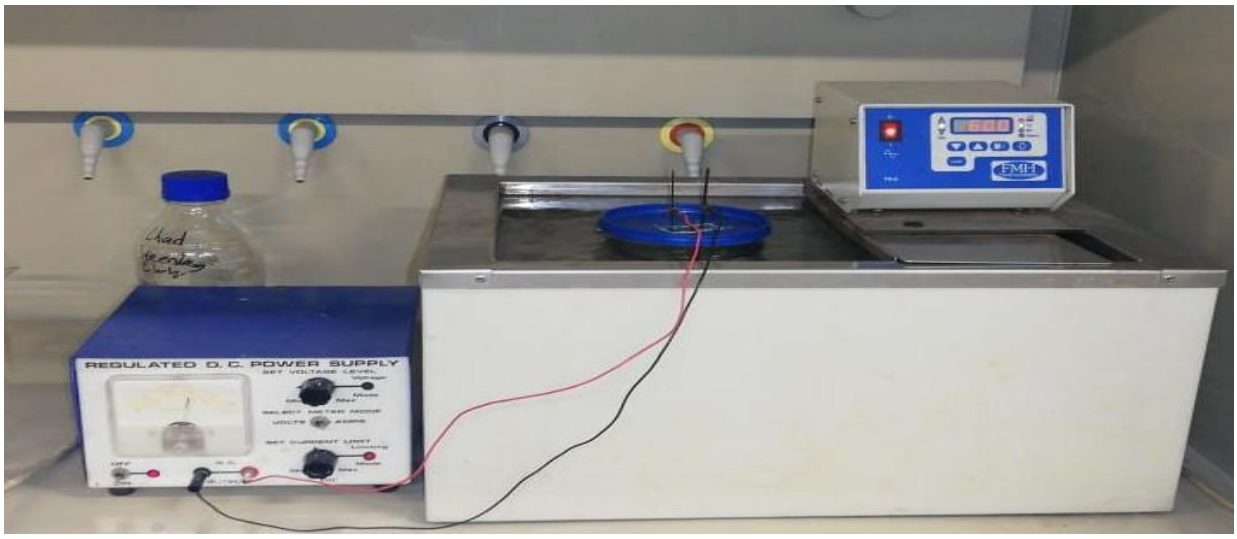

Photograph 3- 3: Electrochemical Oxidation Set-up

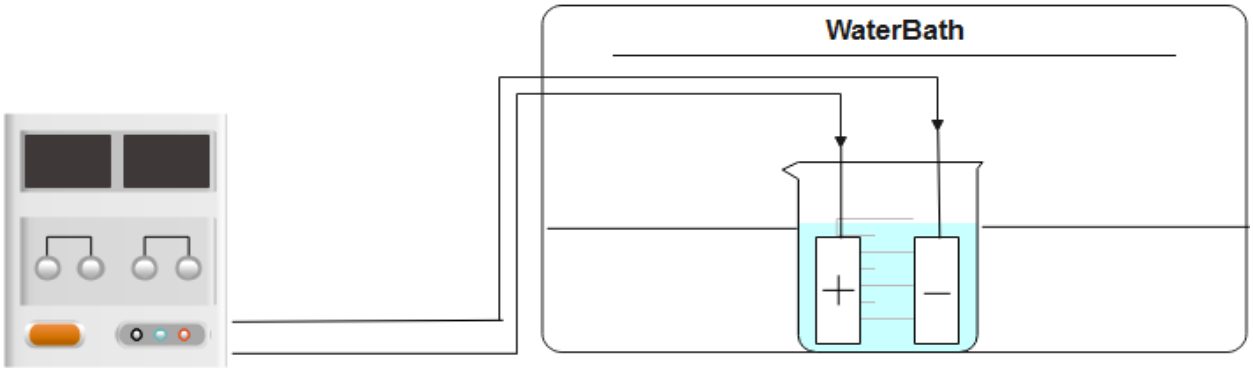

Figure 3- 2: Schematic Diagram of EO Process

Figure 3-3 shows a schematic diagram of the integrated treatment process of carwash wastewater.

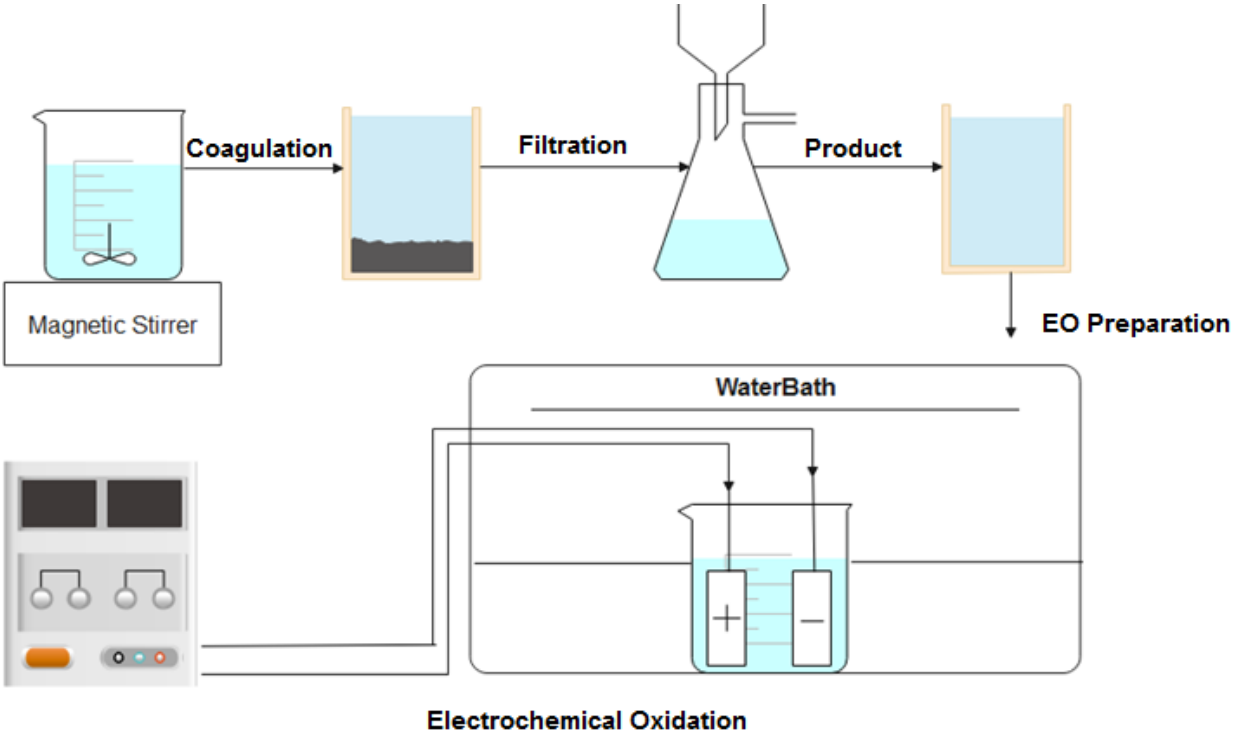

Figure 3- 3: Hybrid Treatment Process

3.5 Chemical Analysis

Conductivity, pH, and turbidity were measured using, calibrated conductivity, pH, and turbidity meters (Hanna Instruments), respectively. CWW was characterized by a high concentration of chemical oxygen demand (COD), oil and grease (O&G), and surfactants. COD was measured by a reactor digestion method using a Hanna instrument. In brief, the measurement of parameters by Hanna instruments involves the addition of a sample solution into a reagent containing vial, which is heated for a specified period, then cooled to room temperature. The concentration of the parameter sought is then measured using Hanna's COD and multiparameter instrument. The range of the COD vials was 0 - 10000 mg/L. Hanna's COD and multiparameter instrument measured colour and COD concentration. Furthermore, FOG and anionic surfactant analysis were done off-site at an accredited analytical facility.

3.6 Design of Experiments

Design Expert software was employed to develop the experimental runs to be performed. The type of design chosen was Response Surface Methodology, specifically the Box-Behnken design. Design expert software version 10.0 (Stat-Ease Inc, Minneapolis, USA) was used to generate 26 experimental runs. The factor's range and levels are presented in Tables 3-2.

Table 3- 2: Factorial Design of Experiments

	Name	Units	Low	Middle	High
A	Initial pH	-	-1 (2)	0 (7)	1 (12)
B	Current Density	mA/cm^2	-1 (1)	0 (5.5)	1 (10)
C	Electrolyte	M	-1 (0.01)	0 (0.055)	1 (0.1)

In the experimental design one center point was chosen, therefore 13 runs were produced by the software. All experimental runs were duplicated; therefore 26 electrochemical oxidation runs were performed. The conditions for each run can be seen in table 3-3.

Table 3- 3: Experimental Runs

	Factor 1	Factor 2	Factor 3
Run	pH	Current Density (mA/cm^2)	Electrolyte (M)
1	-1	-1	0
2	-1	-1	0
3	-1	0	1
4	-1	0	1
5	-1	0	-1
6	-1	0	-1
7	1	0	-1
8	1	0	-1

9	0	-1	-1
10	0	-1	-1
11	0	1	-1
12	0	1	-1
13	1	-1	0
14	1	-1	0
15	0	0	0
16	0	0	0
17	-1	1	0
18	-1	1	0
19	1	0	1
20	1	0	1
21	0	-1	1
22	0	-1	1
23	1	1	0
24	1	1	0
25	0	1	1
26	0	1	1

The RSM Box-Behnken design (BBD) was applied to develop the appropriate experimental conditions. The BBD design indicated the random order of experimental runs to be followed.

3.7 Research Apparatus

The following equipment, consumables and apparatus were used during the experimental runs to collect data to determine the removal efficiencies for COD and turbidity from CCW before and after the chemical coagulation and the electrochemical oxidation process.

3.7.1 Storage Containers & Glassware

- 2 x 25 L Plastic Container for collecting and storing carwash wastewater.
- 1 litre beaker for coagulation.
- 1 litre beaker for electrochemical oxidation.
- 1 litre glass Schott bottles were used for storage of samples.

3.7.2 Equipment

- A FMH Circulator was used to heat up the water in the water-bath to maintain a constant temperature of 60°C. It is manufactured by FMH Instruments and it was purchased from Lab Supply in Cape Town, South Africa.

Photograph 3- 4: FMH Circulator

- A Digital Hotplate Magnetic Stirrer was used during the chemical coagulation process to alter between rapid and slow mixing. This instrument is manufactured by Dragon Laboratory Instruments and the specific model used was a MS-H-Pro. It was purchased from Select Science.

Photograph 3- 5: Magnetic Stirrer

- A COD Test Tube Heater was used to heat up the COD vials to the desired temperature of 150°C. This product is manufactured by Hanna Instruments, and the model number for the product is HI839800. It was purchased at their office in Cape Town, South Africa.

Photograph 3- 6: COD Test Tube Heater

- A Water & Wastewater Multiparameter Photometer was used to determine the COD values in this study. The instrument is manufactured by Hanna Instruments and the model number for the product is HI83399-02. It was purchased from their office in Cape Town, South Africa.

Photograph 3- 7: Multiparameter Photometer

- A Crison Basic 20 pH – Meter was used in this study to determine the pH of various samples. This product is manufactured by Crison Instruments and was purchased from the manufacturer, who are situated in Barcelona, Spain.

Photograph 3- 8: Crison pH meter

- An analytical balance was used to determine the amount of coagulant dosage for pre-treatment experimental runs. The analytical balance used in this study was a Kern analytical balance. It was purchased from Merck. Merck is situated in Darmstadt, Germany.

Photograph 3- 9: Kern Analytical Balance

- The turbidity of samples was determined using a turbidity meter called Turb 355 IR. It is manufactured by Xylem Analytics. The instrument was purchased from Labotec. They are in Midrand, South Africa.

Photograph 3- 10: Turb 355 IR

3.7.3 Materials

High-grade chemicals and reagents were used for this research. Sodium chloride (NaCl), sulphuric acid (H_2SO_4) and sodium hydroxide (NaOH) were purchased from Merck. All solutions used in this study were prepared using water from an ultrapure Milli-Q purification system (MQ, Millipore). For pH adjustment, 1 M H_2SO_4 and/or 1 M NaOH was used in all experiments.

COD high reagent vials were used to determine the amount of COD present in various samples. All reagent vials (H93754C) were purchased from Hanna Instruments, from the office situated in Cape Town, South Africa.

The coagulant used in this study (PAC) was supplied by Marlyn Chemicals. They are situated in Klipriver, South Africa.

The electrodes used in this study were IrO_2-Ta_2O_5/Ti anodes. The electrodes were purchased from NMT Electrodes (PTY) LTD. They are situated in Pinetown, South Africa.

3.7.4 Sludge Characterization

The sludge generated by the coagulation process was characterized by using Fourier-transform infrared spectroscopy. The functional groups in the sludge were identified using FTIR by indicating the relative wavelengths (cm^{-1}) of the peaks.

The FTIR analysis was performed off-site at an accredited analytical facility.

Chapter 4:

Results

&

Discussion

Chapter 4: Results & Discussion

4.1 Introduction

This chapter presents the results obtained with the removal of pollutants from industrial carwash wastewater using a laboratory bench scale integrated CC and EO process. The major pollutants were COD and anionic surfactants. The pollutant levels before and after degradation were used to evaluate how efficient the integrated process was. All experimental runs were conducted in randomized order and were repeated.

4.2 Car Wash Wastewater Characteristics

The characteristics of the raw carwash wastewater is tabulated below and the parameters which were investigated are COD, FOG, surfactants and turbidity. This study consisted of investigating these parameters for real carwash wastewater. The characteristics of the wastewater can be seen in table 4-1.

Table 4- 1: Raw Carwash Wastewater

Real Carwash Wastewater		
Parameter	**Unit**	**Value**
COD	mg/L	1220
FOG	mg/L	48.2
Surfactant	mg/L	25.9
Turbidity	NTU	99.4
pH	-	7.08

4.3 Preliminary Treatment

4.3.1 Coagulation

The coagulation process, with poly aluminum chloride (PAC) as coagulant, was used as a pre-treatment step before electrochemical oxidation. First the most favourable dosage was determined in terms of COD, FOG, surfactants, and turbidity removal. The dosages of PAC which were investigated were 60, 80, and 100 mg/L, respectively.

In Figure 4-1, the coagulation results are displayed at their respective dosages and corresponding removal percentages of anionic surfactants, FOG's, COD, and turbidity. The objective was to determine which coagulant dosage is best suited as the initial step before the electrochemical oxidation experiments.

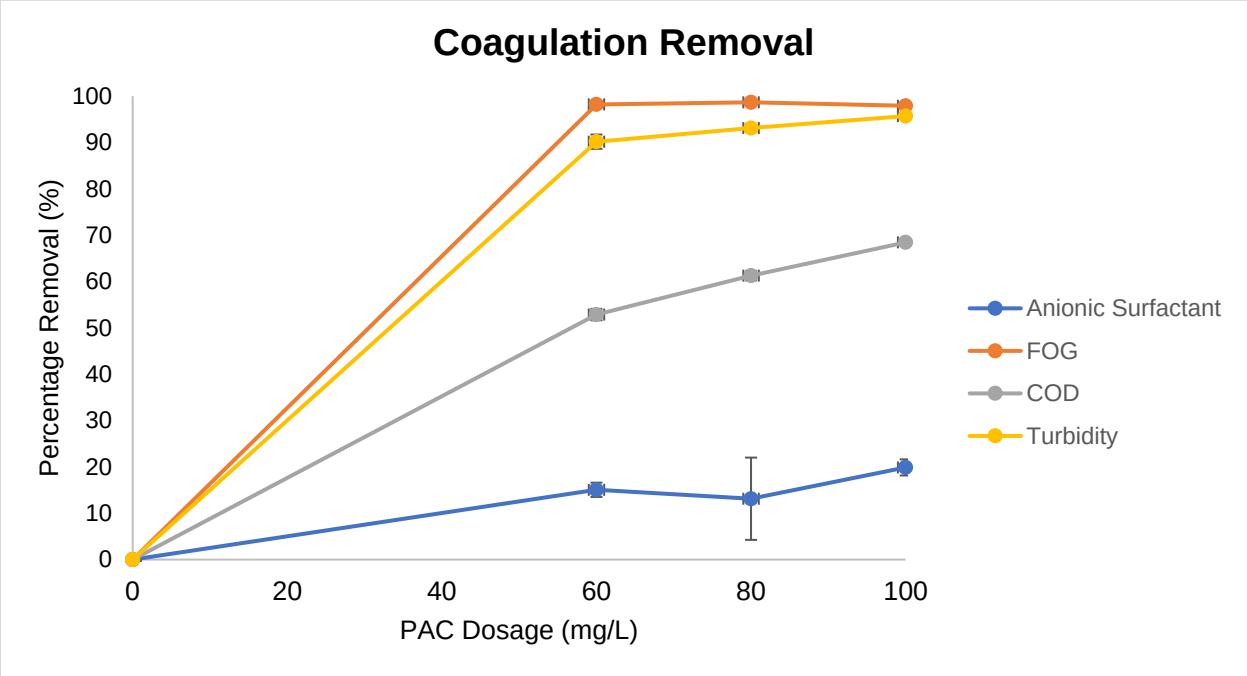

Figure 4- 1: Coagulation Removal Efficiencies

As shown in Figure 4-1, there is no significant difference between the three dosages in terms of FOG removal. All three dosages achieved ± 98 percentage removal, therefore, this parameter was not an influential factor in determining the most suitable dosage for the electrochemical oxidation process. Baddor et al. (2014) performed coagulation on CWW and obtained a removal

efficiency of 86.57 percent using natural coagulant, bentonite. In this study the highest FOG removal was found to be 98.67 percent using 80 mg/L PAC coagulant. It should be noted that there is quite a significant difference of 12 percent between the natural and the PAC coagulant. Hidayah et al. (2019) treated industrial wastewater by means of coagulation comparing various coagulants. They found that when using 20 mg/L of PAC, FOG percentage removal was found to be 91.3%.

During the turbidity removal, all three dosages managed to achieve removal percentages above 90%. However, the 100 mg/L dosage performed significantly better than the other two dosages. This can also be seen in Photograph 4-1. Using 100 mg/L achieved a turbidity removal of 95.7%, compared to the 90.17% and 93.12% for the 60 and 80 mg/L dosages, respectively. Mohamed et al. (2014) compared natural and chemical coagulants when treating CWW. The highest turbidity removal efficiency of 95% was achieved using the natural coagulant, Strychnos Potatorum. Their results are consistent with the highest turbidity removal found during this study, of 95.7 percentage removal efficiency with 100 mg/L PAC. Yang et al. (2010) compared PAC and aluminum sulphate to treat yellow river water and found that PAC performed significantly better. Using 15 mg/L of PAC it achieved a turbidity removal of 96.3%.

Bazrafshan et al. (2012) achieved a COD removal percentage of 86.44 when using 100 mg/L PAC as a coagulant to treat CWW. In this study COD removal percentages were found to be 52.87, 61.27, and 68.44 at PAC coagulant dosages of 60, 80, and 100 mg/L, respectively. At a 100 mg/L PAC coagulant dosage, the study by Bazrafshan et al. (2012), achieved a better COD percentage removal at a COD feed concentration of 924.17 mg/L. A possible explanation for this discrepancy could be due to the difference in feed concentration, where this study started with a COD feed concentration of 1220 mg/L. It can be concluded that the COD percentage removal is directly proportional to the increase in coagulant dosage (Bazrafshan et al., 2012).

Anionic surfactant percentage removal efficiencies were found to be 15.06, 13.13, and 19.88% for the PAC dosage of 60, 80, and 100 mg/L, respectively. There was no significant difference between the 60 and 80 mg/L dosages, but a small increase at 100 mg/L. This is consistent with Bazrafshan et al. (2012), where the anionic surfactant removal percentage increased with an increase in coagulant dosage. In the same study, the CWW was also dosed with 100 mg/L of PAC coagulant and achieved a removal efficiency of 77.73%, compared to the 19.88% removal found in this study. The possible explanation to this big discrepancy in percentage removal is due

to the 24-hour waiting period before the first treatment, thus, allowing some impurities to settle down and separated before any experimental run.

Table 4- 2: Coagulation Removal Percentages

	% Removal			
Dosage (mg/L)	Turbidity	COD	Anionic Surfactants	FOG
60	90.17	52.87	15.06	98.22
80	93.12	61.27	13.13	98.67
100	**95.7**	**68.44**	**19.88**	97.93

As mentioned before the FOG results are quite close to one another, therefore, it could not be an influential factor when choosing the most desirable dosage. Based on the highlighted values shown in Table 4-2, the most favourable dosage was found to be 100 mg/L. This PAC coagulant dosage will be used as the chemical coagulation pretreatment step before all electrochemical oxidation (EO) experimental runs. In Photograph 4-1, it can be seen how the colour changed with a change of the three different PAC coagulant dozing. The far right with the 100 mg/L PAC sample bottle shows the best clarity.

Photograph 4- 1: PAC coagulation at three different dosages

4.3.2 Sludge Characterization

After coagulation was performed, the samples were filtered to remove the sludge before the electrochemical oxidation process. The sludge samples generated at optimum operating conditions were characterized using FTIR measurements for PAC, to identify the functional groups in the samples. The sludge can be seen in photograph 4-2. FTIR analysis was performed on the sludge at a range of 450 - 3450 cm^{-1} wavelengths.

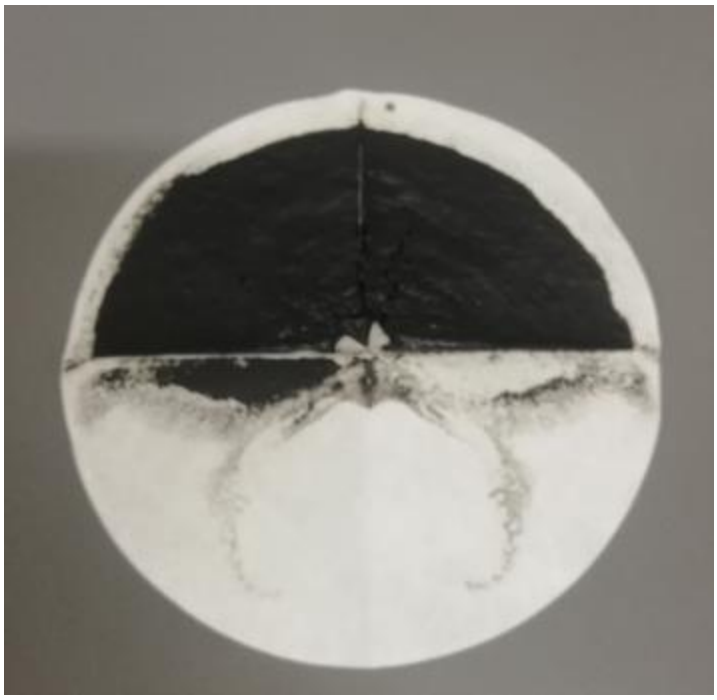

Photograph 4- 2: PAC coagulated Sludge

Photograph 4-2 shows the sludge filtered after the coagulation process where an FTIR analysis was performed on the coagulated sludge. As seen from FTIR spectra of the coagulant sludge (Figure 4-2), the peaks 2924 cm^{-1}, 2851 cm-^{1}, 1640 cm^{-1}, 1458 cm^{-1}, and 1000 cm^{-1} are presented. The strong peak at 1000 cm^{-1} is assigned to Al-O-H bending. The presence of these bands indicated that the generated sludge for Al mostly includes hydroxides (Gönder et al., 2017). The peak at 1458 cm^{-1} is attributed to O-H bending vibration (Aswathy et al., 2016). According to Lal & Garg (2017), the peak at 1640 cm^{-1} is an indication of O-H bending of H_2O. The formation of O-H groups may incorporate components of water, alcohol and phenol. The peaks at 2851 cm^{-1} and 2924 cm^{-1} is attributed to C-H strong vibration (Kaufmann, 2012).

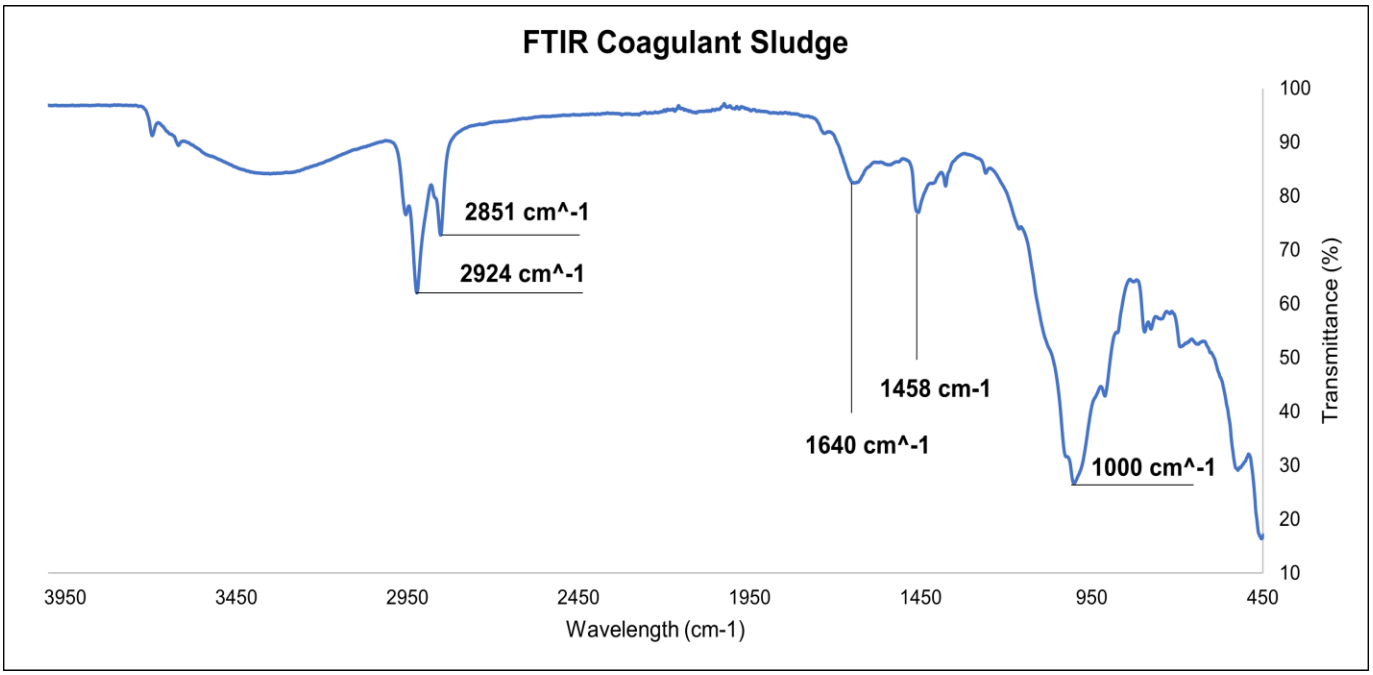

Figure 4- 2: Sludge FTIR Analysis

Table 4-3 provides an overview of the wave numbers (cm^{-1}) and their respective band assignments for each peak identified for the FTIR analysis of the coagulated sludge.

Table 4- 3: Functional groups of coagulated sludge

Wave Number (cm^{-1})	Band Assignments	Reference
2924 & 2851	C-H strong vibration	Kaufmann, (2012)
1640	OH bending of H_2O	Lal & Garg, (2017)
1458	OH bending Vibration	Aswathy et al., (2016)
1000	Al-OH bending	Gönder et al., (2017)

It can be concluded that the coagulated PAC sludge has functional groups which could bind pollutants like alcohols, phenols and alkanes. The hydroxyl group is strongly associated with pollutants and heavy metal ions (Gomes et al., 2007).

4.4 Electrochemical Oxidation of Carwash Wastewater

During the electrochemical oxidation (EO) experimental runs, the CWW feed was pretreated with a chemical coagulation (100 mg/L PAC as coagulant) step. Design Expert software was employed to develop the twenty-six (26) experimental runs to be performed in order to investigate the problem at hand. The factor range and levels are presented in Tables 3-2 (Chapter 3). In the experimental design, one center point was chosen, therefore, 13 runs were produced. All experimental runs were duplicated; therefore 26 electrochemical oxidation (EO) runs were performed. The conditions for experimental runs are demonstrated in Table 3-3 (Chapter 3).

A 3-level factor BBD was applied to develop the appropriate experimental conditions that influenced the COD, surfactant, FOG, and turbidity removal efficiencies from CWW. Initial pH (2, 7, 12); electrolyte NaCl concentration (0.01, 0.055, 0.1M); current density (1, 5.5, 10 $mA.cm^{-2}$) were taken as the process parameters. The design BBD indicated random order of experimental runs to be followed. The EO experimental parameters that were kept constant throughout are electrolysis time of 24 hours; system temperature at 60˚C; and the electrode spacing of approximately 1 cm.

4.4.1 Chemical Oxygen Demand (COD) Removal

The elimination of organic matter in the carwash wastewater was assessed from the decay of the chemical oxygen demand (COD), which was measured using a HANNA spectrophotometer. Figure 4-3 displays the COD concentration and the average percentage removal at each experimental condition. Figure 4-4 displays the COD percentage removal with experimental parameter detail. The COD percentage removal ranges from a minimum of 70.49 for experimental run 11 (pH 7, current density 1 $mA.cm^{-2}$, NaCl 0.1M) to a maximum of 97.13 for experimental run 9 (pH 2, current density 10 $mA.cm^{-2}$, NaCl 0.055M).

Table 4-4 summarizes the COD percentage removal and shows the effect of current density. It can be observed that an increase in current density promotes the removal of COD, however increasing current density results in an increase in the energy consumption (Panizza & Cerisola, 2010).

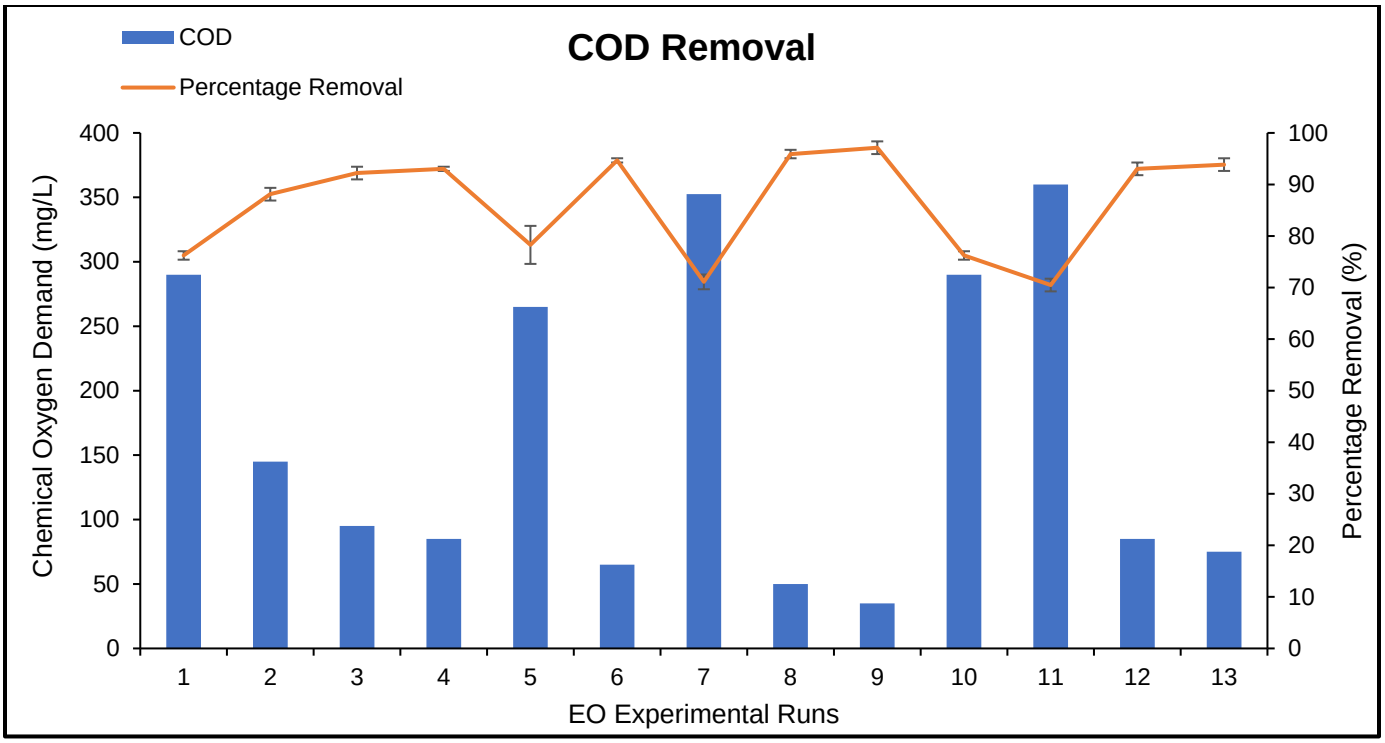

Figure 4- 3: Electrochemical Oxidation COD Removal

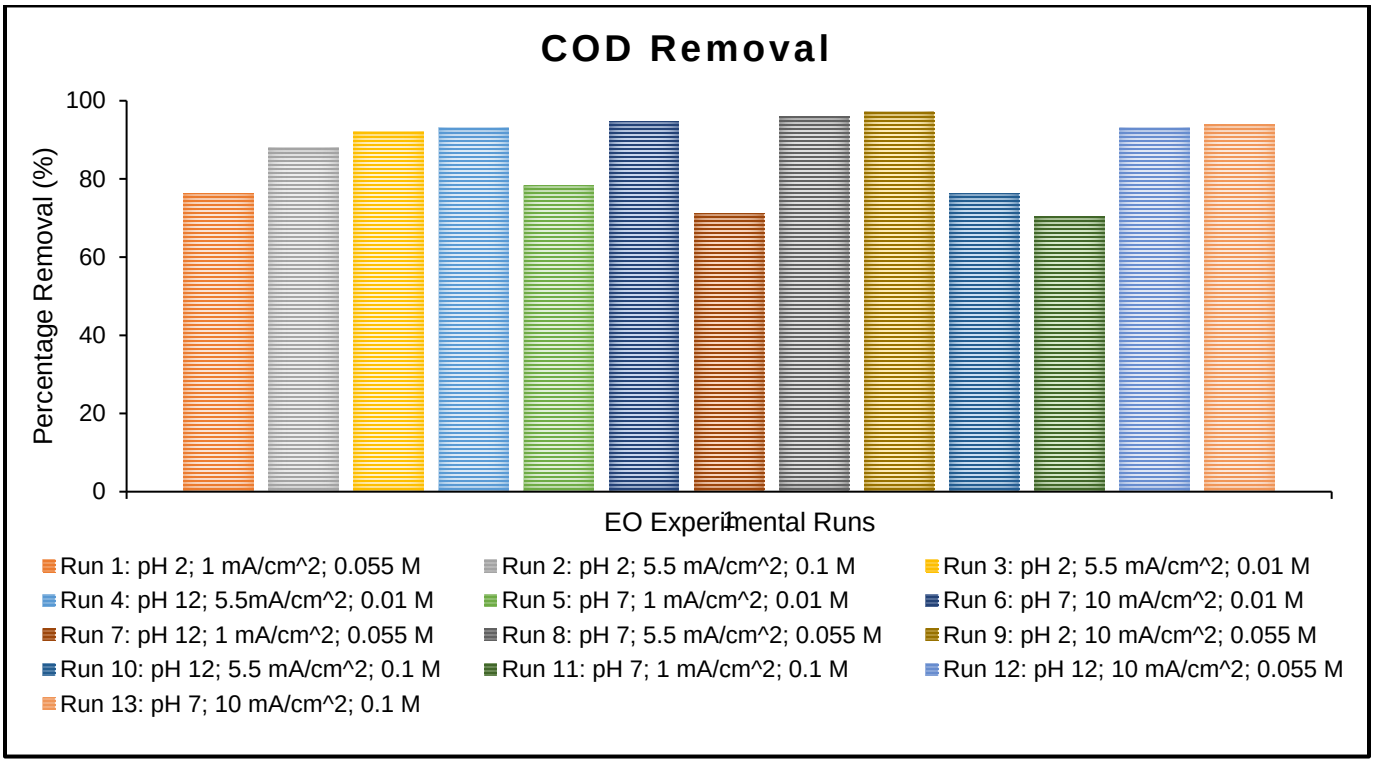

Figure 4- 4: COD Percentage Removal at various Experimental Conditions

The noticeable effect can be observed at low current densities (1 $mA.cm^{-2}$), where the COD percentage removal for experimental runs 1, 5 ,7 and 11 are all below 80%, It seems that the electrolyte (NaCl) concentration does not have any visible effect, whereas the high pH (experimental run 7, pH 12 and 11, pH 7) at lower current density (1 $mA.cm^{-2}$) has a distinct influence on the COD percentage removal (71.11 and 70.49%).

The electrochemical removal of COD was due to direct oxidation, as well as indirect oxidation (Wang et al., 2020). In direct oxidation, the organic pollutants are oxidized on the surface of the electrode and the products are then released into the bulk solution. At the cathode, the reactions which occur are hydrogen production and H_2O_2 formation. The amount of hydrogen bubbles produced is dependent on the current intensity being applied. At higher currents, the bubble concentration increases and the mixing rate is higher (Gonzalez-Rivas et al., 2019). This explains why at higher current densities more favourable results were obtained. The reactions which occur during direct oxidation can be seen below:

$$H_2O \rightarrow H^+ + HO\bullet + e^- \qquad \text{(Eq. 4-1)}$$

$$2HO\bullet + R \rightarrow RO + H_2O \qquad \text{(Eq. 4-2)}$$

In indirect oxidation a mediator is generated in-situ. Once generated the mediator then reacts with organic pollutants in the bulk solutions. In waters where chlorides exist, a very efficient amount of free chlorine can be generated, however, the pH value may affect the oxidation rate as it determines the primary active chloro-species present in the wastewater (Urtiaga & Ortiz, 2009; Gonzalez-Rivas et al., 2019). This explains the significant difference of COD removal observed at lower pH values (2 & 7) and at higher pH (12). The chemical reactions which occur at different levels of pH in chlorinated waters is as follows (Martínez-Huitle & Panizza, 2018):

$$2Cl^- \rightarrow Cl_2 + 2e^- \qquad \text{(Eq. 4-3)}$$

$$Cl_2 + H_2O \rightarrow HOCl + H^+ + Cl^- \qquad \text{(Eq. 4-4)}$$

$$HOCl \rightarrow H^+ + OCl^- \qquad \text{(Eq. 4-5)}$$

Table 4- 4: COD Results Summarized

Current Density $mA.cm^{-2}$	Experimental Run	Electrolyte (NaCl) M	pH	Average COD percentage removal	COD effluent concentration level (mg/L)
1	1	0.055	2	76.23	290
	5	0.010	7	78.28	265
	7	0.055	12	71.11	353
	11	0.100	7	70.49	360
5.5	2	0.100	2	88.11	145
	3	0.010	2	92.21	95
	4	0.010	12	93.03	85
	8	**0.055**	**7**	**95.90**	**50**
	10	0.100	12	76.23	290
10	**6**	**0.010**	**7**	**94.67**	**65**
	9	**0.055**	**2**	**97.13**	**35**
	12	0.055	12	93.03	85
	13	**0.100**	**7**	**93.85**	**75**

The experimental runs performed at current densities of 5.5. and 10 $mA.cm^{-2}$ performed very well with COD removal efficiencies above 90%. The effect of initial pH has a significant effect on the removal of COD as well. This can be seen by the experimental runs performed at an initial pH of 2 performing considerably better than at the higher pH values. This is attributed to the formation of chlorine at strong acidic conditions (pH < 3.3) as it is the strongest oxidant which can be formed in chlorinated waters (Urtiaga & Ortiz, 2009).

Mohan et al. (2007) performed a study implementing electrochemical oxidation and found that when using NaCl as a supporting electrolyte, the rate of degradation of pollutions increased with supporting electrolyte concentrations. In this study it is difficult to conclude whether increasing the NaCl concentration has a significant effect on the removal of COD, as even at the lowest molarity there have been experimental runs with sufficient COD removal (Runs 3, 4, and 6). However, the addition of NaCl is significant as it provides the addition of chloride ions in order to induce indirect oxidation (Urtiaga & Ortiz, 2009). Therefore, it can be concluded that at all electrolyte conditions the amount of NaCl is enough for the removal of COD in this study.

According to the South African National Water Act, 1998 (Act No. 36 of 1998), for wastewater to meet the requirements to be used for irrigation purposes, the limit for COD is 75 mg/L. From Figure 4-3 and Table 4-4, only four experimental runs (6, 8, 9 and 13) meet that requirement. Out of the four runs which satisfied the objective, three of which implements a current density of 10 mA/cm^2, this illustrates the formation of hydrogen bubbles being more excessive at higher current densities as described by Gonzalez-Rivas et al. (2019), thus resulting in more favourable removal efficiencies. The experimental run which obtained the highest COD removal (97.13%) was experimental run 9 at conditions of pH: 2, current density: 10 mA/cm^2, and NaCl: 0.055 M. The minimum concentration of COD at experimental run 9 was 35 mg/L.

4.4.2 Anionic Surfactant Removal

Anionic surfactants are the main constituent of most commercial detergents and soaps used in carwash garages, these are transferred into the wastewater during the car-washing process. The decay of the surfactant during the electrochemical oxidation treatment is shown in Figures 4-5 and 4-6. Both percentage removal and concentration levels (mg/l) are shown. All experimental runs were done in duplication with average values plotted.

The removal rates for the anionic surfactants range between 46.33% (Run 7) and 99.22% (Run 13). From the results displayed and based on the large range between the lowest removal and highest removal for the anionic surfactants, it is evident that the experimental conditions play a significant role.

Current density seems to play a significant role in the removal of anionic surfactants. This is notable by observing that most of the runs performed at 1 mA/cm^2 had poor anionic surfactant removal (Run 5, 7, and 11), with the lowest being 46.33% at experimental run 7. Conversely, experimental runs performed at 10 mA/cm^2 showed remarkable anionic surfactant removal efficiencies, with one exception (Run 12 – 82.63%). The other runs all displayed anionic removal efficiencies above 96%, with the highest being 99.22% at experimental run 13. Koparal et al. (2006) reported an increase in the applied current density resulted in an increase in the removal efficiency of anionic surfactants. This is consistent with the results in terms of current density in this study, therefore, it can be concluded that the current density is directly proportional to the removal efficiency of anionic surfactants.

During the direct oxidation process, hydroxyl radicals were produced on the surface of the anode. The IrO_2 coated on the surface of the electrode directly interacted with the oxygen on the surface, thus, a high valence state of IrO_3 was produced. Therefore, the two mentioned states of active oxygen are proposed to have participated in the electrochemical process to oxidize the anionic surfactants. The equations can be seen as follows (Wang et al., 2020):

$$IrO_2 + H_2O \rightarrow IrO_2(\bullet OH) + H^+ + e^- \quad \text{(Eq. 4-6)}$$

$$IrO_2(\bullet OH) \rightarrow IrO_3 + H^+ + e^- \quad \text{(Eq. 4-7)}$$

$$IrO_3 + R \rightarrow IrO_2 + RO \quad \text{(Eq. 4-8)}$$

$$2IrO_2(\bullet OH) + R \rightarrow ROO + 2IrO_2 + 2H^+ + 2e^- \quad \text{(Eq. 4-9)}$$

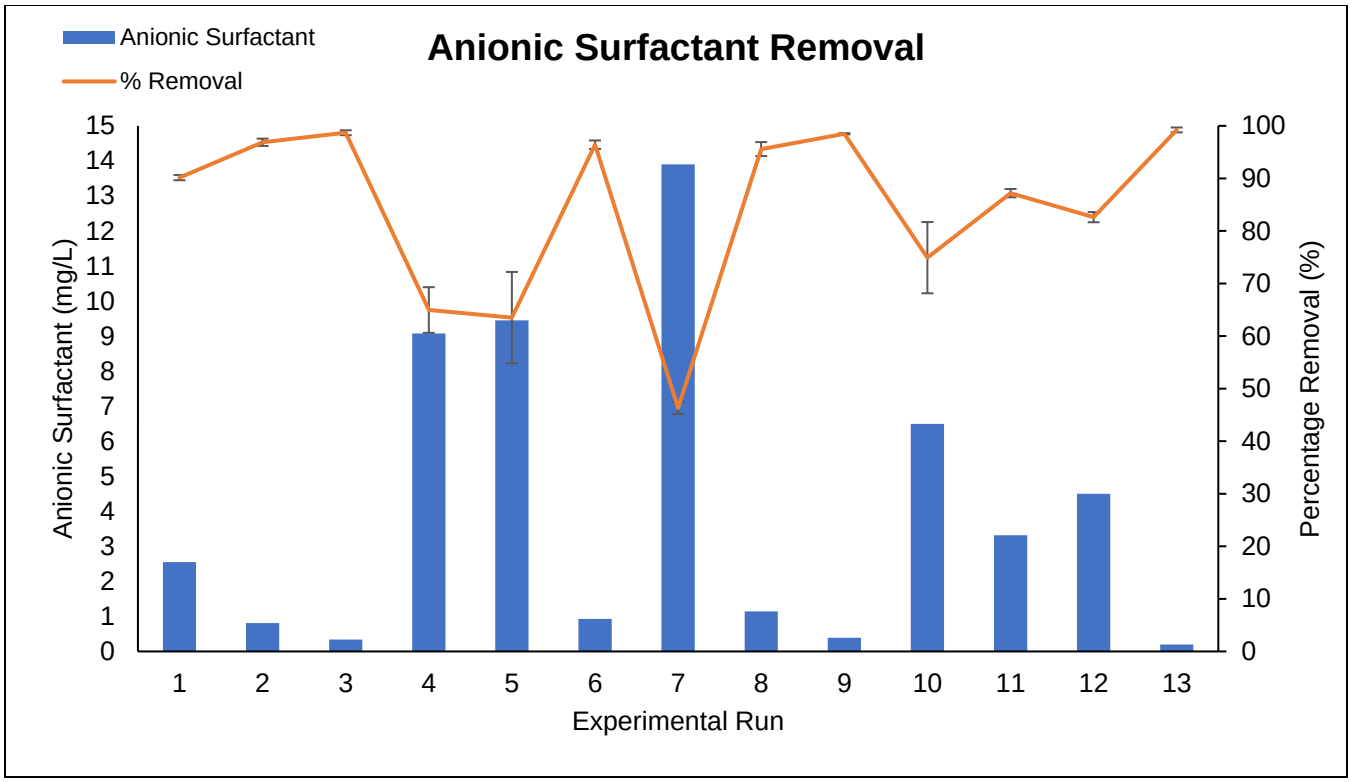

Figure 4- 5: Electrochemical Oxidation Anionic Surfactant Removal

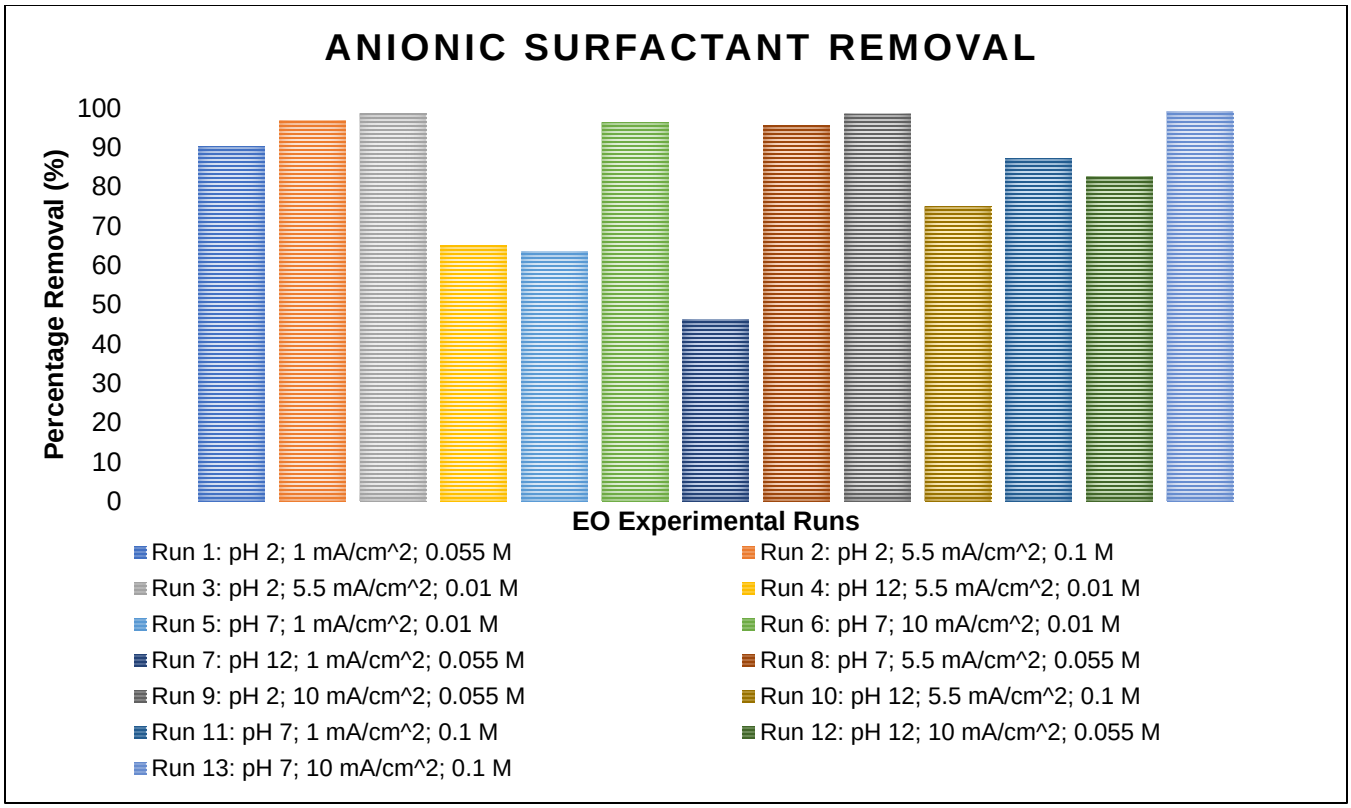

Figure 4- 6: Anionic Surfactant Conditions & Removal %

Table 4- 5: Surfactant Results Summarized

Current Density $mA.cm^{-2}$	Experimental Run	Electrolyte (NaCl) M	pH	Average Surfactant percentage removal	Surfactant effluent concentration level (mg/L)
1	1	0.055	2	90.15	2.550
	5	0.010	7	63.51	9.450
	7	0.055	12	46.33	13.90
	11	0.100	7	87.20	3.315
5.5	**2**	**0.100**	**2**	**96.87**	**0.810**
	3	**0.010**	**2**	**98.69**	**0.340**
	4	0.010	12	64.96	9.075
	8	**0.055**	**7**	**95.58**	**1.145**
	10	0.100	12	74.92	6.495
10	**6**	**0.010**	**7**	**96.41**	**0.930**
	9	**0.055**	**2**	**98.49**	**0.390**
	12	0.055	12	82.63	4.500
	13	**0.100**	**7**	**99.23**	**0.200**

The removal of anionic surfactants is strongly dependent on the initial pH. This is apparent as at a pH value of 2, the removal of anionic surfactants are all above 90% (R1 – 90.15%, R2 – 96.86%, R3 – 98.69%, and R9 – 98.49%), while at a pH value of 12 very poor anionic surfactant removal efficiencies were obtained, with the lowest being 46.33% at run 7 and highest at run 12 with a removal efficiency of 82.63%. At the pH value of 7 it is difficult to conclude as it ranges from 63.51% at run 5, to 99.23% at run 13, however, the effects of the other parameters should be considered as well. Gu et al. (2006) found that the removal of anionic surfactants was favoured at lower pH values and their findings are consistent with the results presented in this study. The reason for high anionic surfactant removal observed at lower pH values is due to the chlorine evolution reaction being favoured (Czarnetzki & Janssen, 1992; Scialdone et al., 2009). Chlorine is the oxidant formed at such strong acidic conditions, according to Urtiaga & Ortiz, (2009) it is the strongest oxidant which can be formed in chlorinated waters, therefore it explains why such high removal efficiencies were observed at the pH value of 2.

The effect of electrolyte molarity does not seem to have a significant effect on the removal of anionic surfactants when it is adjusted. This can be observed from run 2 and 3, having the same conditions except for electrolyte molarity (R2 – 0.1 M; R3 – 0.01 M). Run 3 has a slightly higher removal efficiency of 98.69%, compared to 96.87% of run 2. Since there is no significant difference between the two runs, it can be concluded that the removal of anionic surfactants is more dependent on current density and the effect of initial pH than varying the electrolyte molarity, however, the addition of the electrolyte is significant as in the presence of chloride ions oxidation is optimized (Deng & Englehardt, 2015; Panizza et al., 2005).

To meet the requirements for the irrigation with wastewater, according to the South African National Water Act, 1998 (Act No. 36 of 1998) the limit for anionic surfactants is 2.5 mg/L. From Figure 4-5 it can be observed that six experimental runs meet the requirements according to the National Water Act. Those 6 experimental runs are 2, 3, 6, 8, 9, and 13. The experimental run which obtained the highest anionic surfactant removal (99.22%) was experimental run 13 with conditions of pH: 7, current density: 10 mA/cm^2, and 0.1 M using NaCl. The anionic surfactant concentration of experimental run 13 was found to be 0.2 mg/L.

4.4.3 Turbidity Removal

Figure 4-7 shows the percentage removal of turbidity for the electrochemical oxidation experiments performed in this study.

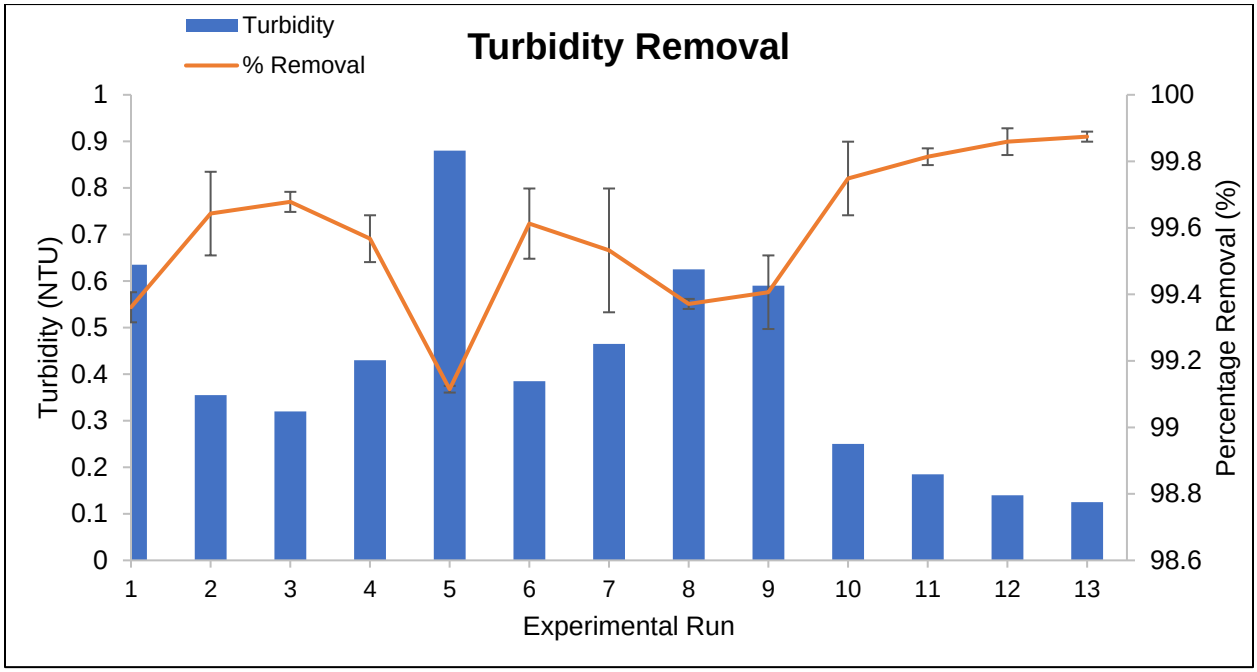

Figure 4- 7: Electrochemical Oxidation Turbidity Removal

Turbidity was not declared a major pollutant as in the pre-treatment process where the removal of turbidity was above 95%. It can therefore be concluded that the removal efficiency of turbidity is sufficient for all experimental conditions. Juárez et al. (2015) performed a combined process of electrocoagulation and electrochemical oxidation for the treatment of carwash wastewater with a turbidity percentage removal was 98.4. According to Sarmadi et al. (2020), combined processes are the most attractive option for the remediation of carwash wastewater. This is proven in this study where the coagulation process removed the suspended solids which contributed to the high turbidity of the carwash wastewater, therefore, electrochemical oxidation further removed most of the remaining suspended particles in solution.

4.4.4 Fat, oil and Grease (FOG) Removal

FOG does not mix with water, and when CWW that contain FOG are disposed of in the water sources without treatment, the FOG portion of the water can float to the surface and solidify, causing environmental problems.

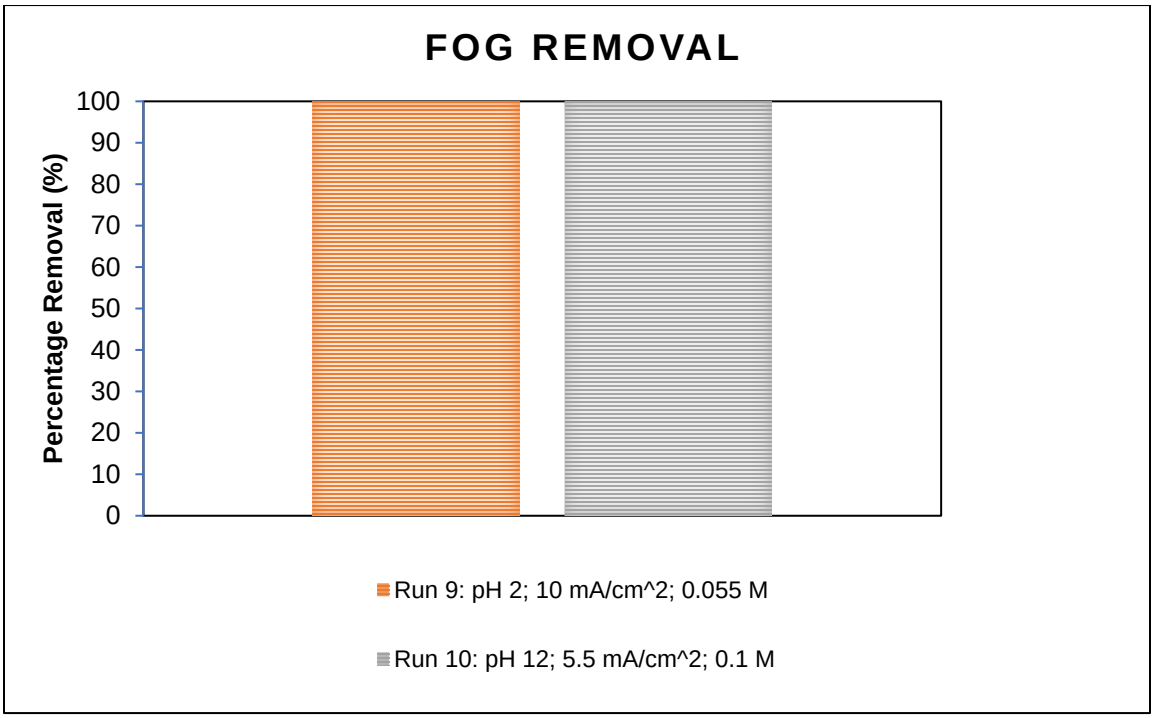

Figure 4- 8: EO FOG Removal

Almost 100% of the FOG has been removed during the PAC coagulation process as pre-treatment. For this reason, random FOG analysis was performed on two pre-selected electrochemical oxidation samples to confirm complete removal. The EO experimental runs considered were experimental runs 9 and 10. In Figure 4-8 it is shown that both conditions achieved 100% FOG removal. Juárez et al. (2015) concur and reported 100 percent FOG removal after an integrated EC-EO treatment process of carwash wastewater. Bhatti et al. (2011) reported 96% removal of oil from carwash wastewater after implementing a multiple treatment process which included aeration, coagulation and chemical oxidation. This shows that the statement made by Sarmadi et al. (2020) is accurate as many favourable results are reported for the remediation of carwash wastewater using hybrid processes.

4.4.5 COD and Surfactant removal comparison

COD and anionic surfactant percentage removal during the electrochemical oxidation process are compared in Figure 4-9. The Manhattan like chart (anionic surfactant) follows the same trend as the line chart (COD), where the increase and decrease at the same experimental conditions, are similar.

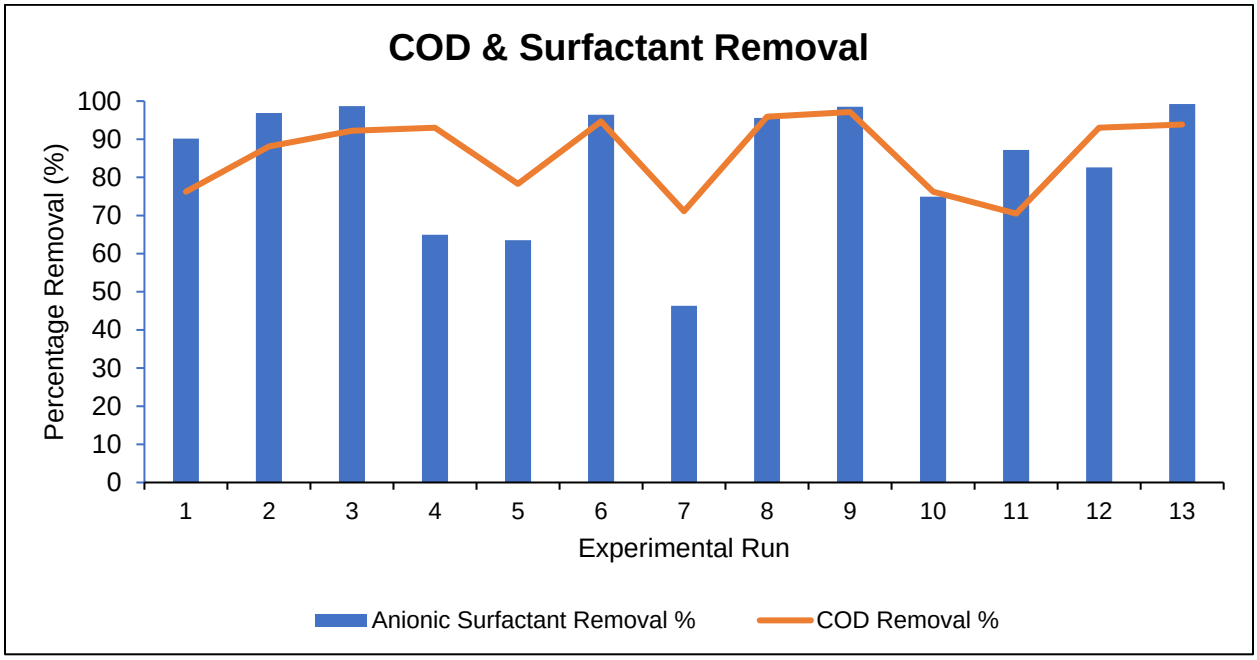

Figure 4- 9: Electrochemical Oxidation COD and Anionic Surfactant Comparison

The discharge limit for wastewater into water resources, is 75 and 2.5 mg/L for COD and anionic surfactants, respectively. Table 4-6 summarises the experimental runs (6, 8, 9 and 13) which comply with the COD and anionic national discharge standards. Direct oxidation (on the surface of the anode) is proposed for the favourable results observed at higher current densities, while indirect oxidation is the proposed mechanism which takes place at the lower pH (evolution of strong oxidant: chlorine), however, it is possible that both mechanisms can occur, as described by Wang et al. (2020). This is apparent as in Run 9 (pH: 2, CD: 10 mA/cm^2) very high removal efficiencies were achieved for COD (97.13%) and anionic surfactants (98.49%). This indicates both direct and indirect oxidation occurred in experimental run 9.

Table 4- 6: Experimental Runs which comply with discharge standards

	Removal			
	COD		Anionic Surfactants	
Run No	%	Value (mg/L)	%	Value (mg/L)
6	94.67	65	96.41	0.930
8	95.90	50	95.58	1.145
9	97.13	35	98.49	0.390
13	93.85	75	99.23	0.200

4.5 Energy Consumption

Figure 4-10 displays the specific energy consumption vs current density. The highest removal rates for COD and anionic surfactants are displayed at the specific current density with the corresponding energy consumption.

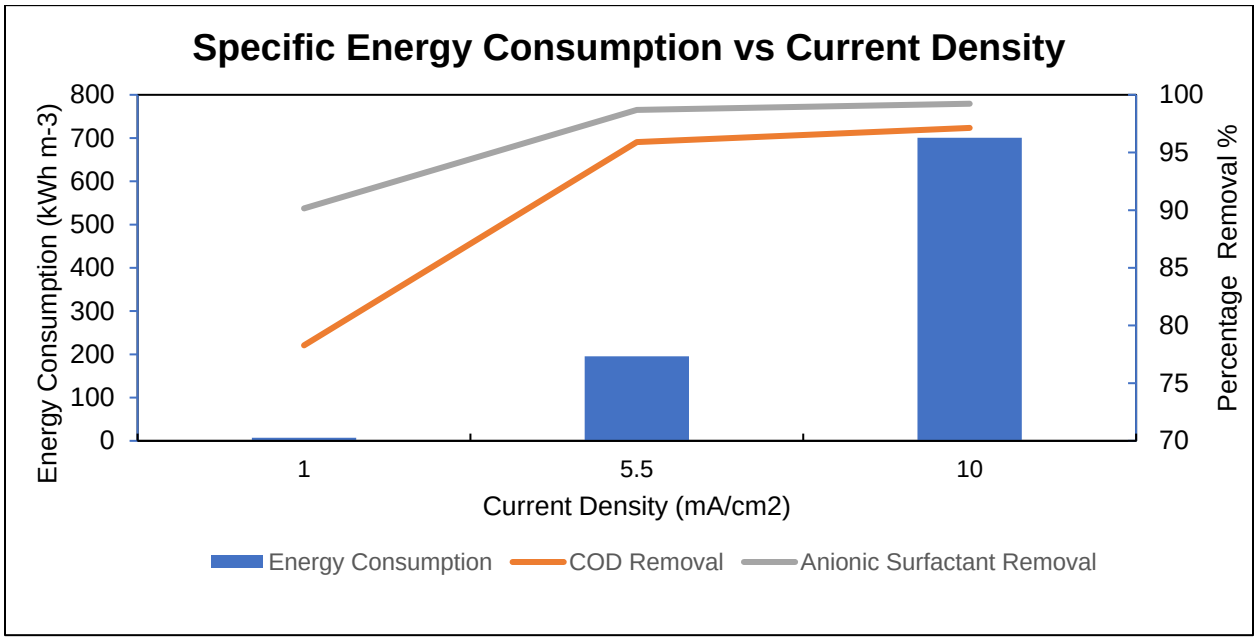

Figure 4- 10: Specific Energy Consumption vs Current Density

Panizza & Cerisola (2010) reported that increasing the applied current increases the energy consumption as well, which is clear from Figure 4-10. While 1 mA/cm^2 shows the lowest energy consumption, the removal for COD and anionic surfactants is not enough to meet the objectives of this study. The current density at 10 mA/cm^2 shows the most favourable results when looking at the removal percentage. However, the extremely high energy consumption of 700.8 kWh m^{-3} is of great concern. There is no drastic difference between the removal of COD and anionic surfactants between 5.5 & 10 mA/cm^2, but the difference in energy consumption is quite significant. The current density almost doubles, but the energy consumption increases 4 times (10 mA/cm^2 – 700.8 kWh m^{-3}; 5.5 mA/cm^2 – 195.36 kWh m^{-3}). Therefore, it can be deduced, that the optimal current density was found to be 5.5 mA/cm^2 with a corresponding 195.36 kWh m^{-3} specific energy consumption. According to Deng & Englehardt (2015), 5 mA/cm^2 is the minimum current density required to achieve effective oxidation of organics, thus the findings reported here concur with the statement made by those authors.

4.6 Instantaneous Current Efficiency

Instantaneous current efficiency (ICE) is a term used to measure the amount of current intensity on the destruction of pollutants. COD is the pollutant to be investigated with the ICE formula (Chapter 2) as follows:

$$\%ICE = FV\left(\frac{[COD]_0 - [COD]_t}{8I\Delta t}\right) x\ 100 \qquad (Eq.\ 4-10)$$

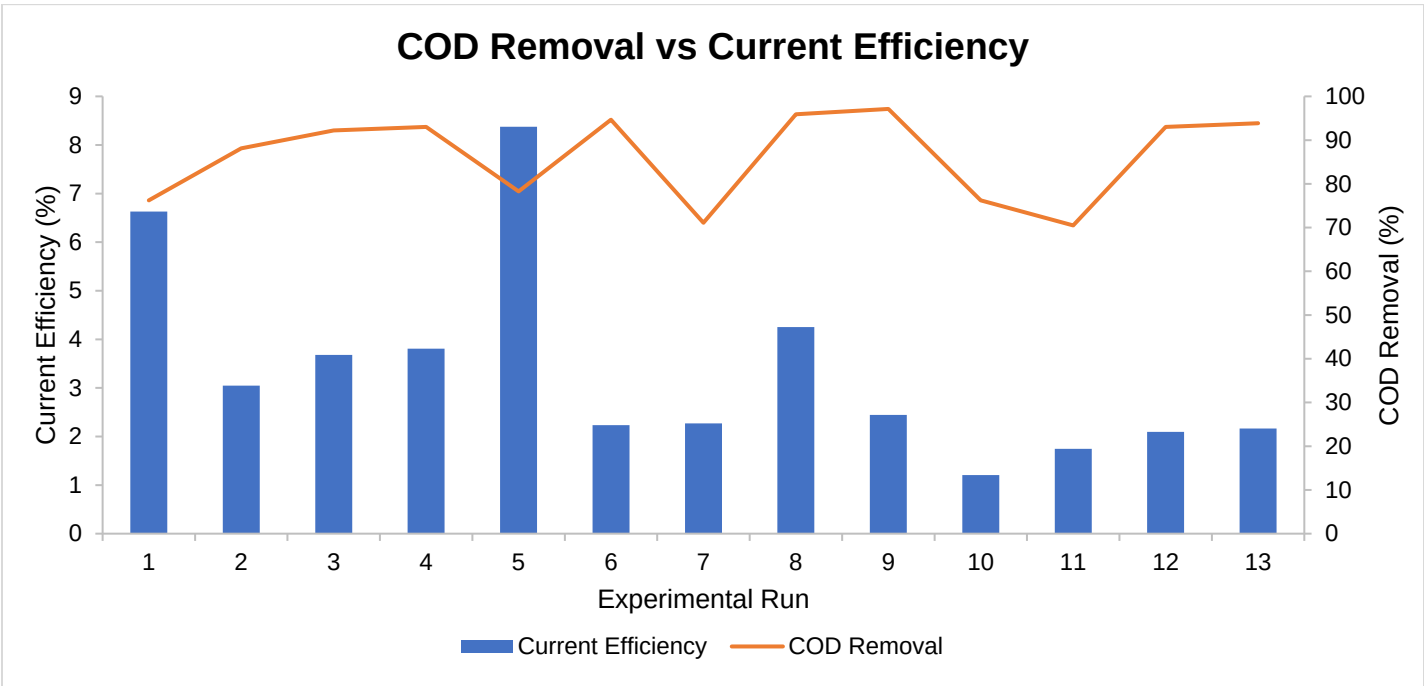

Figure 4- 11: COD Removal vs Current Efficiency

Figure 4-11 shows the COD removal and the current efficiency at each electrochemical oxidation experimental run plotted on the same chart. It is apparent that the most efficient experimental runs were at the lower current densities with the worst COD removal. Experimental run 5 achieved the highest current efficiency of 8.38%, but the COD removal efficiencies were much lower than expected. Panizza & Cerisola (2010) compared PbO_2 & BDD to treat carwash wastewater. For PbO_2 at the end of 8 hours the current efficiency was approximately 3%, while in the case of BDD after 5 hours it was around 5%. These values are consistent with the current efficiencies at the end of the electrochemical oxidation processes.

Photograph 4- 3: Initial, Coagulation, and Electrochemical Oxidation

Photograph 4-3 shows (from left to right) Initial (feed), pre-treated (CC) carwash wastewater, and final treated (EO) carwash wastewater.

Chapter 5:

Optimization using RSM

Chapter 5: Optimization using Response Surface Methodology (RSM)

5.1 Introduction

This chapter deals with the design of the experiments using the software package called Design Expert. Response surface methodology (RSM) is a collection of mathematical and statistical techniques based on the fit of a polynomial equation to the experimental data with the objective of statistically predicting and understanding the system's behaviour (Bezerra et al., 2008). It was used to statistically analyze the data and to develop statistical models that can be used to fully understand the individual effects and the interactions between the independent variables. Based on the dependent and independent variables and constraints identified, the model was selected to depict the outputs of the EO process. The aim was to predict the response of COD and anionic surfactant removal and to optimize the process to achieve the desired outcomes. The BBD model was applied considering the number of factors and levels at which these factors were required to be tested.

5.2 EO performance predicted using RSM and BOX Behnken Design (BBD)

The Box-Behnken Design (BBD) was used in this study. It is a quadratic design approach where each factor can be tested on three levels, only. The BBD default setting reduces average prediction variances, resulting in the development of a robust model with outstanding prediction characteristics. The model investigated the influence of pH (A), current density (B) and electrolyte molarity (C) on the EO process using COD and anionic surfactant removal. The experimental results in this study indicated that the removal of these pollutants was significantly affected by these parameters. The interaction of the parameters is discussed in this section for both COD and anionic surfactant removal.

5.2.1 Chemical Oxygen Demand

The design matrix indicating experimental run order and output data for the BDD can be seen in Table 5-1. The data obtained from the 26 experiments that were conducted was used to develop a polynomial quadratic equation, as shown in Equations 5-1 in terms of coded factors.

Table 5- 1: Box-Behnken Design output results for COD removal

	Factors			COD Removal (%)	
Run	A: pH	B: CD (mA/cm^2)	C: NaCl (M)	Experimental Value	Predicted Value
1	2	1	0.055	77.05	76.84
2	2	1	0.055	75.41	76.84
3	2	5.5	0.1	86.89	89.42
4	2	5.5	0.1	89.34	89.42
5	2	5.5	0.01	90.98	90.44
6	2	5.5	0.01	93.44	90.44
7	12	5.5	0.01	93.44	91.72
8	12	5.5	0.01	92.62	91.72
9	7	1	0.01	81.97	79.43
10	7	1	0.01	74.59	79.43
11	7	10	0.01	95.08	96.59
12	7	10	0.01	94.26	96.59
13	12	1	0.055	69.67	71.25
14	12	1	0.055	72.54	71.25
15	7	5.5	0.055	96.72	95.9
16	7	5.5	0.055	95.08	95.9
17	2	10	0.055	95.9	96.97
18	2	10	0.055	98.36	96.97

19	**12**	**5.5**	**0.1**	**75.41**	**77.99**
20	**12**	**5.5**	**0.1**	**77.05**	**77.99**
21	**7**	**1**	**0.1**	**69.26**	**68.57**
22	**7**	**1**	**0.1**	**71.72**	**68.57**
23	**12**	**10**	**0.055**	**94.26**	**92.41**
24	**12**	**10**	**0.055**	**91.8**	**92.41**
25	**7**	**10**	**0.1**	**92.62**	**92.69**
26	**7**	**10**	**0.1**	**95.08**	**92.69**

The reliability, quality and accuracy of the fitted quadratic model were evaluated using analysis of variance (ANOVA), as shown in Table 5-2.

$$\text{COD Removal \%} = 95.9 - 2.53625A + 10.32187B - 3.68813C + 0.25625AB - 3.17625AC + 1.7425BC - 4.22625A^2 - 7.3B^2 - 4.2775C^2$$

Equation 5-1

The experimental and predicted values of COD removal for the 26 experiments presented in Table 5-1, where the results clearly indicated that a maximum COD removal of 98,36% was achieved with experiment 18, at pH, current density and electrolyte molarity of 2, 10 mA/cm^2 and 0.055 M, respectively. A close correlation between experimental and predicted values were found when a fair agreement was reached for the R^2 predicted.

The analysis of variance was used to evaluate the determination coefficient, lack of fit and the importance of the linear, quadratic and interaction effects on the response of the independent variables. The p-value was used to determine the significance of the coefficient and the interaction strength of the combined factors.

The significance of the models is confirmed by high F-values and low p-values (Sun et al., 2016). The models were significant as confirmed by low probability values of less than 0.0001 and high F-values of 44.58 for COD removal efficiency. The reported F-values imply that there is only a 0.01% chance that their difference could be due to noise. For this study, the lack of fit for the model was insignificant, which shows that the data fitted the model well.

Fit statistics are also shown in Table 5-2 where the coefficient of determination R^2 is a statistical parameter that measures how well the data fits the line. Adjusted R^2 is a version of R^2 that is always smaller than $R^{2,}$ and predicted R^2 measures the predictive accuracy of the model. A model is considered well fitted when the R^2 value is greater than 0.8 (Najib et al., 2017). R^2, adjusted R^2, and predicted R^2 were found to be 0.9616, 0.9401, and 0.9010 for COD efficiency removal. For this study, predicted and adjusted R^2 agreed with this. Adequate precision measures the signal-to-noise ratio, and a ratio greater than 4 is desirable. The value of adequate precision was 18.784 COD efficiency removal, which indicates an adequate signal.

Table 5- 2: Analysis of variance (ANOVA) of the quadratic model for COD removal

Analysis of Variance Table [Partial sum of squares – Type III]					
Source	**Sum of Squares**	**Degree of freedom**	**Mean Square**	**F-Value**	**p-value Prob > F**
Model	2385.23	9	265.03	44.58[1]	< 0.0001[1]
A - pH	102.92	1	102.92	17.31	0.0007[1]
B – Current Density	1704.66	1	1704.66	286.71	< 0.0001[1]
C - Electrolyte	217.64	1	217.64	36.61	< 0.0001[1]
AB	0.53	1	0.53	0.088	0.7701[2]
AC	80.71	1	80.71	13.57	0.0020[1]
BC	24.29	1	24.29	4.09	0.0603[2]
A^2	81.65	1	81.65	13.73	0.0019[1]
B^2	243.61	1	243.61	40.97	< 0.0001[1]
C^2	83.64	1	83.64	14.07	0.0017[1]
Residual	95.13	16	5.95	-	-
Lack of Fit	40.94	3	13.65	3.27[2]	0.0556[2]
Pure Error	54.19	13	4.17	-	-
Cor Total	2480.36	25	-	-	-
Standard deviation	2.44	-	-	R-squared	0.9616
mean	86.17	-	-	Adjusted R-squared	0.9401
Coefficient of variance %	2.83	-	-	Predicted R-squared	0.9010

[1] Significant; [2] Not Significant

A. Validation of Model (COD)

After the regression model was developed, the fitted model was tested to ensure that it provided an accurate approximation to the real system. Three types of model diagnostics were used for verification, namely: the normal, residual and predicted vs experimental plot.

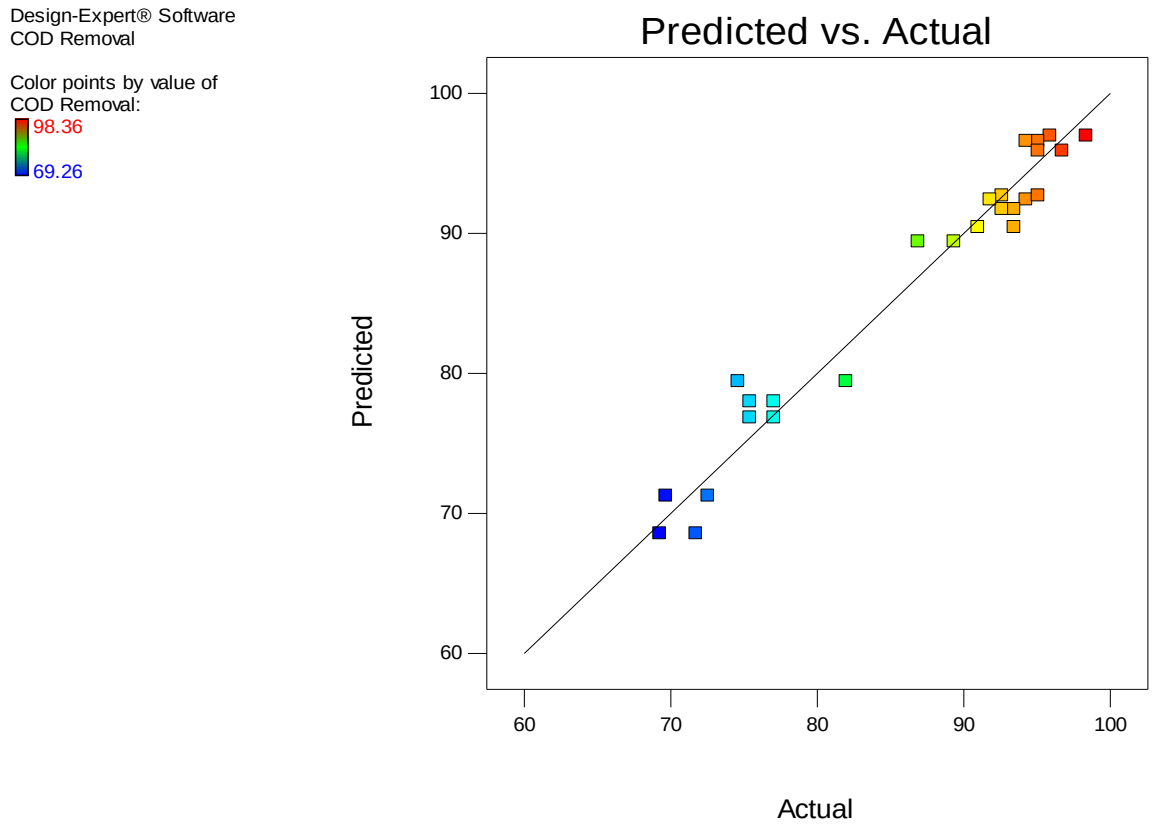

Figure 5- 1: Predicted vs experimental COD removal values

Figure 5-1 shows a plot of predicted vs. actual values for the COD % removal in this study. Essentially what this graph indicates is, if the point lies on the diagonal line, the predicted value is the same or very close to the actual value. As seen from figure 5-1, all the points are very close to the diagonal line which gives an indication that the model used is significant and quite accurate for the predictions made. According to Zainal-abideen et al. (2012), predicted vs actual plots assist in judging whether the model is satisfactory or not. Figure 5-1 indicates an adequate agreement between experimental data and the outputs of the model.

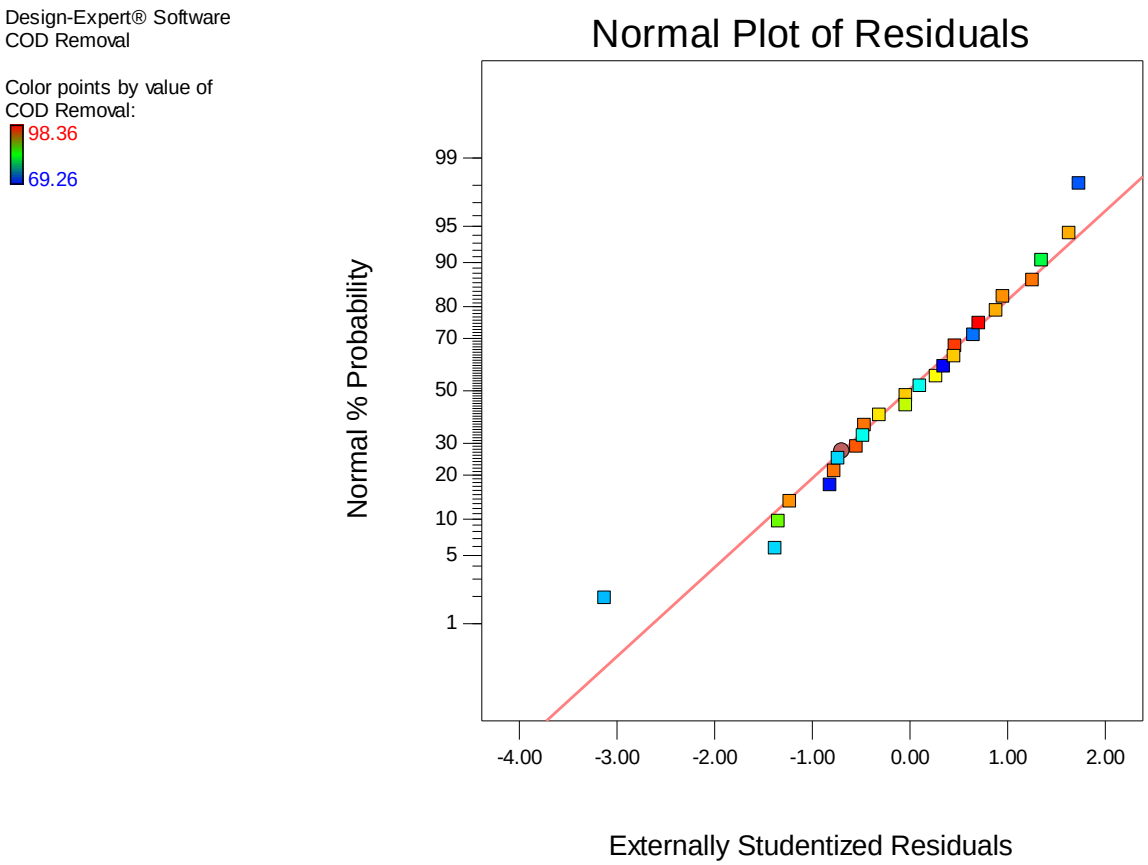

Figure 5- 2: Normal Plot of Residuals

Figure 5-2 shows a normal plot of residuals graph for the COD data generated in this study. Zhang et al. (2011) states that if the points on the plot follow a straight line the residuals are normally distributed. According to Montgomery (2013), the plot of normal % probability vs residuals will resemble a straight line if the underlying error distribution is normal, as shown in figure 5-2 the points for the most part resemble a straight line, therefore, the underlying error distribution can be said to be normal for the COD data.

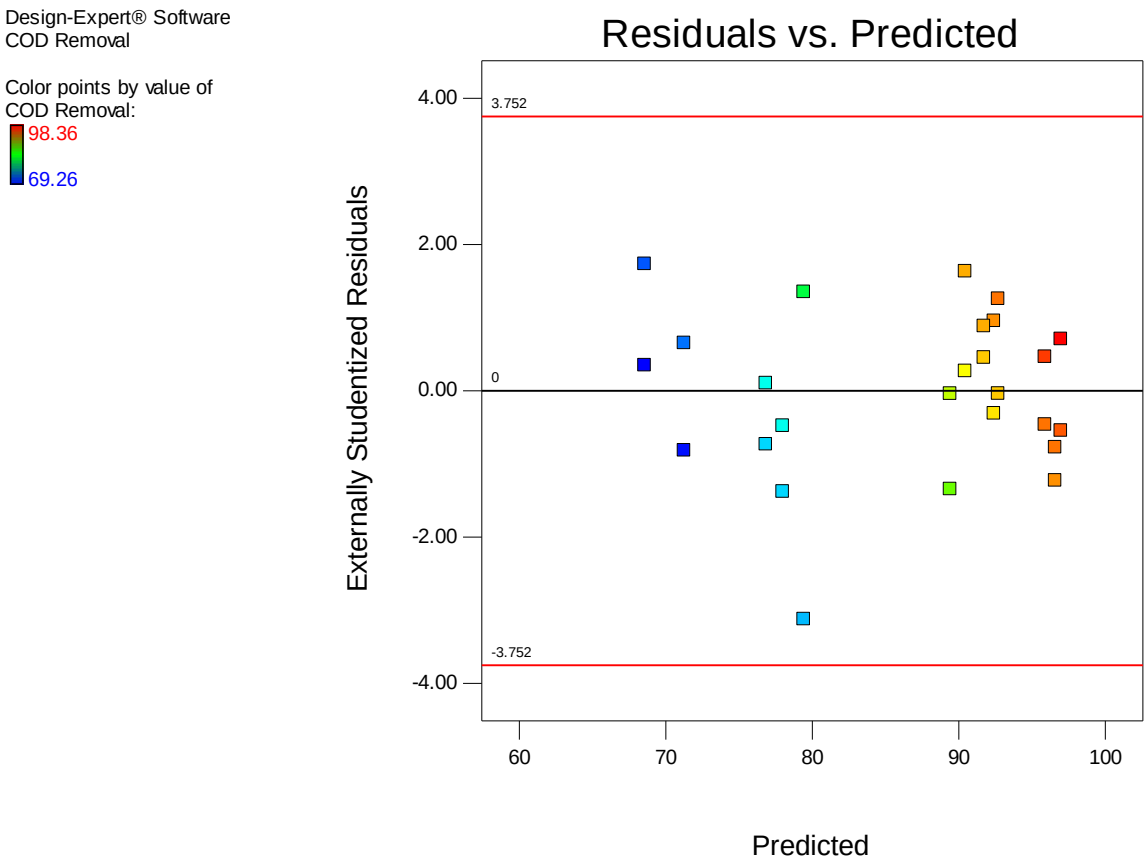

Figure 5- 3: Plot of externally studentized residuals vs predicted response (COD)

The residuals vs. predicted graph for the COD data can be seen in figure 5-3. According to Montgomery (2013), an indication that the model is correct is that there is no obvious pattern or structure shown by the residuals. From figure 5-3 it can be seen that it is in accordance with the statement made by the author as the points are all scattered randomly.

B. Analysis of Response (COD)

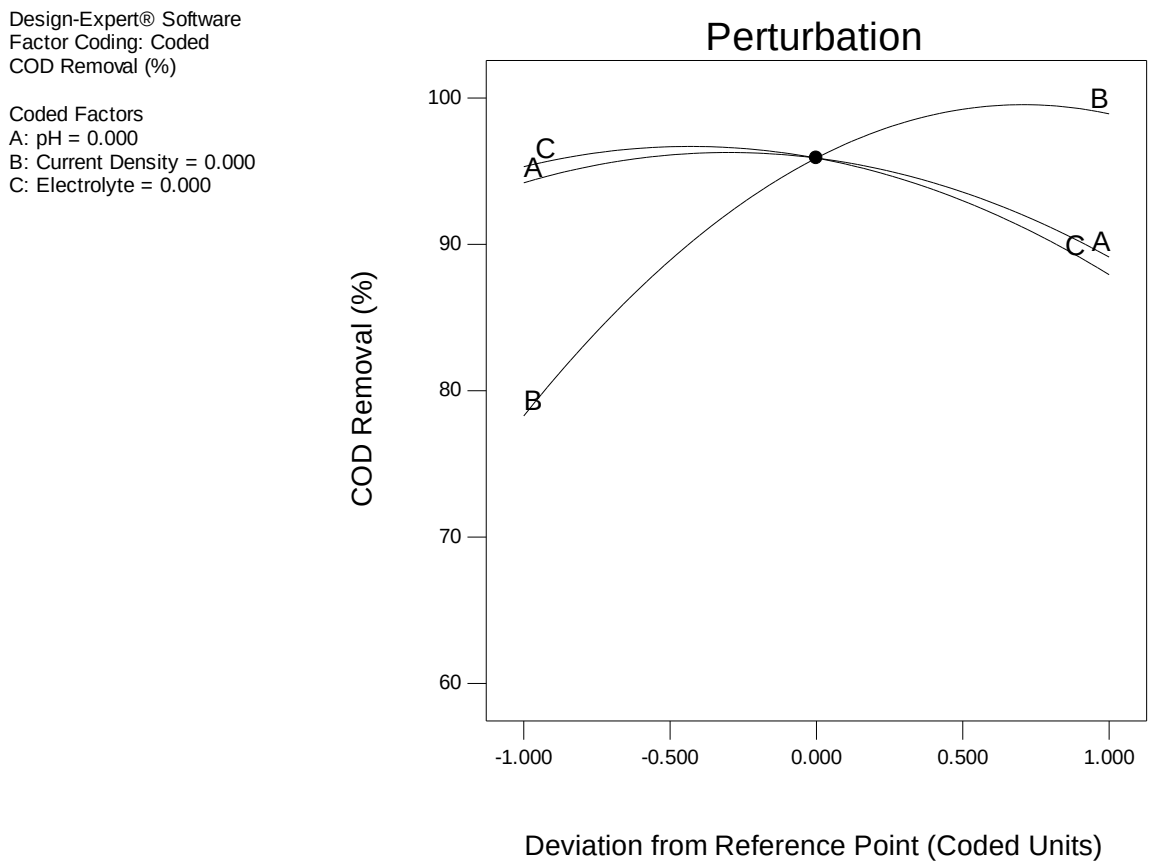

Figure 5- 4: COD Perturbation

The Perturbation plot for COD data can be seen in figure 5-4. Kusuma & Mahfud (2016) states that a Perturbation plot compares all factors at a selected point in the design space. The factors considered in figure 5-4 are pH, current density and electrolyte molarity on removal of COD. The reference point (black dot) is the centre points for the three factors. This graph indicates that the factor A (pH) has the highest COD removal at the coded unit – 1. This suggests that the most favourable COD removal occurs at the lowest pH value in the design space. The plot clearly indicates the most influential factor among the three factors is factor B (current density). The most favourable COD removal percentage was found at the coded factor + 1, significantly higher than at the coded unit – 1. Therefore, it can be concluded that COD removal is proportional to current density. Factor C (electrolyte molarity) indicates the most favourable COD removals occur at the – 1 coded unit, however, the factor with the most influence on the COD removal is current density.

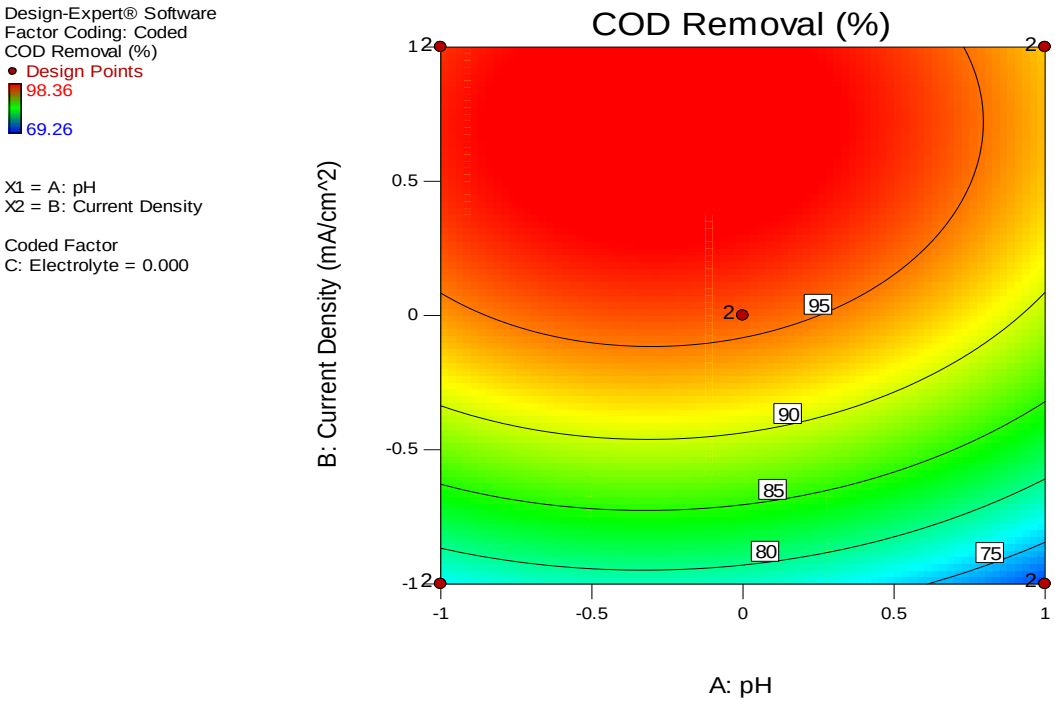

Figure 5- 5: COD Contour (pH & Current Density)

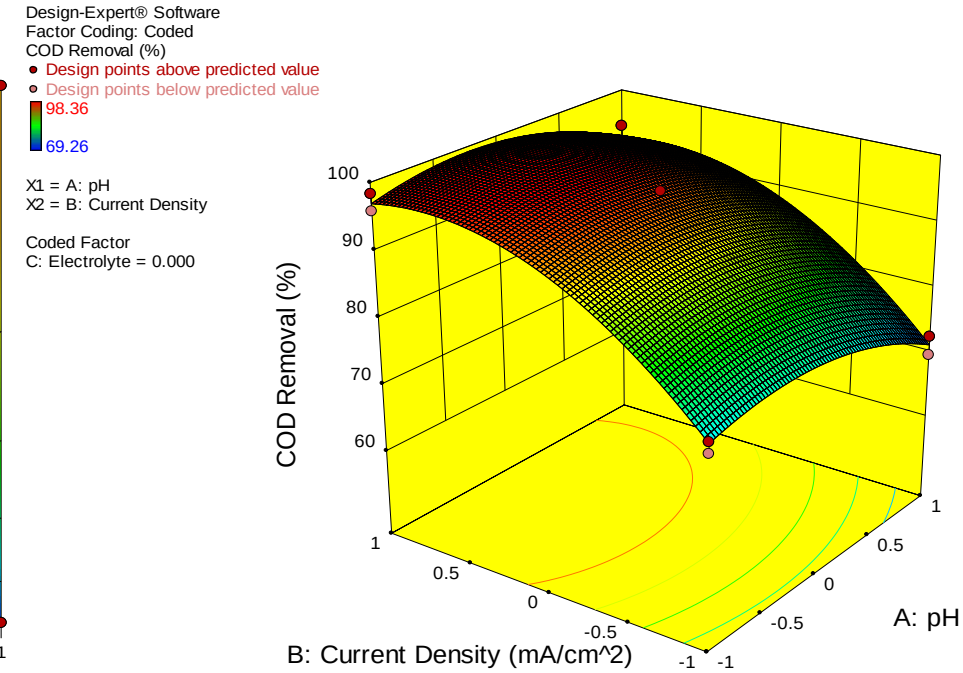

Figure 5- 6: COD 3D (pH & Current Density)

Figure 5-5 and 5-6 shows the contour and 3D graphs for the factor's pH and current density, with the electrolyte being constant, so that the relationship between factors A and B can be determined. It can be seen from the graphs that lower pH values and high current densities are needed to achieve optimal COD removal efficiencies. Current density seems to play a critical role in achieving high COD removal, however, this is not maintained at high pH as it can be seen from figure 5-6. Thus, it can be concluded that current density is directly proportional to COD removal and pH is inversely proportional to the removal of COD. Therefore, ideal coded factors are +1 for current density & - 1 for pH. In terms of actual factors, it converts to a current density of 10 mA/cm^2 and a pH of 2, to obtain optimal COD removal. The high COD removals is attributed to Cl_2 being the active chloro species at low pH values (<3.3) as it is a strong oxidant (Urtiaga & Ortiz, 2009).

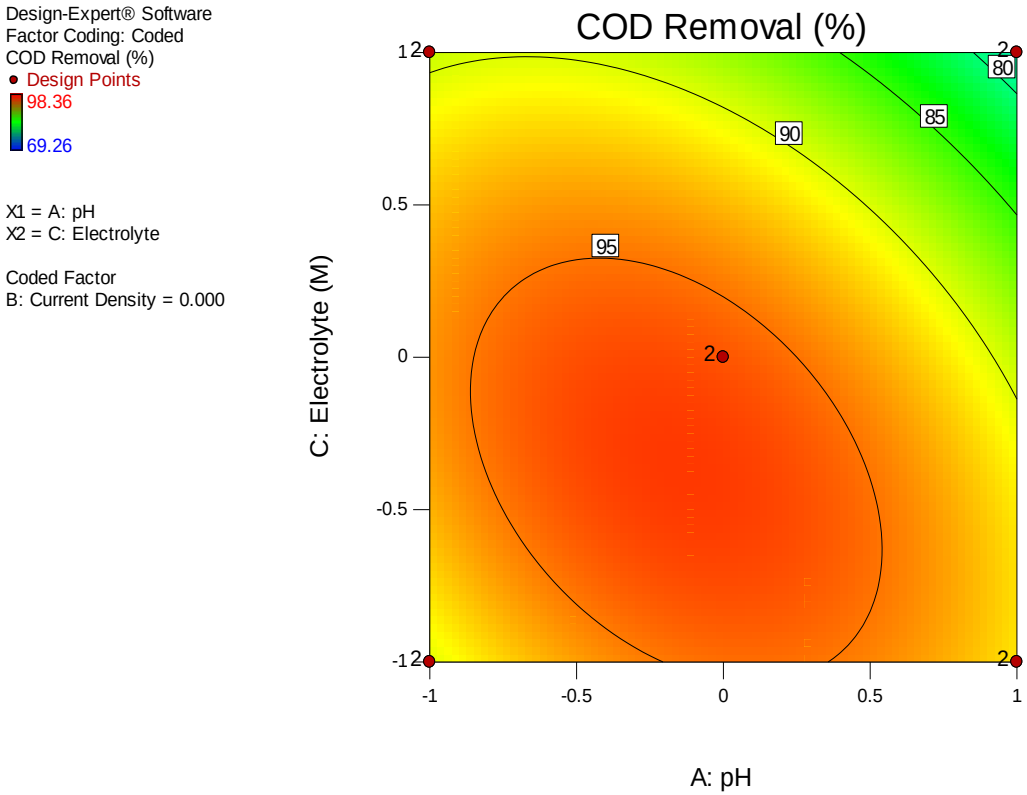

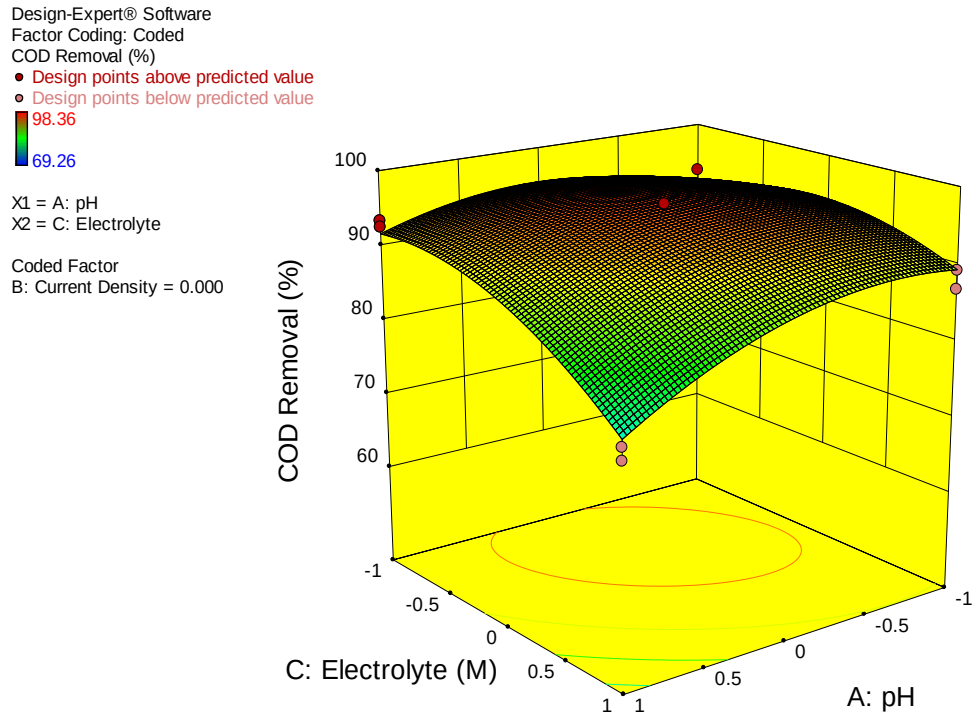

Figure 5- 7: COD Contour (pH & Electrolyte)

Figure 5- 8: COD 3D (pH & Electrolyte)

Figures 5-7 and 5-8 are the contour and 3D graphs for the factors A (pH) and C (electrolyte), with factor B (current density) staying constant at the coded factor of 0. Between the compared factors, the graphs suggest that the most influential factor between the two is the pH. This can be seen by figure 5.7, at coded factors +1 for pH & electrolyte molarity, the COD removal is around 80%, however as the pH level decreases there is a significant change in the COD removal, reaching up to 95%. Optimal COD removal for the factors are approximately – 0.75 < pH < + 0.5 and -1 < Electrolyte < + 0.4 in terms of coded factors. This converts to the actual factors of 3.25 < pH < 9.5 and 0.01 M < electrolyte < 0.073 M. The 3D graph takes the shape of a maximum point, as described by Montgomery, (2013).

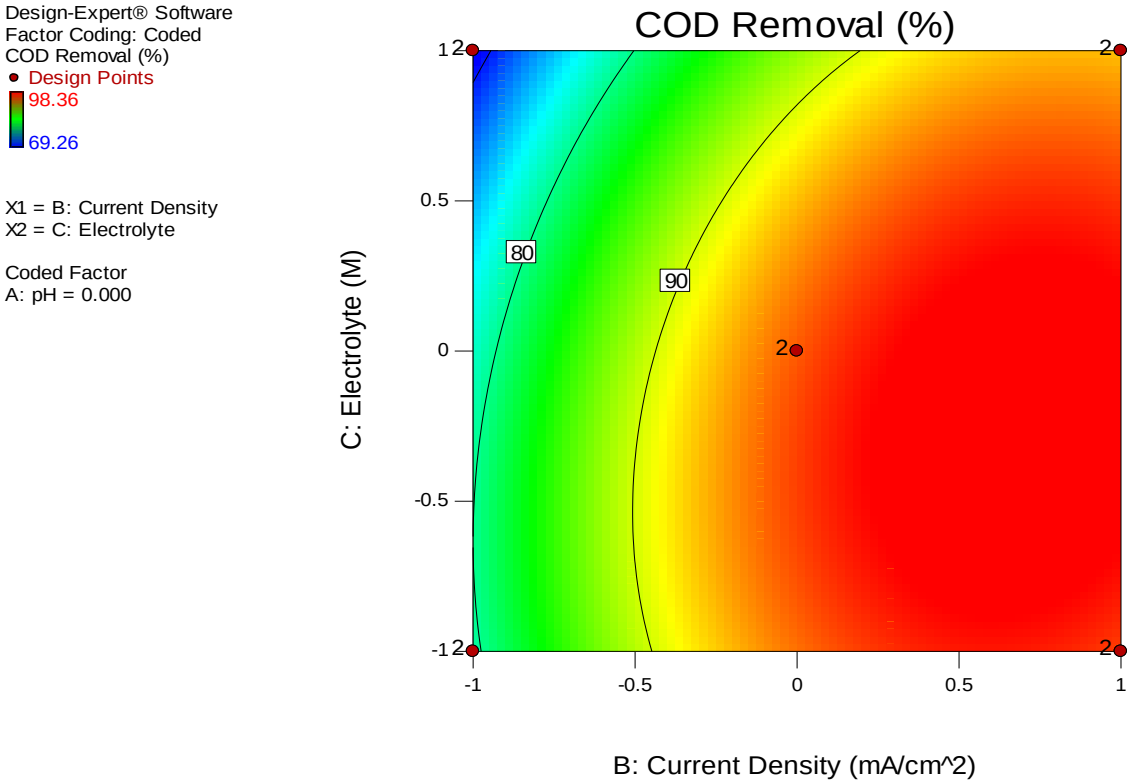

Figure 5- 9:COD Contour (Current Density & Electrolyte)

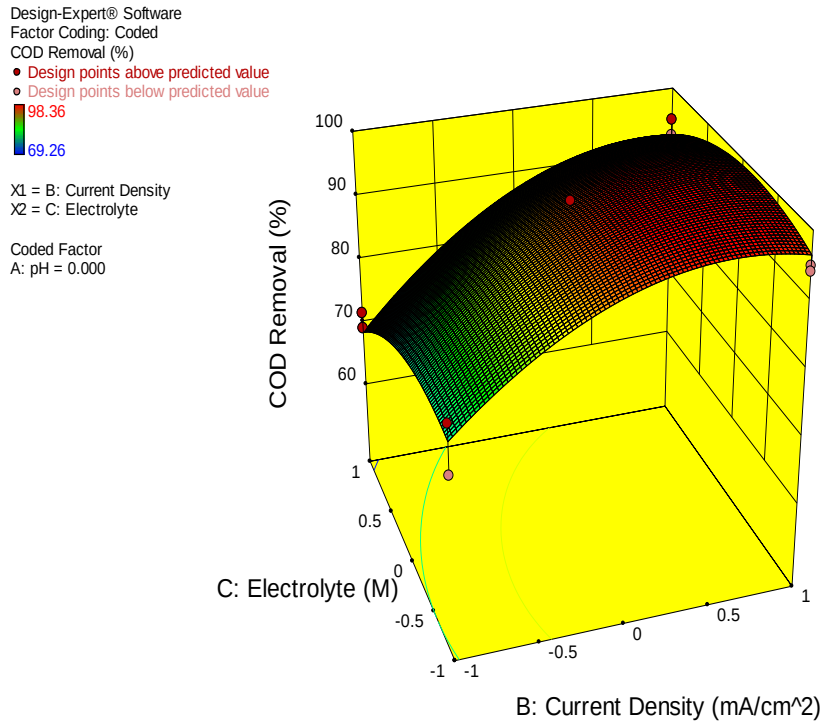

Figure 5- 10: COD 3D (Current Density & Electrolyte)

Figures 5-9 and 5-10 displays the contour and 3D graphs for the factors B (current density) and C (electrolyte), with pH staying constant at its centre point. Between the two factors, the driving force for COD removal is current density. This is clearly illustrated by figure 5-10, COD removal is proportional to the increase in current density and the electrolyte molarity does not seem to be that influential. At the highest level for current density, COD removal is close to 100 percent for all levels of electrolyte molarity, therefore, it can be concluded that the most influential factor between these two is current density. Optimal COD removal is achieved at a current density of 10 mA/cm^2 for the ranges of 0.01 M < Electrolyte < 0.1 M. Panizza & Cerisola (2010) found that optimal results were found at higher current densities and that's consistent with the results illustrated in figure 5-10.

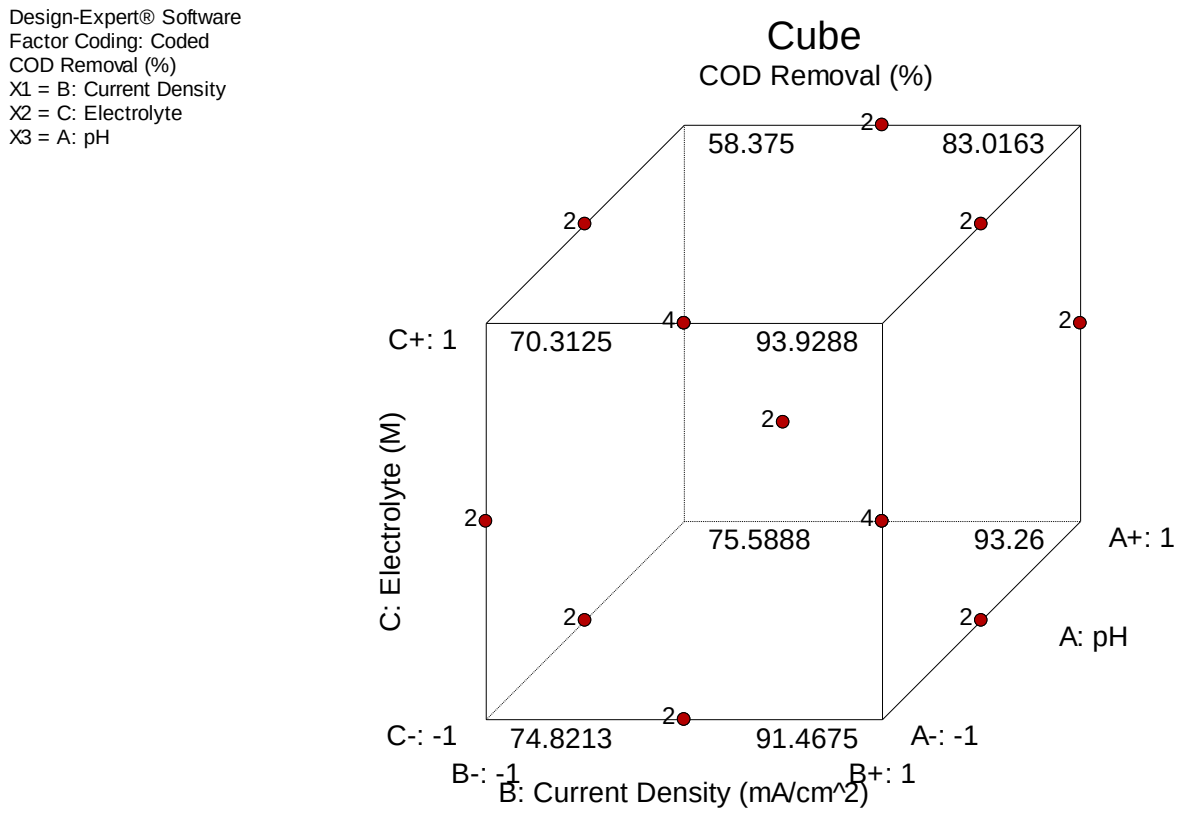

Figure 5- 11: COD Box Behnken

Figure 5-11 shows the cube generated by the Design Expert software for the removal of COD for the factors pH, current density and electrolyte molarity. The cube illustrates that the most influential factor for COD removal is current density, followed by pH. Electrolyte molarity does not seem to be a critical factor in this instance. Operating conditions to achieve optimal COD removal are high current density, low pH, and low electrolyte molarity. According to figure 5-11, 93.93% of COD removal is obtained at the factors, pH -1 and current density + 1. This converts to actual factors of 10 mA/cm^2 for current density, at a pH of 2. As discussed in chapter 4, with regards to the COD results, favourable conditions were found in literature at low pH and high current densities (Urtiaga & Ortiz, 2009; Panizza & Cerisola, 2010a).

5.2.2 Anionic Surfactant Model

The design matrix for BBD can be seen in table 5-3 for the anionic surfactant data.

Table 5- 3: Anionic Surfactant Predicted vs Actual

	Factors			Anionic Surfactant Removal (%)	
Run	**A: pH**	**B: CD (mA/cm^2)**	**C: NaCl (M)**	**Experimental**	**Predicted**
1	**2**	**1**	**0.055**	**90.66**	**89.72**
2	**2**	**1**	**0.055**	**89.95**	**89.72**
3	**2**	**5.5**	**0.1**	**96.18**	**99.69**
4	**2**	**5.5**	**0.1**	**97.57**	**99.69**
5	**2**	**5.5**	**0.01**	**98.22**	**96.91**
6	**2**	**5.5**	**0.01**	**99.15**	**96.91**
7	**12**	**5.5**	**0.01**	**60.62**	**62.14**
8	**12**	**5.5**	**0.01**	**69.31**	**62.14**
9	**7**	**1**	**0.01**	**54.83**	**65.86**
10	**7**	**1**	**0.01**	**72.2**	**65.86**
11	**7**	**10**	**0.01**	**97.22**	**98.64**
12	**7**	**10**	**0.01**	**95.6**	**98.64**
13	**12**	**1**	**0.055**	**47.49**	**46.79**
14	**12**	**1**	**0.055**	**45.17**	**46.79**
15	**7**	**5.5**	**0.055**	**94.25**	**95.58**
16	**7**	**5.5**	**0.055**	**96.91**	**95.58**
17	**2**	**10**	**0.055**	**98.38**	**98.02**
18	**2**	**10**	**0.055**	**98.61**	**98.02**

19	**12**	**5.5**	**0.1**	**68.15**	**76.69**
20	**12**	**5.5**	**0.1**	**81.7**	**76.69**
21	**7**	**1**	**0.1**	**86.41**	**84.94**
22	**7**	**1**	**0.1**	**87.99**	**84.94**
23	**12**	**10**	**0.055**	**81.66**	**83.20**
24	**12**	**10**	**0.055**	**83.59**	**83.20**
25	**7**	**10**	**0.1**	**98.76**	**96.87**
26	**7**	**10**	**0.1**	**99.69**	**96.87**

The reliability, quality and accuracy of the fitted quadratic model were evaluated using analysis of variance (ANOVA), as shown in Table 5-3. The polynomial quadratic equation can be seen in equation 5-2.

Anionic Surfactant Removal % = 95.58 – 14.43938A + 11.17562B + 4.33125C + 7.02625AB +2.94250AC – 5.21750BC – 9.43312A^2 – 6.70812B^2 – 2.28438C^2

Equation 5-2

The experimental and predicted values of anionic surfactant removal for the 26 experiments is presented in Table 5-3, where the results clearly indicated that a maximum anionic surfactant removal of 99,69% was achieved with experiment 26, at pH, current density and electrolyte molarity of 7, 10 mA/cm^2 and 0.01 M, respectively. A close correlation between experimental and predicted values were found as indicated by the R^2 predicted.

The analysis of variance was used to evaluate the determination coefficient, lack of fit and the importance of the linear, quadratic and interaction effects on the response of the independent variables. The p-value was used to determine the significance of the coefficient and the interaction strength of the combined factors.

The significance of the models is confirmed by high F-values and low p-values (Sun et al., 2016). The models were significant as confirmed by low probability values of less than 0.0001 and high

F-values of 31.68 for anionic surfactant removal efficiency. The reported F-values imply that there is only a 0.01% chance that their difference could be due to noise. For this study, the lack of fit for the model was insignificant, which shows that the data fitted the model well.

Fit statistics are also shown in Table 5-4 where the coefficient of determination R^2 is a statistical parameter that measures how well the data fits the line. Adjusted R^2 is a version of R^2 that is always smaller than R^2 and predicted R^2 measures the predictive accuracy of the model. A model is considered well fitted when the R^2 value is greater than 0.8 (Najib et al., 2017). R^2, adjusted R^2, and predicted R^2 were found to be 0.9469, 0.9170, and 0.8633 for Anionic Surfactant efficiency removal. For this study, predicted and adjusted R^2 agreed with this. Adequate precision measures the signal-to-noise ratio, and a ratio greater than 4 is desirable. The value of adequate precision was 17.46 Anionic Surfactant efficiency removal, which indicates an adequate signal.

Table 5-4 shows the ANOVA for the anionic surfactant model

Table 5- 4: ANOVA Anionic Surfactant

Analysis of Variance Table [Partial sum of squares – Type III]					
Source	**Sum of Squares**	**df**	**Mean Square**	**F-Value**	**p-value Prob > F**
Model	6803.22	9	755.91	31.68[1]	< 0.0001
A - pH	3335.93	1	3335.93	139.81	< 0.0001[1]
B – Current Density	1998.31	1	1998.31	83.75	< 0.0001[1]
C - Electrolyte	300.16	1	300.16	12.58	0.0027[1]
AB	394.95	1	394.95	16.55	0.0009[1]
AC	69.27	1	69.27	2.90	0.1078
BC	217.78	1	217.78	9.13	0.0081[1]
A^2	406.78	1	406.78	17.05	0.0008[1]
B^2	205.71	1	205.71	8.62	0.0097[1]
C^2	23.86	1	23.86	1.00	0.3322
Residual	381.76	16	23.86	-	-
Lack of Fit	88.59	3	29.53	1.31[2]	0.3134
Pure Error	293.18	13	22.55	-	-
Cor Total	7184.99	25	-	-	-
Standard deviation	4.88	-	-	R-squared	0.9469
mean	84.24	-	-	Adjusted R-squared	0.9170
Coefficient of variance %	5.8	-	-	Predicted R-squared	0.8633

[1] Significant; [2] Not Significant

I. Validation of Model (Anionic Surfactants)

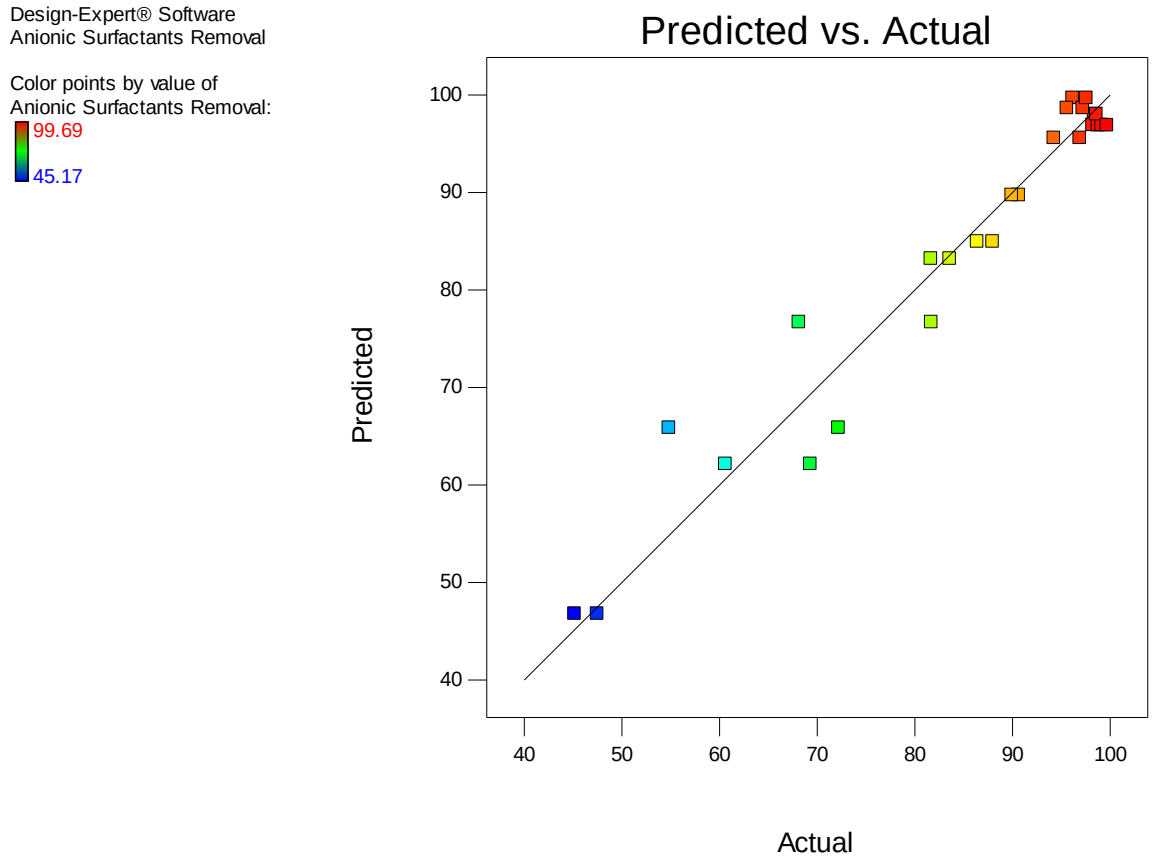

Figure 5- 12: Anionic Surfactant Predicted vs. Actual

Figure 5-12 illustrates the predicted values vs the actual values. According to Zainal-abideen et al. (2012), this plot is used to assist in determining whether the model is satisfactory or not. As seen from figure 5-12, most of the points lie very close to the ideal diagonal line, with an exception for two points. This is an indication that the model used is satisfactory and can accurately predict the anionic surfactant removal for the factors pH, current density and electrolyte molarity during the electrochemical oxidation process.

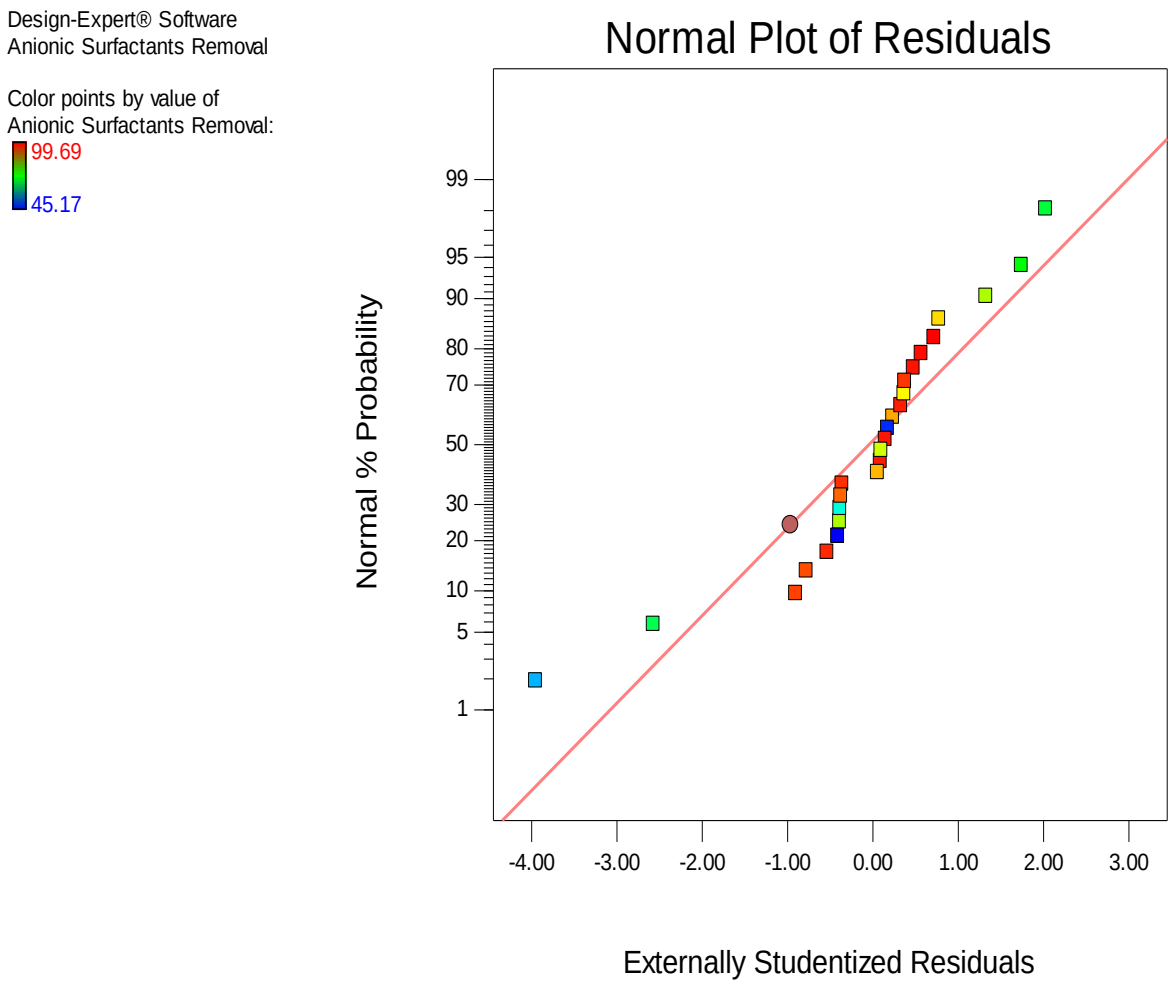

Figure 5- 13: Anionic Surfactants Normal Plot of Residuals

Figure 5-13 shows the normal plot of residuals for the anionic surfactant data. Montgomery (2013) states that if the underlying error distribution is normal, the plot will resemble a straight line, he also states that moderate departure from normality is of little concern, as this is notable from figure 5-13, therefore according to figure 5-13 and the statement made by the author, it can be concluded that the underlying error distribution is normal for the anionic surfactants.

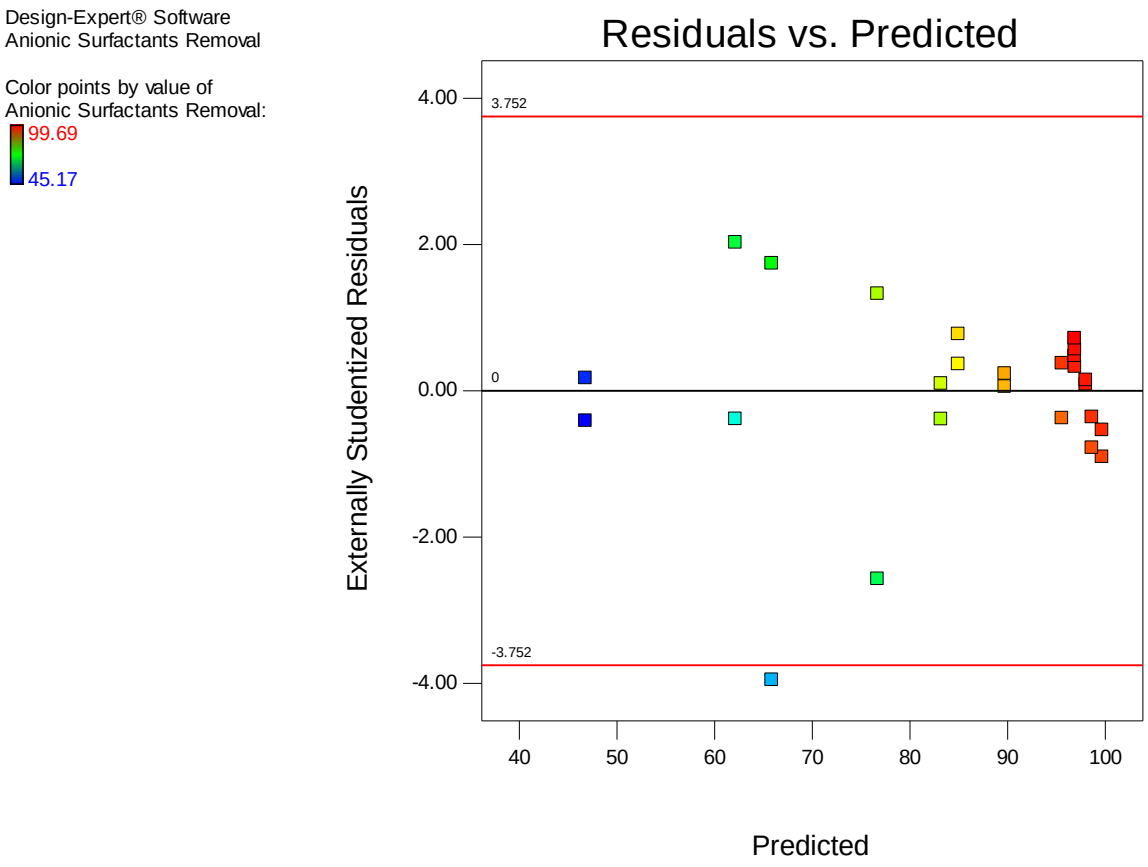

Figure 5- 14: Anionic Surfactants Residuals vs. Predicted

Figure 5-14 shows the plot of the externally studentized residuals vs predicted values for the anionic surfactant data set. The points in figure 5-14 can be seen to be random and not forming any particular structure, this is an indication that the model is correct according to (Montgomery, 2013).

II. Analysis of Response (Anionic Surfactant)

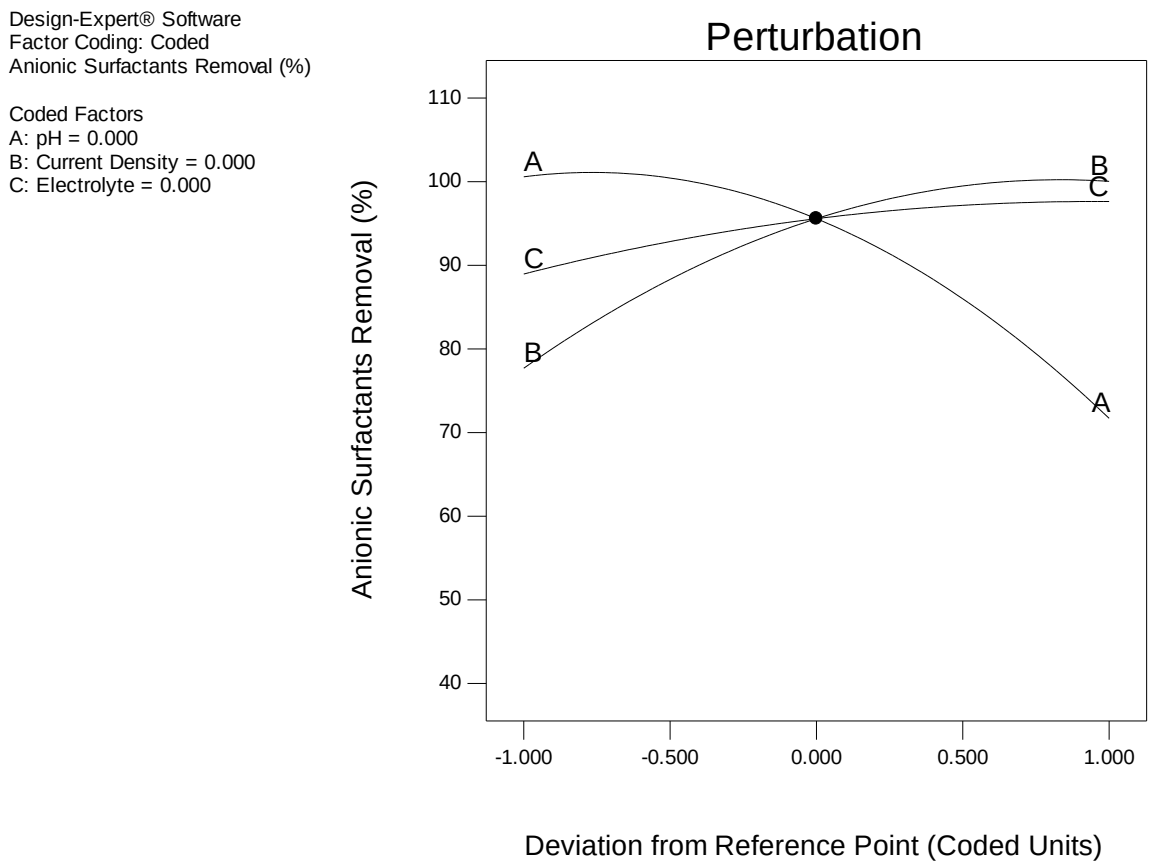

Figure 5- 15: Anionic Surfactants Perturbation

The Perturbation plot is used to compare all factors at a selected point (Kusuma & Mahfud, 2016). The factors are A (pH), B (current density), and C (electrolyte molarity) for the electrochemical oxidation process on the removal of anionic surfactants is shown in figure 5-15. It is quite apparent that factors A and B are the most influential factors out of the three. Factor A seems to be the most significant factor. This can be seen by the vast difference in anionic surfactant removal at unit – 1 (±100%), and unit + 1 (± 75%). Factor C does not seem to have a significant effect on the anionic surfactant removal. It is notable that there is an increase in anionic surfactant removal at unit 1, however, it is only a slight increase and not as impactful as factors A and B.

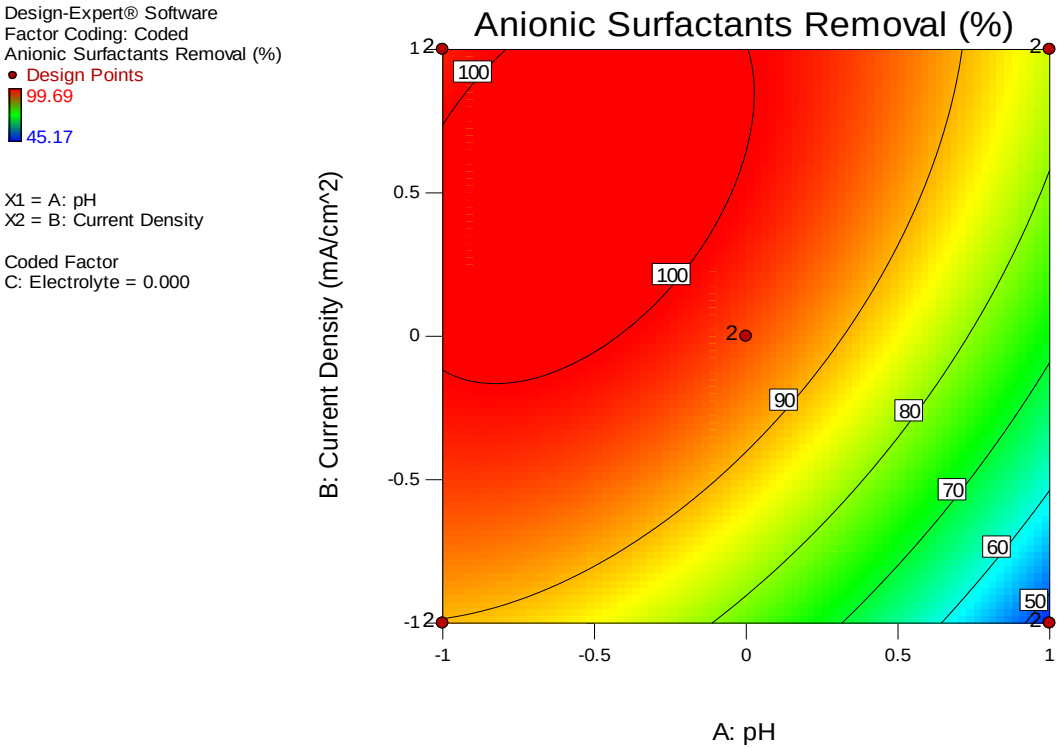

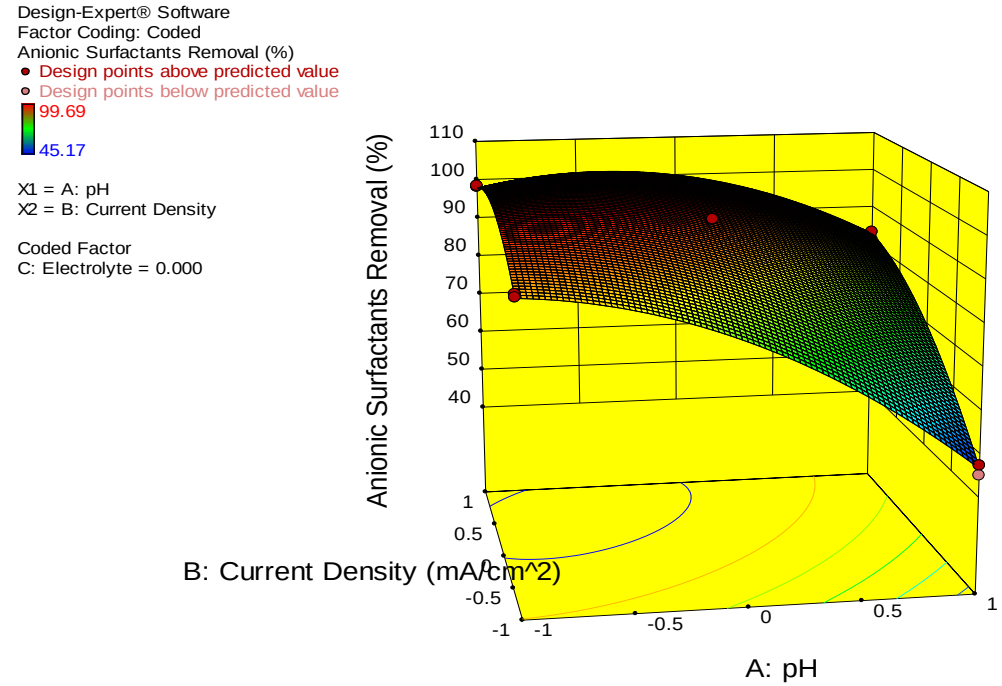

Figure 5- 16: Anionic Surfactants Contour (pH & CD)

Figure 5- 17: Anionic Surfactants 3D (pH & CD)

The contour and 3D graphs for the anionic surfactant removal are shown in figures 5-16 and 5-17, respectively, for factors A and B, which represents pH and current density, while the electrolyte molarity remains constant. There appears to be a linear relationship for both pH and current density, on the removal of anionic surfactants. For pH, the most favourable results were at the lower coded levels, while for current density it was at the higher coded levels, therefore, it can be concluded that the removal of anionic surfactants is directly proportional to current density and inversely proportional to pH. Optimal results were found at approximately 0 to + 1 for current density and between - 1 and – 0.5. In terms of actual factors, optimal results for the removal of anionic surfactants were found between the ranges of 5.5 to 10 mA/cm^2 for current density and between the pH values of 2 and 4.5. Lissens et al. (2003) reported that an optimal initial pH of 10 was found for their EO process for the removal of anionic and cationic surfactants, however, poor removal is shown at similar pH values for this study. Gu et al. (2006) reported an initial pH of 5 or lower achieved favourable anionic surfactant degradation, which is in line with the findings of this study.

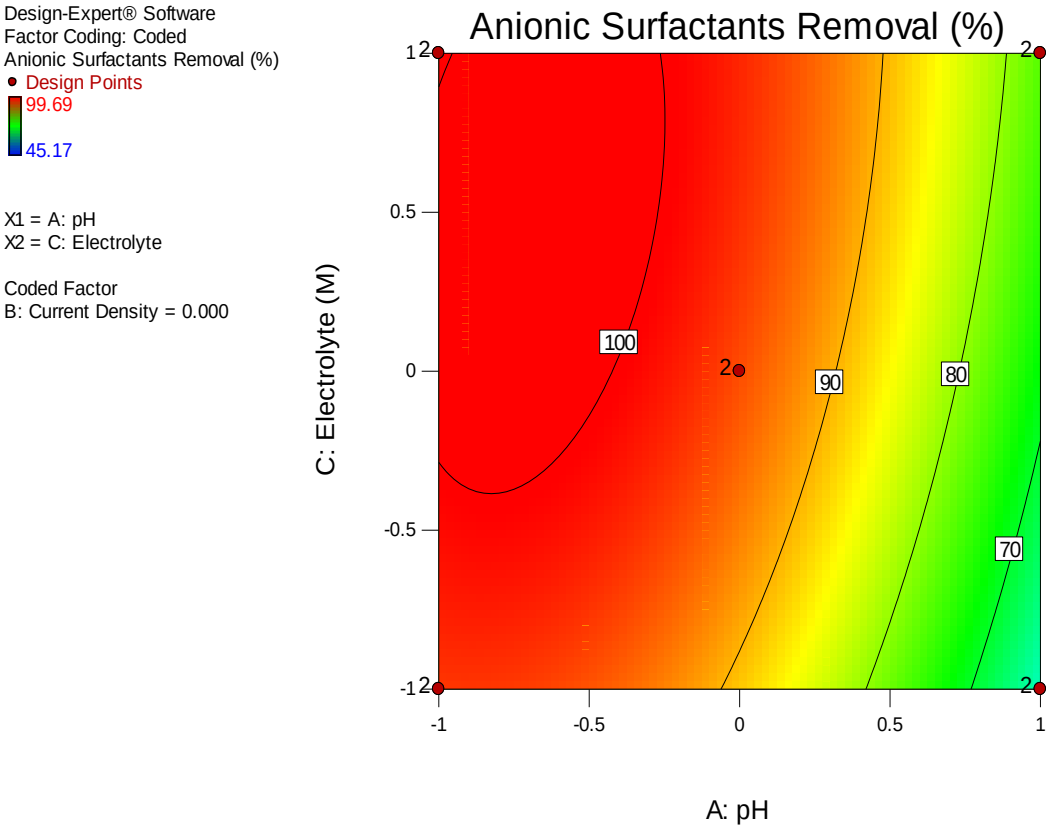

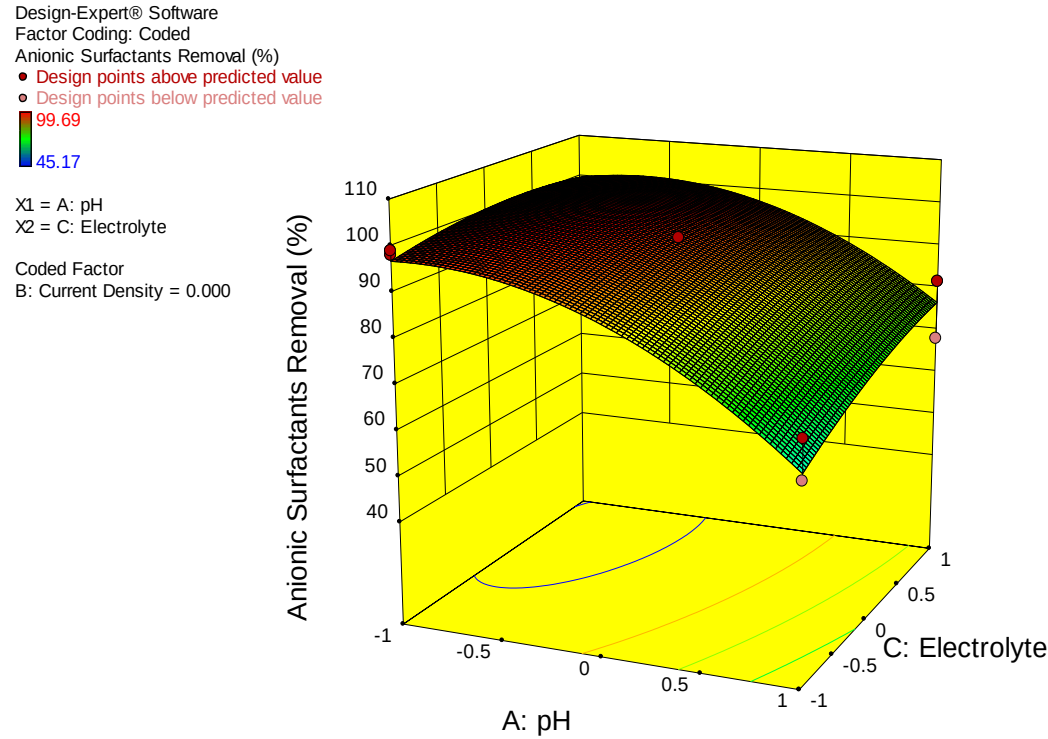

Figure 5- 18: Anionic Surfactants Contour (pH & NaCl)

Figure 5- 19: Anionic Surfactants 3D (pH & NaCl)

Figures 5-18 and 5-19 display the contour and 3D graphs for the removal of anionic surfactants for factors A (pH) and C (electrolyte molarity). The driving factor out of these two factors is pH. This can be seen at pH factor + 1 and NaCl +1, the anionic surfactant removal is between 70 and 80 percent, however, at the factors, pH -1 and +1, anionic surfactants are completely removed. This concludes that the most influential factor is pH. Optimal anionic surfactant removal was found at – 0.5 < pH < -1 and -0.4 < NaCl < + 1. This converts to values for pH being in the range of 2 – 4.5 and NaCl molarity values being between 0.037 – 0.1 M. Figure 5-19 takes the shape of a maximum point as described by Montgomery (2013).

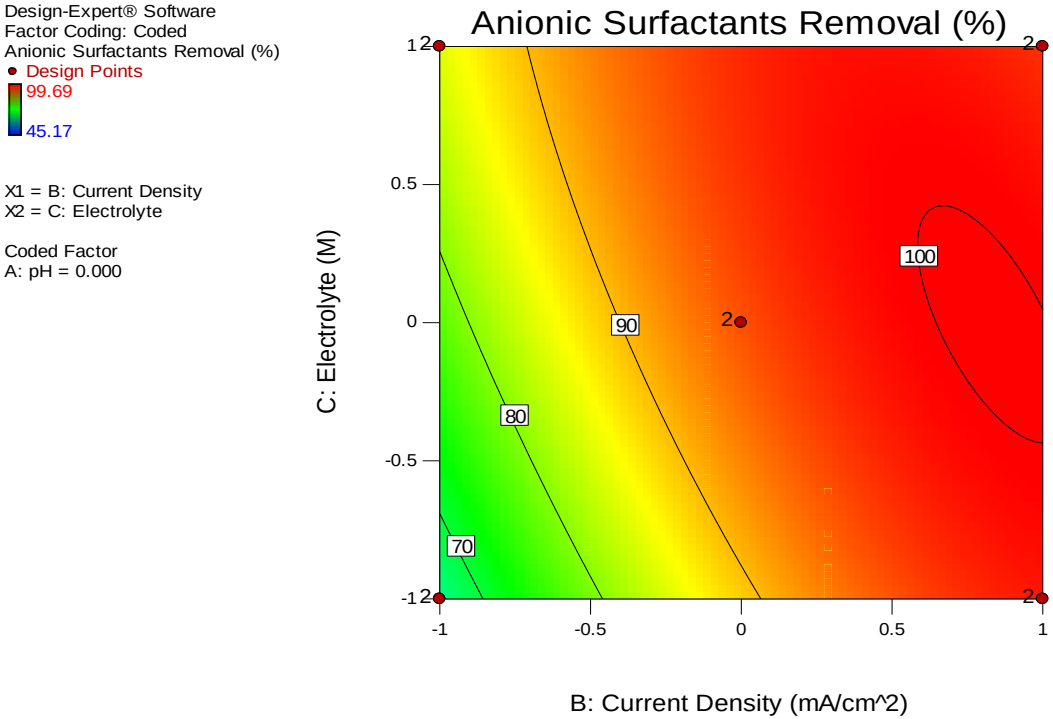

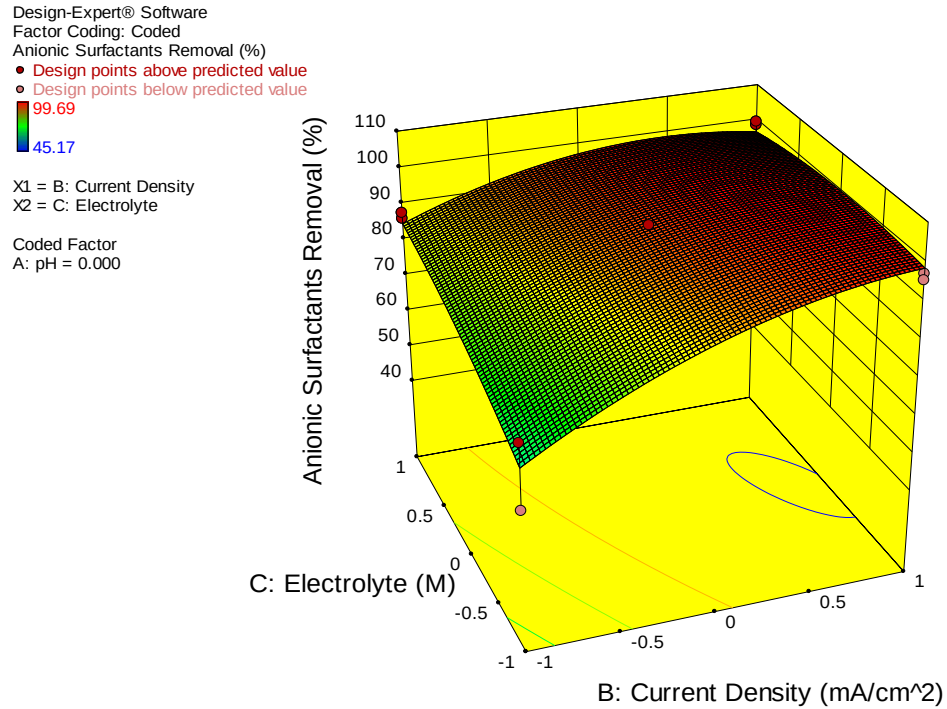

Figure 5- 20: Anionic Surfactants Contour (CD & NaCl)

Figure 5- 21: Anionic Surfactants 3D (CD & NaCl)

Figures 5-20 and 5-21 displays the contour and 3D graphs for current density and electrolyte molarity on the removal of anionic surfactants. Current density is clearly the more influential factor between the factors being compared, in terms of achieving high anionic surfactant removal. Anionic surfactant removal is directly proportional to the increase in current density. There is no clear relationship between the electrolyte molarity and anionic surfactant removal. It seems to be more of a supporting factor to the current density to achieve optimal anionic surfactant removal. The most favourable results can be seen between 0.5 < CD < 1 & - 0.5 < NaCl < 0.5. This converts to actual values of 7.75 – 10 mA/cm^2 for current density and 0.0325 – 0.0775 M for electrolyte molarity. Koparal et al. (2006) reported that an increase in current density resulted in higher removal efficiencies of anionic surfactants. Their findings are consistent with the results obtained in this study.

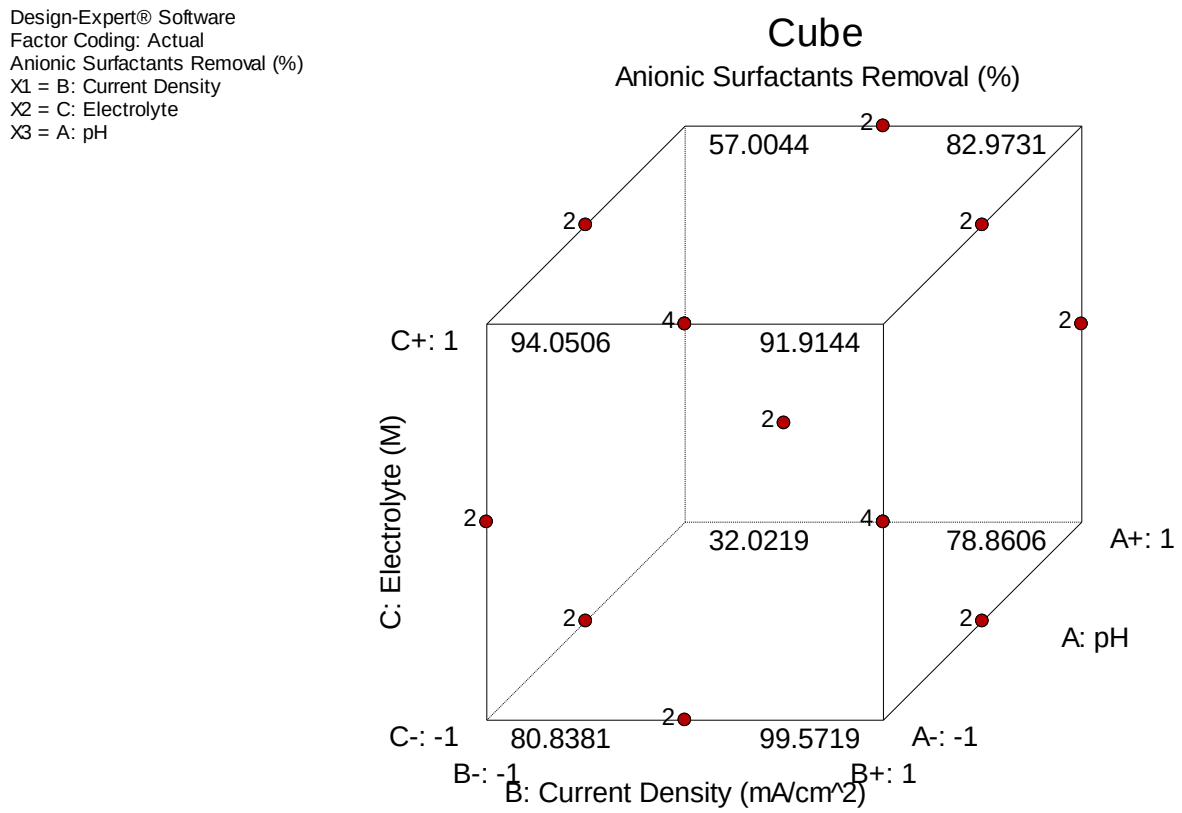

Figure 5- 22: Anionic Surfactants Box Behnken

Figure 5-22 shows the cube generated by the DesignExpert software for the removal of anionic surfactants for the factors pH, current density and electrolyte molarity. The cube illustrates that the two factors which are critical for the highest anionic surfactant removal are current density and pH. This is notable from figure 5.22 at CD of +1 and pH of – 1, the anionic surfactant removal is 99.57%. The actual factors being a current density of 10 mA/cm^2 at a pH of 2. These factors correspond to findings by Koparal et al. (2006) and Gu et al. (2006). The addition of NaCl is significant as well. Panizza et al. (2005) reported that in the presence of chlorine ions surfactants were completely oxidized due to the electrogenerated chlorine, therefore, this highlights the significance of adding NaCl as an electrolyte for the removal of anionic surfactants.

5.3 Optimization Using RSM

Using the program Design Expert, based on the experimental results and the model developed by the software, it optimized the process by predicting the process variables to maximize the COD and anionic surfactant removal efficiencies. The optimization factors can be seen in table 5-5.

Table 5- 5: Optimization Factors

Factors	Coded	Actual	Unit
A (pH)	-0.789	3.055	-
B (CD)	0.901	9.5545	mA/cm^2
C (NaCl)	0.086	0.05887	M

The analysis of response graphs can be seen in figures 5-23, 5-24, 5-25, and 5-26.

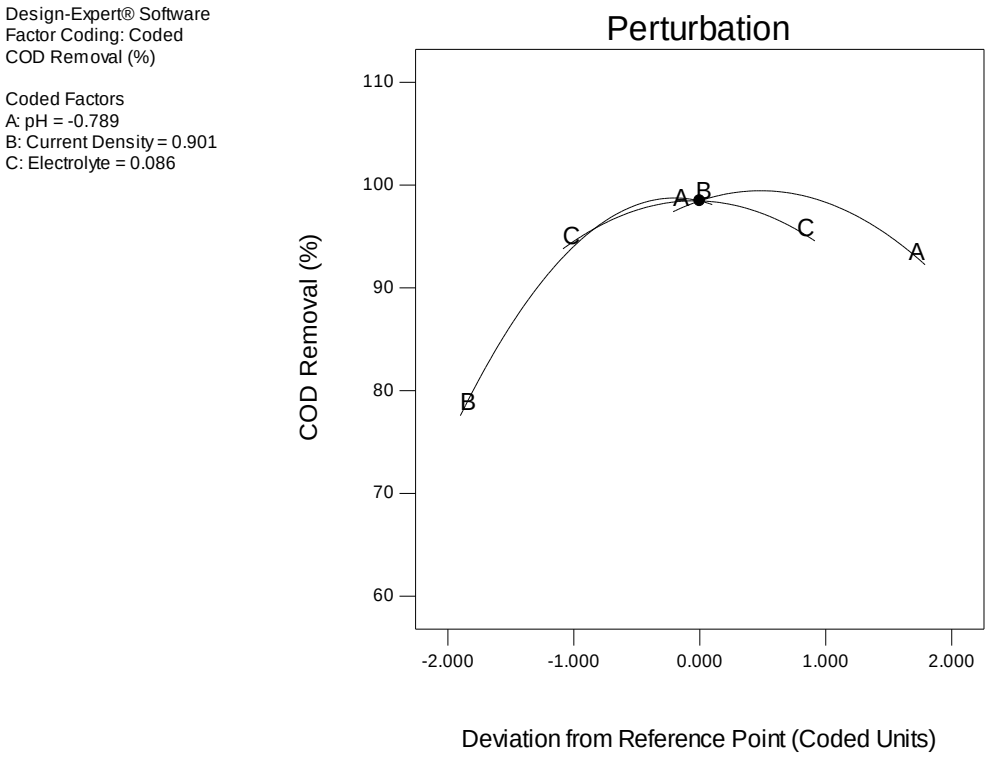

Figure 5- 23: Optimized COD Perturbation

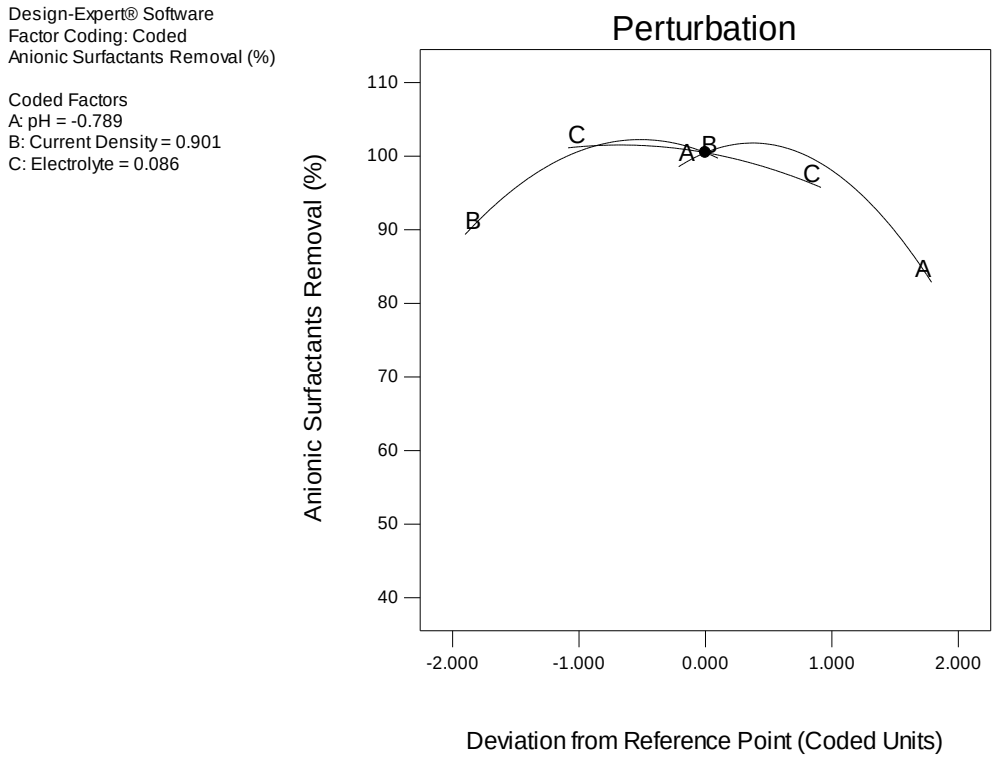

Figure 5- 24: Optimized Anionic Surfactants Perturbation

Figure 5-23 shows the graph for the Perturbation of the optimized factors for the removal of COD, while figure 5-24 shows the graph for the Perturbation of the optimized factors for the removal of anionic surfactants.

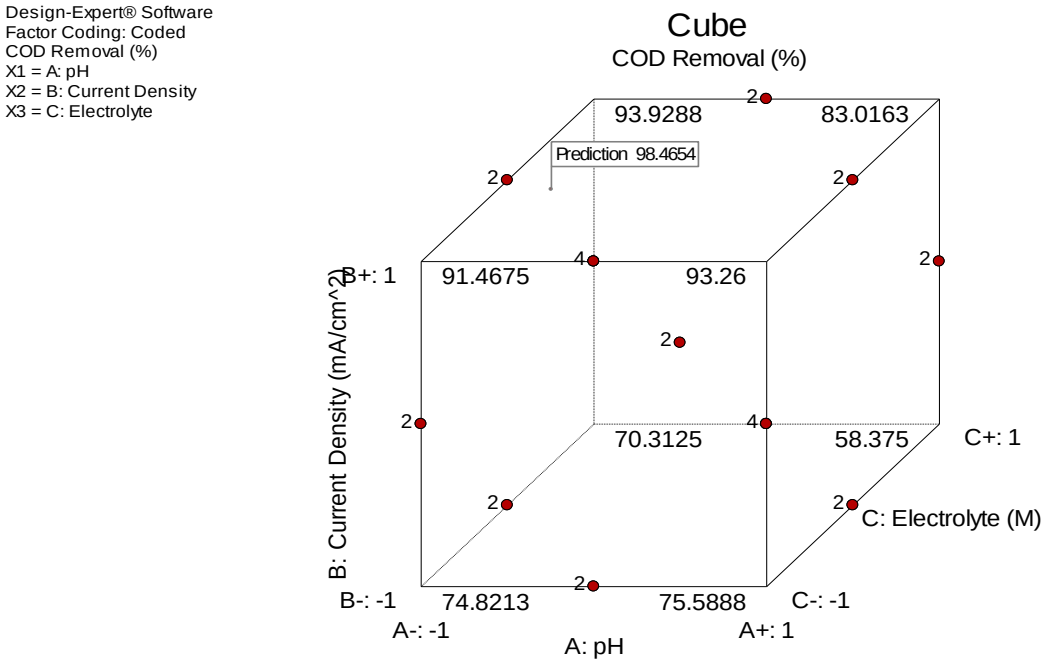

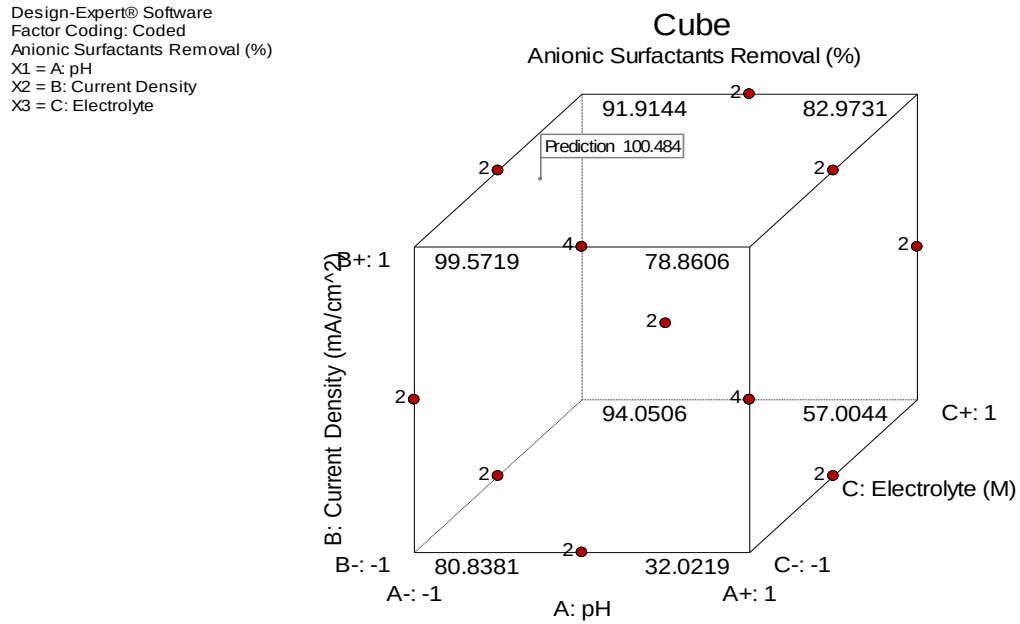

Figure 5- 25: Optimized COD Box Behnken

Figure 5- 26: Optimized Anionic Surfactants Box Behnken

Figure 5-25 shows the Box Behnken cube for the COD removal and figure 5-26 shows the Box Behnken cube for the anionic surfactant removal for the optimized factors given in table 5-5. At a pH of 3.055, current density of 9.55 mA/cm^2 and an electrolyte molarity of 0.059 M, the prediction for COD and anionic surfactant removal is 98.57 and 100%, respectively.

Chapter 6:

Conclusion & Recommendation

Chapter 6: Conclusion and Recommendation

6.1 Conclusion

In this study, the treatment of carwash wastewater (CWW) consisted of two consecutive treatment steps: chemical coagulation (CC) using PAC and electrochemical oxidation (EO) using Ti/IrO_2–Ta_2O_5 anodes. The results obtained from this work include the pollutant removal efficiency of both processes.

In the first step various dosages of the PAC coagulant were investigated in a batch reactor. The 100 mg/L concentration was found to be the most suitable dosage to be used as a pre-treatment for the electrochemical oxidation process. The removal efficiencies of COD, FOG, anionic surfactants, and turbidity was found to be 68.44%, 97.93%, 19.88%, and 95.7%, respectively.

For the second step, the electrochemical oxidation experimental runs removed nearly 100% of turbidity and FOG, however, only four experimental runs were able to satisfy the objectives by achieving a final COD ≤ 75 mg/L, and a final concentration of anionic surfactants of ≤ 2.5 mg/L. The experimental run which obtained the highest COD removal of 97.13% was at experimental conditions of starting pH of 2; current density of 10 mA/cm^2 and electrolyte (NaCl) concentration of 0.055 M. The highest anionic surfactant removal of 99.22% was obtained at experimental conditions of starting pH of 7; current density of 10 mA/cm^2 and electrolyte (NaCl) concentration of 0.1 M.

The optimization of the EO process was conducted using the Box Behnken Design (BBD). From the ANOVA results, it was observed that the P-value was less than 0.0001 for the model developed, achieving an R^2 value of 0.96, when experimental and modelled results were compared. A quadratic equation obtained from the BBD was developed to predict the removal of COD and anionic surfactants from CWW. The optimum conditions were found to be starting pH of 2 and 7; NaCl concentration 0.055 and 0.1 M; current density of 10 and 10 mA/cm^2, to obtain a maximum removal efficiency of 98% and 99% for COD and anionic surfactants, respectively.

The integrated treatment CC-EO process was able to reduce COD and other pollutants levels by 97% and 99%, respectively. This resulted in a treated effluent that complies with the discharge and reuse standards, thus making it a viable process for the treatment of CCW.

6.2 Recommendation

1. Investigating alternative coagulants for the removal of anionic surfactants with the CC process.

2. Other MMO anodes should be utilized with the removal of pollutants to minimize experimental running time that will result in lower operating cost.

3. Powdered activated carbon should be used as a polishing step to lower pollutant levels, such as of anionic surfactants; for recycling and reuse application during the CC-EO process.

References

Alicia, I., Boluarte, R., Andersen, M., Kumar, B., Chang, C., Bagshaw, S., Farago, L., Jegatheesan, V. & Shu, L. 2016. International Biodeterioration & Biodegradation Reuse of car wash wastewater by chemical coagulation and membrane bioreactor treatment processes. *International Biodeterioration & Biodegradation*: 1–5. http://dx.doi.org/10.1016/j.ibiod.2016.01.017.

Asghar, A., Aziz, A., Raman, A., Mohd, W. & Wan, A. 2014. A Comparison of Central Composite Design and Taguchi Method for Optimizing Fenton Process. *The Scientific World Journal*, 2014(869120): 1–14. https://doi.org/10.1155/2014/869120.

Asha, M.N., Chandan, K.S., Harish, H.P., NikhileswarReddy, S., Sharath, K.S. & Liza, G.M. 2016. Recycling of Waste Water Collected from Automobile Service Station. *Procedia Environmental Sciences*, 35: 289–297. http://linkinghub.elsevier.com/retrieve/pii/S1878029616300986.

Aswathy, P., Gandhimathi, R., Ramesh, S.T. & Nidheesh, P. V. 2016. Removal of organics from bilge water by batch electrocoagulation process. *Separation and Purification Technology*, 159: 108–115. https://doi.org/10.1016/j.seppur.2016.01.001.

Baddor, Ilham Muniar;Abdel-magid, Isam Mohammed; Farhoud, Nahed; Alshami, Shibli, Ahamd, Fleih Hassan; Olabi, A. 2014. Study of Car Wash Wastewater Treatment by Adsorption. *International Conference of Engineering, Information Technology, and Science*: 2–22.

Banchon, C., Castillo, A. & Posligua, P. 2017. Chemical interactions to cleanup highly polluted automobile service station wastewater by bioadsorption-coagulation-flocculation. *Journal of Ecological Engineering*, 18(1): 1–10.

Barrios, J.A., Becerril, E., De León, C., Barrera-Díaz, C. & Jiménez, B. 2015. Electrooxidation treatment for removal of emerging pollutants in wastewater sludge. *Fuel*, 149: 26–33. http://dx.doi.org/10.1016/j.fuel.2014.10.055.

Bazrafshan, E., KordMostafapoor, F., Soori, M.M. & Mahvi, A.H. 2012. Application of combined chemical coagulation and electrocoagulation process to carwash wastewater treatment. *Fresen Environ Bull*, 21(9a): 2694–2701.

Bezerra, M.A., Santelli, R.E., Oliveira, E.P., Villar, L.S. & Escaleira, L.A. 2008. Response

surface methodology (RSM) as a tool for optimization in analytical chemistry. *Talanta*, 76(5): 965–977. https://doi.org/10.1016/j.talanta.2008.05.019.

Bhatti, Z.A., Mahmood, Q., Raja, I.A., Malik, A.H., Khan, M.S. & Wu, D. 2011. Chemical oxidation of carwash industry wastewater as an effort to decrease water pollution. *Physics and Chemistry of the Earth*, 36(9–11): 465–469. http://dx.doi.org/10.1016/j.pce.2010.03.022.

Bottero, J.Y., Cases, J.M., Fiessinger, F. & Polrier, J.E. 1980. Studies of hydrolyzed aluminum chloride solutions. 1. Nature of aluminum species and composition of aqueous solutions. *Journal of Physical Chemistry*, 84(22): 2933–2939.

Bratby, J. 1980. Coagulation and flocculation: With an emphasis on water and wastewater treatment. *Filtration & Separation*: 55–58. http://www.ircwash.org/sites/default/files/253-80CO-1277.pdf.

Comninellis, C., Kapalka, A., Malato, S., Parsons, S.A., Poulios, I., & Mantzavinos, D. 2008. Advanced oxidation processes for water treatment: advances and trends for R&D. *Journal of Chemical Technology & Biotechnology*, 83(May): 1163–1169.

da Costa, P.R.F., da Silva, D.R., Martínez-huitle, C.A. & Garcia-segura, S. 2016. Fuel station effluent treatment by electrochemical technology. *JEAC*, 763: 97–103. http://dx.doi.org/10.1016/j.jelechem.2015.12.038.

Czarnetzki, L.R. & Janssen, L.J.J. 1992. Formation of hypochlorite, chlorate and oxygen during NaCl electrolysis from alkaline solutions at an RuO2/TiO2 anode. *Journal of Applied Electrochemistry*, 22(4): 315–324.

Deng, Y. & Englehardt, J.D. 2015. Electrochemical oxidation for landfill leachate treatment. , 27(2007): 380–388.

Department of Water Affairs-South Africa. 2013. Government Gazette N°36820, 6 September 2013. , (36820): 3–31. http://extwprlegs1.fao.org/docs/pdf/saf126916.pdf.

Durakovic, B. 2018. Design of Experiments Application , Concepts , Examples : State of the Art. , 5(3).

Ebeling, J.M., Sibrell, P.L., Ogden, S.R. & Summerfelt, S.T. 2003. Evaluation of chemical coagulation-flocculation aids for the removal of suspended solids and phosphorus from intensive recirculating aquaculture effluent discharge. *Aquacultural Engineering*, 29(1–2):

23–42.

Environmental Protection Agency. 2002. *Water Treatment Manuals: Coagulation, flocculation & Clarification*. http://www.epa.ie/pubs/advice/drinkingwater/EPA_water_treatment_mgt_coag_flocc_clar2.pdf.

Fajardo, A.S., Seca, H.F., Martins, R.C., Corceiro, V.N., Freitas, I.F., Quinta-ferreira, M.E. & Quinta-ferreira, R.M. 2017. Electrochemical oxidation of phenolic wastewaters using a batch-stirred reactor with NaCl electrolyte and Ti / RuO 2 anodes. *Journal of Electroanalytical Chemistry*, 785: 180–189. http://dx.doi.org/10.1016/j.jelechem.2016.12.033.

Feng, Y., Yang, L., Liu, J. & Logan, B.E. 2016. Electrochemical technologies for wastewater treatment and resource reclamation. *Environ. Sci.: Water Res. Technol.*, 2(5): 800–831. http://xlink.rsc.org/?DOI=C5EW00289C.

Ferreira, S.L.C., Bruns, R.E., Ferreira, H.S., Matos, G.D., David, J.M., Brand, G.C., Silva, E.G.P., Reis, P.S., Souza, A.S. & Santos, W.N.L. 2007. Box-Behnken design : An alternative for the optimization of analytical methods. , 597: 179–186.

Gaitonde, V.N., Manjaiah, M., Maradi, S., Karnik, S.R., Petkar, P.M. & Davim, J.P. 2017. *7 - Multiresponse optimization in wire electric discharge machining (WEDM) of HCHCr steel by integrating response surface methodology (RSM) with differential evolution (DE)*. Elsevier Ltd. http://dx.doi.org/10.1016/B978-0-85709-481-0.00007-0.

Gilpavas, E., Dobrosz-gómez, I. & Gómez-garcía, M.Á. 2018. Journal of Water Process Engineering Optimization of sequential chemical coagulation - electro-oxidation process for the treatment of an industrial textile wastewater. *Journal of Water Process Engineering*, 22(November 2017): 73–79. https://doi.org/10.1016/j.jwpe.2018.01.005.

Gomes, J.A.G., Daida, P., Kesmez, M., Weir, M., Moreno, H., Parga, J.R., Irwin, G., Mcwhinney, H., Grady, T., Peterson, E. & Cocke, D.L. 2007. Arsenic removal by electrocoagulation using combined Al – Fe electrode system and characterization of products. , 139: 220–231.

Gönder, Z.B., Balcıoğlu, G., Vergili, I. & Kaya, Y. 2017. Electrochemical treatment of carwash wastewater using Fe and Al electrode: Techno-economic analysis and sludge characterization. *Journal of Environmental Management*, 200: 380–390.

Gonzalez Rivas, N., Reyes-Perez, H. & Barrera-Diaz, C.E. 2019. A mini review on recent advances in water and wastewater electrodisinfection. *ChemElectroChem*, 6(7): 1978–1983.

Gosling, S.N. & Arnell, N.W. 2016. A global assessment of the impact of climate change on water scarcity. : 371–385.

Gu, L., Wang, B., Ma, H. & Kong, W. 2006. Catalytic oxidation of anionic surfactants by electrochemical oxidation with CuO-Co2O3-PO43-modified kaolin. *Journal of Hazardous Materials*, 137(2): 842–848.

Gude, V.G. 2017. Desalination and water reuse to address global water scarcity. *Reviews in Environmental Science and Biotechnology*, 16(4): 591–609.

Hanjra, M.A. & Qureshi, M.E. 2010. Global water crisis and future food security in an era of climate change. *Food Policy*, 35(5): 365–377. http://dx.doi.org/10.1016/j.foodpol.2010.05.006.

Hidayah, E.N., Amalia, A., Putro, R.K.H. & Putranto, D. 2019. Effect of Coagulant to Enhance Floatation Performance in Removing Organic and Grease. *ISRM: Science and Technology for People Empowerment*, 2018(2018): 266–269.

Jacyna, J., Kordalewska, M. & Markuszewski, M.J. 2019. Design of Experiments in metabolomics-related studies: An overview. *Journal of Pharmaceutical and Biomedical Analysis*, 164: 598–606.

Juárez, H.R., Díaz, C.B.-, Hernández, I.L.-, Fall, C. & Bilyeu, B. 2015. A Combined Electrocoagulation-Electrooxidation Process for Carwash Wastewater Reclamation. , 10: 6754–6767.

Jury, W.A. & Vaux, H.J. 2007. The Emerging Global Water Crisis: Managing Scarcity and Conflict Between Water Users. *Advances in Agronomy*, 95(07): 1–76.

Kaufmann, E.N. 2012. Characterization of Materials. In *Characterization of Materials*. John Wiley & Sons, Inc.: 1104–1133.

Kaur, P., Kushwaha, J.P. & Sangal, V.K. 2017. Evaluation and disposability study of actual textile wastewater treatment by electro-oxidation method using Ti/RuO2anode. *Process Safety and Environmental Protection*, 111: 13–22. http://dx.doi.org/10.1016/j.psep.2017.06.004.

Kiran, S.A., Arthanareeswaran, G., Thuyavan, Y.L. & Ismail, A.F. 2015. Ecotoxicology and Environmental Safety In fl uence of bentonite in polymer membranes for effective treatment of car wash ef fl uent to protect the ecosystem. : 1–7.

Koparal, A.S., Onder, E. & Ogutveren, U.B. 2006. Removal of linear alkylbenzene sulfonate from a model solution by continuous electrochemical oxidation. , 197: 262–272.

Kumar, N.S. & Chauhan, M.S. 2018. Treatment of Car Washing Unit Wastewater — A Review. In *Water Quality Management*. Springer Singapore: 247–255.

Kusuma, H.S. & Mahfud, M. 2016. Response Surface Methodology for Optimization Studies of Microwave- assisted Extraction of Sandalwood Oil. , 7(6): 1958–1971.

Lal, K. & Garg, A. 2017. Physico-chemical treatment of pulping effluent : Characterization of flocs and sludge generated after treatment. *Separation Science and Technology*, 52(9): 1583–1593.

Larsen, T.A., Hoffmann, S., Lüthi, C., Truffer, B. & Maurer, M. 2016. Emerging solutions to the water challenges of an urbanizing world. *Science*, 352(6288): 928–933.

Lau, W.J., Ismail, A.F. & Firdaus, S. 2013. Car wash industry in Malaysia: Treatment of car wash effluent using ultrafiltration and nanofiltration membranes. *Separation and Purification Technology*, 104: 26–31. http://dx.doi.org/10.1016/j.seppur.2012.11.012.

Linares-Hernández, I., Barrera-Díaz, C., Bilyeu, B., Juárez-Garcíarojas, P. & Campos-Medina, E. 2010. A combined electrocoagulation – electrooxidation treatment for industrial wastewater. , 175: 688–694.

Lissens, G., Pieters, J., Verhaege, M., Pinoy, L. & Verstraete, W. 2003. Electrochemical degradation of surfactants by intermediates of water discharge at carbon-based electrodes. , 48: 1655–1663.

Mäkelä, M. 2017. Experimental design and response surface methodology in energy applications : A tutorial review. *Energy Conversion and Management*, 151(August): 630–640. http://dx.doi.org/10.1016/j.enconman.2017.09.021.

Manojkumar, N., Muthukumaran, C. & Sharmila, G. 2020. Journal of King Saud University – Engineering Sciences A comprehensive review on the application of response surface methodology for optimization of biodiesel production using different oil sources. *Journal of King Saud University - Engineering Sciences*, (xxxx).

https://doi.org/10.1016/j.jksues.2020.09.012.

Martínez-Huitle, C.A. & Panizza, M. 2018. Electrochemical oxidation of organic pollutants for wastewater treatment. *Current Opinion in Electrochemistry*, 11(1): 62–71.

Moazzem, S., Wills, J., Fan, L., Roddick, F. & Jegatheesan, V. 2018. Performance of ceramic ultrafiltration and reverse osmosis membranes in treating car wash wastewater for reuse. *Environmental Science and Pollution Research*, 25(9): 8654–8668.

Mohamed, M.A., Jaafar, J., Ismail, A.F., Othman, M.H.D. & Rahman, M.A. 2017. *Fourier Transform Infrared (FTIR) Spectroscopy*. Elsevier B.V. http://dx.doi.org/10.1016/B978-0-444-63776-5.00001-2.

Mohamed, M.S.R., Kutty, N.M.I. & Kassim, A.H.M. 2014. Efficiency of Using Commercial and Natural Coagulants in Treating Car Wash Wastewater Treatment. *Australian Journal of Basic and Applied Sciences Aust. J. Basic & Appl. Sci*, 8(816): 227–234. www.ajbasweb.com.

Mohammadi, M.J., Takdastan, A., Jorfi, S., Neisi, A., Farhadi, M., Yari, A.R., Dobaradaran, S. & Khaniabadi, Y.O. 2017. Electrocoagulation process to Chemical and Biological Oxygen Demand treatment from carwash grey water in Ahvaz megacity, Iran. *Data in Brief*, 11: 634–639.

Mohan, N., Balasubramanian, N. & Basha, C.A. 2007. Electrochemical oxidation of textile wastewater and its reuse. *Journal of Hazardous Materials*, 147(1–2): 644–651.

Montgomery, D.C. 2013. *Design and Analysis of Experiments Eighth Edition*. Eighth. John Wiley & Sons, Inc.

Muddemann, T., Haupt, D., Sievers, M. & Kunz, U. 2019. Electrochemical Reactors for Wastewater Treatment. , (5): 142–156.

Myburgh, D.P., Aziz, M., Roman, F., Jardim, J. & Chakawa, S. 2019. Removal of COD from Industrial Biodiesel Wastewater Using an Integrated Process: Electrochemical-Oxidation with IrO2-Ta2O5/Ti Anodes and Chitosan Powder as an Adsorbent. *Environmental Processes*, 6(4): 819–840.

Nadzirah, Z., Nor Haslina, H., Mohd Adib, M.R. 2015. Studies On the Preparation of Activated Carbon Sugarcane Bagasse On Removal of Chemical Oxygen Demand , Alkalinity and Oil and grease of Car Wash Wastewater. , 9(12): 15–20.

Najib, T., Solgi, M., Farazmand, A., Heydarian, S.M. & Nasernejad, B. 2017. Optimization of sulfate removal by sulfate reducing bacteria using response surface methodology and heavy metal removal in a sulfidogenic UASB reactor. *Biochemical Pharmacology*. http://dx.doi.org/10.1016/j.jece.2017.06.016.

Oluwole, A.J.O., Ikhu-Omoregbe, D.I. & Jideani, V.A. 2020. Physicochemical properties of african catfish mucus and its effect on the stability of soya milk emulsions. *Applied Sciences (Switzerland)*, 10(3).

Othmer, K. 2007. Kirk-Othmer Encyclopedia of Chemical Technology. In *Encyclopedia of Chemical Technology*.

Panizza, M. & Cerisola, G. 2010a. Applicability of electrochemical methods to carwash wastewaters for reuse. Part 1: Anodic oxidation with diamond and lead dioxide anodes. *Journal of Electroanalytical Chemistry*, 638(1): 28–32. http://dx.doi.org/10.1016/j.jelechem.2009.10.025.

Panizza, M. & Cerisola, G. 2010b. Applicability of electrochemical methods to carwash wastewaters for reuse . Part 2 : Electrocoagulation and anodic oxidation integrated process. *Journal of Electroanalytical Chemistry*, 638(2): 236–240. http://dx.doi.org/10.1016/j.jelechem.2009.11.003.

Panizza, M., Delucchi, M. & Cerisola, G. 2005. Electrochemical degradation of anionic surfactants. *Journal of Applied Electrochemistry*, 35(4): 357–361.

Pernitsky, D.J. & Edzwald, J.K. 2003. Solubility of polyaluminium coagulants. *Journal of Water Supply: Research and Technology - AQUA*, 52(6): 395–406.

Priya, M. & Jeyanthi, J. 2019. Removal of COD , oil and grease from automobile wash water effluent using electrocoagulation technique . *Microchemical Journal*, 150(July): 104070. https://doi.org/10.1016/j.microc.2019.104070.

Radjenovic, J. & Sedlak, D.L. 2015. Challenges and Opportunities for Electrochemical Processes as Next- Generation Technologies for the Treatment of Contaminated Water.

Raju, G.B., Karuppiah, M.T., Latha, S.S., Parvathy, S. & Prabhakar, S. 2008. Treatment of wastewater from synthetic textile industry by electrocoagulation-electrooxidation. *Chemical Engineering Journal*, 144(1): 51–58.

Ren, X., Zhang, Y. & Chen, H. 2019. WATER ENVIRONMENTAL POLLUTION AND STATE OF

THE ART TREATMENT Graywater treatment technologies and reuse of reclaimed water for toilet flushing.

Sahu, O.P. & Chaudhari, P.K. 2013. Review on Chemical treatment of Industrial Waste Water Review on Chemical treatment. *Journal of Applied Science Environmental Management*, 17(2): 241–257.

Sarmadi, M., Foroughi, M., Najafi Saleh, H., Sanaei, D., Zarei, A.A., Ghahrchi, M. & Bazrafshan, E. 2020. Efficient technologies for carwash wastewater treatment: a systematic review. *Environmental Science and Pollution Research*, 27(28): 34823–34839.

Scialdone, O., Randazzo, S., Galia, A. & Silvestri, G. 2009. Electrochemical oxidation of organics in water : Role of operative parameters in the absence and in the presence of NaCl. *Water Research*, 43(8): 2260–2272. http://dx.doi.org/10.1016/j.watres.2009.02.014.

da Silva, A.J.C., dos Santos, E.V., de Oliveira Morais, C.C., Martínez-Huitle, C.A. & Castro, S.S.L. 2013. Electrochemical treatment of fresh, brine and saline produced water generated by petrochemical industry using Ti/IrO2-Ta2O5and BDD in flow reactor. *Chemical Engineering Journal*, 233: 47–55.

Sincero, A.P. & Sincero, G.A. 2003. *Physical Chemical Treatment of Water and Wastewater*.

Sun, Y., Wei, J., Ping, J. & Yang, G. 2016. Journal of Natural Gas Science and Engineering Optimization using response surface methodology and kinetic study of Fischer e Tropsch synthesis using SiO 2 supported bimetallic Co e Ni catalyst. *Journal of Natural Gas Science and Engineering*, 28: 173–183. http://dx.doi.org/10.1016/j.jngse.2015.11.008.

Tang, L., Tan, X.J., Cui, F.Y., Zhou, Q. & Yin, J. 2007. Reuse of carwash wastewater with hollow fiber membrane aided by enhanced coagulation and activated carbon treatments. *Water Science and Technology*, 56(12): 111–118.

Tian, Y., Hu, H. & Zhang, J. 2017. Solution to water resource scarcity : water reclamation and reuse. : 5095–5097.

Torres, N.H., Santos, B., Ferreira, L.F.R., Lima, A.S., dos Santos, G.N. & Cavalcanti, E.B. 2019. Chemosphere Real textile effluents treatment using coagulation / flocculation followed by electrochemical oxidation process and ecotoxicological assessment. , 236.

Urtiaga, A. & Ortiz, I. 2009. Contributions of electrochemical oxidation to waste-water treatment : fundamentals. , (March): 1747–1755.

Wahab, M.A., Jellali, S. & Jedidi, N. 2010. Ammonium biosorption onto sawdust: FTIR analysis, kinetics and adsorption isotherms modeling. *Bioresource Technology*, 101(14): 5070–5075. http://dx.doi.org/10.1016/j.biortech.2010.01.121.

Wahid, Z. & Nadir, N. 2013. Improvement of One Factor at a Time Through Design of Experiments 1. , 21: 56–61.

Wang, H., Wang, J., Bo, G., Wu, S. & Luo, L. 2020. Degradation of pollutants in polluted river water using Ti/IrO2–Ta2O5 coating electrode and evaluation of electrode characteristics. *Journal of Cleaner Production*, 273: 123019. https://doi.org/10.1016/j.jclepro.2020.123019.

Wei, N., Zhang, Z., Liu, D., Wu, Y., Wang, J. & Wang, Q. 2015. Coagulation behavior of polyaluminum chloride: Effects of pH and coagulant dosage. *Chinese Journal of Chemical Engineering*, 23(6): 1041–1046.

Yang, Z., Gao, B. & Yue, Q. 2010. Coagulation performance and residual aluminum speciation of Al 2 (SO 4) 3 and polyaluminum chloride (PAC) in Yellow River water treatment. *Chemical Engineering Journal*, 165(1): 122–132. http://dx.doi.org/10.1016/j.cej.2010.08.076.

Yu, P., Yin, M. & Zhou, W. 2018. Trends in Food Science & Technology Design of experiments and regression modelling in food fl avour and sensory analysis : A review. *Trends in Food Science & Technology*, 71(January 2017): 202–215. https://doi.org/10.1016/j.tifs.2017.11.013.

Zainal-abideen, M., Aris, A., Yusof, F. & Majid, Z.A. 2012. Optimizing the coagulation process in a drinking water treatment plant - Comparison between traditional and statistical experimental design jar tests. , (September 2014).

Zaleschi, L., Teodosiu, C., Cretescu, I. & Rodrigo, M.A. 2012. A comparative study of electrocoagulation and chemical coagulation processes applied for wastewater treatment. *Environmental Engineering and Management Journal*, 11(8): 1517–1525.

Zambrano, J. & Min, B. 2019. Environmental Technology & Innovation Comparison on efficiency of electrochemical phenol oxidation in two different supporting electrolytes (NaCl and Na 2 SO 4) using Pt / Ti electrode. *Environmental Technology & Innovation*, 15: 100382. https://doi.org/10.1016/j.eti.2019.100382.

Zaneti, R., Etchepare, R. & Rubio, J. 2011. Car wash wastewater reclamation. Full-scale

application and upcoming features. *Resources, Conservation and Recycling*, 55(11): 953–959. http://dx.doi.org/10.1016/j.resconrec.2011.05.002.

Zhang, H., Ran, X., Wu, X. & Zhang, D. 2011. Evaluation of electro-oxidation of biologically treated landfill leachate using response surface methodology. *Journal of Hazardous Materials*, 188(1–3): 261–268.

Appendices:

Appendix A:

Raw Data

Appendix A: Raw Data

Raw Carwash Wastewater Data

Table A- 1: CWW Data

Real Carwash Wastewater			
Parameter	**Unit**	**Sample 1**	**Sample 2**
COD	mg/L	1200	1240
FOG	mg/L	40.4	56
Surfactant	mg/L	26	25.8
Turbidity	NTU	87.8	111
pH	-	7.09	7.07

Coagulation Data

Table A- 2: Coagulation Data

Coagulation Data							
COD (mg/L)		**Anionic Surfactants (mg/L)**		**FOG (mg/L)**		**Turbidity (NTU)**	
60 (mg/L)	Duplication	60 (mg/L)	Duplication	60 (mg/L)	Duplication	60 (mg/L)	Duplication
590	560	21.6	22.4	1.22	0.5	11.3	8.24
80 (mg/L)	Duplication	80 (mg/L)	Duplication	80 (mg/L)	Duplication	80 (mg/L)	Duplication
485	460	24.8	20.2	0.78	0.5	6.07	7.61
100 (mg/L)	Duplication	100 (mg/L)	Duplication	100 (mg/L)	Duplication	100 (mg/L)	Duplication
390	380	21.2	20.3	1	1	4.31	4.24

Electrochemical Oxidation Data

Turbidity

Table A- 3: EO Turbidity Data

Turbidity (NTU)			
Run 1	0.68	Duplicate	0.59
Run 2	0.23	Duplicate	0.48
Run 3	0.29	Duplicate	0.35
Run 4	0.36	Duplicate	0.5
Run 5	0.89	Duplicate	0.87
Run 6	0.49	Duplicate	0.28
Run 7	0.65	Duplicate	0.28
Run 8	0.61	Duplicate	0.64
Run 9	0.7	Duplicate	0.48
Run 10	0.36	Duplicate	0.14
Run 11	0.21	Duplicate	0.16
Run 12	0.18	Duplicate	0.1
Run 13	0.14	Duplicate	0.11

COD

Table A- 4: EO COD Data

COD (mg/L)			
Run 1	280.00	Duplicate	300.00
Run 2	160.00	Duplicate	130.00
Run 3	110.00	Duplicate	80.00
Run 4	80.00	Duplicate	90.00
Run 5	220.00	Duplicate	310.00
Run 6	60.00	Duplicate	70.00
Run 7	370.00	Duplicate	335.00
Run 8	40.00	Duplicate	60.00
Run 9	50.00	Duplicate	20.00
Run 10	300.00	Duplicate	280.00
Run 11	375.00	Duplicate	345.00
Run 12	70.00	Duplicate	100.00
Run 13	90.00	Duplicate	60.00

Anionic Surfactants

Table A- 5: EO Anionic Surfactant Data

Anionic Surfactants (mg/L)			
Run 1	2.42	Duplicate	2.68
Run 2	0.99	Duplicate	0.63
Run 3	0.46	Duplicate	0.22
Run 4	10.20	Duplicate	7.95
Run 5	11.70	Duplicate	7.20
Run 6	0.72	Duplicate	1.14
Run 7	13.60	Duplicate	14.20
Run 8	1.49	Duplicate	0.80
Run 9	0.42	Duplicate	0.36
Run 10	8.25	Duplicate	4.74
Run 11	3.52	Duplicate	3.11
Run 12	4.75	Duplicate	4.25
Run 13	0.32	Duplicate	0.08

FOG

Table A- 6: EO FOG Data

FOG (mg/L)			
Run 9	None detected	Duplicate	None detected
Run 10	None detected	Duplicate	None detected

FTIR Coagulant Sludge Data

Table A- 7: FTIR Data

cm-1	%T
4000	96.88
3999	96.86
3998	96.84
3997	96.83
3996	96.82
3995	96.83
3994	96.83
3993	96.83
3992	96.82
3991	96.8
3990	96.8
3989	96.8
3988	96.8
3987	96.81
3986	96.83
3985	96.84
3984	96.84
3983	96.84
3982	96.84
3981	96.84
3980	96.85
3979	96.86
3978	96.86
3977	96.87
3976	96.85
3975	96.84
3974	96.82
3973	96.81
3972	96.81
3971	96.8
3970	96.8
3969	96.8
3968	96.81
3967	96.81
3966	96.81
3965	96.81
3964	96.8

3963	96.79
3962	96.79
3961	96.81
3960	96.82
3959	96.83
3958	96.83
3957	96.83
3956	96.82
3955	96.82
3954	96.81
3953	96.8
3952	96.79
3951	96.79
3950	96.8
3949	96.81
3948	96.82
3947	96.83
3946	96.82
3945	96.81
3944	96.8
3943	96.8
3942	96.8
3941	96.81
3940	96.82
3939	96.82
3938	96.82
3937	96.82
3936	96.81
3935	96.81
3934	96.82
3933	96.83
3932	96.84
3931	96.85
3930	96.86
3929	96.87
3928	96.87
3927	96.86
3926	96.84
3925	96.82
3924	96.8
3923	96.8

3922	96.8
3921	96.81
3920	96.81
3919	96.8
3918	96.79
3917	96.8
3916	96.81
3915	96.83
3914	96.83
3913	96.82
3912	96.8
3911	96.8
3910	96.8
3909	96.82
3908	96.84
3907	96.86
3906	96.86
3905	96.85
3904	96.83
3903	96.83
3902	96.84
3901	96.86
3900	96.87
3899	96.86
3898	96.85
3897	96.83
3896	96.83
3895	96.83
3894	96.83
3893	96.84
3892	96.84
3891	96.83
3890	96.83
3889	96.83
3888	96.84
3887	96.85
3886	96.86
3885	96.85
3884	96.84
3883	96.83
3882	96.82

3881	96.81
3880	96.81
3879	96.8
3878	96.8
3877	96.8
3876	96.81
3875	96.81
3874	96.82
3873	96.83
3872	96.83
3871	96.84
3870	96.84
3869	96.84
3868	96.84
3867	96.84
3866	96.85
3865	96.85
3864	96.85
3863	96.85
3862	96.85
3861	96.87
3860	96.88
3859	96.88
3858	96.88
3857	96.88
3856	96.9
3855	96.91
3854	96.91
3853	96.9
3852	96.89
3851	96.89
3850	96.9
3849	96.89
3848	96.88
3847	96.86
3846	96.86
3845	96.86
3844	96.86
3843	96.85
3842	96.85
3841	96.85

3840	96.85
3839	96.86
3838	96.86
3837	96.86
3836	96.86
3835	96.87
3834	96.87
3833	96.87
3832	96.87
3831	96.85
3830	96.85
3829	96.85
3828	96.86
3827	96.86
3826	96.86
3825	96.86
3824	96.85
3823	96.83
3822	96.8
3821	96.78
3820	96.77
3819	96.78
3818	96.82
3817	96.86
3816	96.87
3815	96.85
3814	96.83
3813	96.83
3812	96.85
3811	96.86
3810	96.87
3809	96.89
3808	96.92
3807	96.94
3806	96.94
3805	96.93
3804	96.92
3803	96.9
3802	96.87
3801	96.85
3800	96.85

3799	96.87
3798	96.9
3797	96.92
3796	96.92
3795	96.9
3794	96.89
3793	96.9
3792	96.91
3791	96.91
3790	96.9
3789	96.89
3788	96.88
3787	96.88
3786	96.88
3785	96.87
3784	96.87
3783	96.86
3782	96.84
3781	96.83
3780	96.83
3779	96.83
3778	96.83
3777	96.84
3776	96.84
3775	96.85
3774	96.86
3773	96.87
3772	96.88
3771	96.89
3770	96.89
3769	96.87
3768	96.85
3767	96.83
3766	96.82
3765	96.82
3764	96.82
3763	96.82
3762	96.83
3761	96.84
3760	96.85
3759	96.85

3758	96.86
3757	96.85
3756	96.83
3755	96.81
3754	96.79
3753	96.79
3752	96.79
3751	96.8
3750	96.8
3749	96.81
3748	96.83
3747	96.84
3746	96.86
3745	96.86
3744	96.86
3743	96.84
3742	96.83
3741	96.82
3740	96.79
3739	96.75
3738	96.71
3737	96.68
3736	96.67
3735	96.66
3734	96.66
3733	96.67
3732	96.69
3731	96.7
3730	96.69
3729	96.68
3728	96.67
3727	96.65
3726	96.63
3725	96.61
3724	96.57
3723	96.53
3722	96.47
3721	96.39
3720	96.32
3719	96.24
3718	96.17

3717	96.1
3716	96.04
3715	95.97
3714	95.88
3713	95.74
3712	95.56
3711	95.37
3710	95.18
3709	95
3708	94.8
3707	94.58
3706	94.33
3705	94.04
3704	93.7
3703	93.3
3702	92.87
3701	92.44
3700	92.06
3699	91.74
3698	91.49
3697	91.32
3696	91.24
3695	91.26
3694	91.36
3693	91.52
3692	91.73
3691	91.96
3690	92.21
3689	92.47
3688	92.72
3687	92.94
3686	93.12
3685	93.27
3684	93.38
3683	93.46
3682	93.51
3681	93.56
3680	93.6
3679	93.63
3678	93.64
3677	93.63

3676	93.59
3675	93.54
3674	93.49
3673	93.46
3672	93.42
3671	93.35
3670	93.25
3669	93.17
3668	93.11
3667	93.08
3666	93.04
3665	92.99
3664	92.92
3663	92.84
3662	92.76
3661	92.68
3660	92.59
3659	92.51
3658	92.41
3657	92.3
3656	92.19
3655	92.11
3654	92.06
3653	92.04
3652	92.02
3651	91.98
3650	91.9
3649	91.81
3648	91.72
3647	91.66
3646	91.62
3645	91.58
3644	91.55
3643	91.53
3642	91.5
3641	91.49
3640	91.47
3639	91.45
3638	91.42
3637	91.37
3636	91.32

3635	91.26
3634	91.21
3633	91.17
3632	91.13
3631	91.08
3630	90.97
3629	90.77
3628	90.55
3627	90.36
3626	90.21
3625	90.08
3624	89.94
3623	89.8
3622	89.66
3621	89.53
3620	89.44
3619	89.41
3618	89.46
3617	89.55
3616	89.66
3615	89.77
3614	89.88
3613	89.97
3612	90.05
3611	90.11
3610	90.15
3609	90.16
3608	90.17
3607	90.19
3606	90.21
3605	90.22
3604	90.23
3603	90.22
3602	90.2
3601	90.18
3600	90.16
3599	90.14
3598	90.12
3597	90.09
3596	90.07
3595	90.04

3594	90.01
3593	89.97
3592	89.95
3591	89.94
3590	89.93
3589	89.92
3588	89.89
3587	89.83
3586	89.77
3585	89.72
3584	89.67
3583	89.62
3582	89.58
3581	89.54
3580	89.51
3579	89.5
3578	89.5
3577	89.49
3576	89.45
3575	89.39
3574	89.32
3573	89.25
3572	89.19
3571	89.16
3570	89.14
3569	89.12
3568	89.09
3567	89.04
3566	88.97
3565	88.92
3564	88.88
3563	88.86
3562	88.84
3561	88.81
3560	88.77
3559	88.73
3558	88.67
3557	88.62
3556	88.57
3555	88.53
3554	88.47

3553	88.4
3552	88.32
3551	88.25
3550	88.19
3549	88.15
3548	88.12
3547	88.08
3546	88.04
3545	88
3544	87.95
3543	87.91
3542	87.86
3541	87.83
3540	87.8
3539	87.77
3538	87.74
3537	87.71
3536	87.68
3535	87.65
3534	87.62
3533	87.59
3532	87.57
3531	87.55
3530	87.53
3529	87.51
3528	87.49
3527	87.46
3526	87.44
3525	87.42
3524	87.4
3523	87.4
3522	87.4
3521	87.4
3520	87.38
3519	87.36
3518	87.32
3517	87.29
3516	87.26
3515	87.24
3514	87.23
3513	87.2

3512	87.17
3511	87.13
3510	87.1
3509	87.07
3508	87.04
3507	87
3506	86.97
3505	86.93
3504	86.91
3503	86.88
3502	86.85
3501	86.83
3500	86.81
3499	86.8
3498	86.78
3497	86.75
3496	86.71
3495	86.68
3494	86.64
3493	86.61
3492	86.58
3491	86.54
3490	86.5
3489	86.46
3488	86.43
3487	86.4
3486	86.39
3485	86.38
3484	86.36
3483	86.32
3482	86.28
3481	86.25
3480	86.22
3479	86.19
3478	86.16
3477	86.13
3476	86.1
3475	86.08
3474	86.06
3473	86.03
3472	85.99

3471	85.94
3470	85.9
3469	85.87
3468	85.85
3467	85.84
3466	85.83
3465	85.81
3464	85.78
3463	85.74
3462	85.7
3461	85.65
3460	85.61
3459	85.57
3458	85.53
3457	85.5
3456	85.47
3455	85.45
3454	85.43
3453	85.42
3452	85.4
3451	85.39
3450	85.37
3449	85.33
3448	85.29
3447	85.25
3446	85.21
3445	85.18
3444	85.17
3443	85.15
3442	85.13
3441	85.11
3440	85.09
3439	85.07
3438	85.05
3437	85.02
3436	85
3435	84.99
3434	84.98
3433	84.97
3432	84.95
3431	84.94

3430	84.92
3429	84.91
3428	84.9
3427	84.89
3426	84.86
3425	84.83
3424	84.79
3423	84.76
3422	84.73
3421	84.71
3420	84.69
3419	84.68
3418	84.68
3417	84.67
3416	84.66
3415	84.65
3414	84.64
3413	84.62
3412	84.59
3411	84.55
3410	84.52
3409	84.49
3408	84.48
3407	84.49
3406	84.49
3405	84.49
3404	84.48
3403	84.46
3402	84.44
3401	84.43
3400	84.42
3399	84.41
3398	84.39
3397	84.36
3396	84.34
3395	84.34
3394	84.34
3393	84.34
3392	84.34
3391	84.32
3390	84.31

3389	84.3
3388	84.29
3387	84.3
3386	84.3
3385	84.3
3384	84.3
3383	84.3
3382	84.3
3381	84.29
3380	84.27
3379	84.25
3378	84.24
3377	84.23
3376	84.24
3375	84.26
3374	84.26
3373	84.25
3372	84.23
3371	84.21
3370	84.19
3369	84.19
3368	84.2
3367	84.21
3366	84.22
3365	84.22
3364	84.21
3363	84.2
3362	84.19
3361	84.19
3360	84.2
3359	84.22
3358	84.23
3357	84.24
3356	84.24
3355	84.21
3354	84.18
3353	84.15
3352	84.14
3351	84.14
3350	84.16
3349	84.18

3348	84.19
3347	84.19
3346	84.18
3345	84.18
3344	84.2
3343	84.22
3342	84.24
3341	84.25
3340	84.25
3339	84.24
3338	84.23
3337	84.21
3336	84.21
3335	84.21
3334	84.22
3333	84.24
3332	84.27
3331	84.28
3330	84.28
3329	84.27
3328	84.26
3327	84.25
3326	84.25
3325	84.26
3324	84.27
3323	84.27
3322	84.26
3321	84.26
3320	84.26
3319	84.27
3318	84.28
3317	84.29
3316	84.3
3315	84.3
3314	84.3
3313	84.31
3312	84.33
3311	84.35
3310	84.36
3309	84.37
3308	84.37

3307	84.39
3306	84.42
3305	84.44
3304	84.44
3303	84.42
3302	84.41
3301	84.4
3300	84.39
3299	84.38
3298	84.38
3297	84.38
3296	84.38
3295	84.38
3294	84.38
3293	84.39
3292	84.41
3291	84.42
3290	84.43
3289	84.42
3288	84.42
3287	84.42
3286	84.42
3285	84.42
3284	84.44
3283	84.46
3282	84.48
3281	84.5
3280	84.51
3279	84.51
3278	84.52
3277	84.54
3276	84.57
3275	84.6
3274	84.62
3273	84.64
3272	84.66
3271	84.67
3270	84.67
3269	84.66
3268	84.66
3267	84.66

3266	84.68
3265	84.7
3264	84.74
3263	84.77
3262	84.81
3261	84.85
3260	84.88
3259	84.9
3258	84.91
3257	84.92
3256	84.93
3255	84.95
3254	84.98
3253	85.01
3252	85.04
3251	85.07
3250	85.11
3249	85.15
3248	85.17
3247	85.19
3246	85.2
3245	85.21
3244	85.23
3243	85.25
3242	85.27
3241	85.28
3240	85.28
3239	85.29
3238	85.32
3237	85.36
3236	85.4
3235	85.43
3234	85.45
3233	85.46
3232	85.48
3231	85.5
3230	85.52
3229	85.54
3228	85.55
3227	85.57
3226	85.59

3225	85.62
3224	85.64
3223	85.66
3222	85.67
3221	85.69
3220	85.7
3219	85.72
3218	85.74
3217	85.75
3216	85.76
3215	85.78
3214	85.8
3213	85.83
3212	85.88
3211	85.91
3210	85.94
3209	85.96
3208	85.99
3207	86.01
3206	86.03
3205	86.04
3204	86.05
3203	86.07
3202	86.1
3201	86.12
3200	86.14
3199	86.16
3198	86.17
3197	86.18
3196	86.2
3195	86.23
3194	86.27
3193	86.31
3192	86.35
3191	86.39
3190	86.42
3189	86.45
3188	86.47
3187	86.5
3186	86.53
3185	86.55

3184	86.57
3183	86.59
3182	86.61
3181	86.63
3180	86.66
3179	86.69
3178	86.71
3177	86.72
3176	86.73
3175	86.75
3174	86.78
3173	86.82
3172	86.86
3171	86.9
3170	86.92
3169	86.95
3168	86.98
3167	87.01
3166	87.04
3165	87.08
3164	87.11
3163	87.13
3162	87.15
3161	87.17
3160	87.2
3159	87.22
3158	87.24
3157	87.27
3156	87.31
3155	87.37
3154	87.42
3153	87.45
3152	87.47
3151	87.48
3150	87.49
3149	87.52
3148	87.55
3147	87.59
3146	87.61
3145	87.63
3144	87.65

3143	87.67
3142	87.71
3141	87.75
3140	87.79
3139	87.81
3138	87.83
3137	87.84
3136	87.86
3135	87.88
3134	87.91
3133	87.94
3132	87.96
3131	87.99
3130	88.02
3129	88.04
3128	88.06
3127	88.08
3126	88.1
3125	88.13
3124	88.16
3123	88.2
3122	88.24
3121	88.27
3120	88.29
3119	88.31
3118	88.32
3117	88.34
3116	88.37
3115	88.41
3114	88.45
3113	88.48
3112	88.51
3111	88.53
3110	88.55
3109	88.57
3108	88.59
3107	88.61
3106	88.63
3105	88.64
3104	88.65
3103	88.64

3102	88.64
3101	88.64
3100	88.65
3099	88.68
3098	88.71
3097	88.74
3096	88.75
3095	88.76
3094	88.77
3093	88.79
3092	88.82
3091	88.85
3090	88.87
3089	88.9
3088	88.93
3087	88.96
3086	88.98
3085	89
3084	89.01
3083	89.02
3082	89.04
3081	89.06
3080	89.09
3079	89.11
3078	89.13
3077	89.14
3076	89.16
3075	89.17
3074	89.18
3073	89.17
3072	89.17
3071	89.17
3070	89.2
3069	89.24
3068	89.29
3067	89.33
3066	89.35
3065	89.36
3064	89.36
3063	89.36
3062	89.38

3061	89.4
3060	89.43
3059	89.46
3058	89.48
3057	89.51
3056	89.54
3055	89.56
3054	89.59
3053	89.61
3052	89.62
3051	89.64
3050	89.66
3049	89.68
3048	89.7
3047	89.72
3046	89.74
3045	89.76
3044	89.78
3043	89.82
3042	89.85
3041	89.88
3040	89.89
3039	89.9
3038	89.9
3037	89.91
3036	89.94
3035	89.98
3034	90.01
3033	90.02
3032	90.03
3031	90.03
3030	90.04
3029	90.05
3028	90.06
3027	90.08
3026	90.09
3025	90.09
3024	90.09
3023	90.11
3022	90.14
3021	90.17

3020	90.19
3019	90.22
3018	90.23
3017	90.25
3016	90.28
3015	90.3
3014	90.32
3013	90.33
3012	90.32
3011	90.3
3010	90.27
3009	90.26
3008	90.25
3007	90.25
3006	90.25
3005	90.24
3004	90.23
3003	90.22
3002	90.2
3001	90.19
3000	90.17
2999	90.15
2998	90.12
2997	90.09
2996	90.05
2995	90.01
2994	89.98
2993	89.96
2992	89.92
2991	89.88
2990	89.82
2989	89.75
2988	89.66
2987	89.55
2986	89.43
2985	89.3
2984	89.16
2983	89.02
2982	88.87
2981	88.69
2980	88.49

2979	88.25
2978	87.98
2977	87.68
2976	87.35
2975	86.98
2974	86.56
2973	86.09
2972	85.57
2971	85.01
2970	84.41
2969	83.78
2968	83.1
2967	82.39
2966	81.66
2965	80.94
2964	80.25
2963	79.6
2962	79.01
2961	78.46
2960	77.95
2959	77.51
2958	77.14
2957	76.85
2956	76.66
2955	76.57
2954	76.59
2953	76.7
2952	76.9
2951	77.16
2950	77.45
2949	77.72
2948	77.95
2947	78.11
2946	78.18
2945	78.15
2944	78.01
2943	77.76
2942	77.39
2941	76.9
2940	76.3
2939	75.61

2938	74.82
2937	73.96
2936	73.04
2935	72.07
2934	71.05
2933	70.01
2932	68.96
2931	67.92
2930	66.9
2929	65.9
2928	64.95
2927	64.09
2926	63.34
2925	62.74
2924	62.32
2923	62.09
2922	62.07
2921	62.27
2920	62.67
2919	63.23
2918	63.92
2917	64.7
2916	65.52
2915	66.36
2914	67.2
2913	68.02
2912	68.81
2911	69.56
2910	70.25
2909	70.9
2908	71.5
2907	72.07
2906	72.61
2905	73.13
2904	73.62
2903	74.1
2902	74.56
2901	75
2900	75.42
2899	75.82
2898	76.22

2897	76.63
2896	77.04
2895	77.46
2894	77.89
2893	78.33
2892	78.76
2891	79.19
2890	79.6
2889	80.01
2888	80.41
2887	80.8
2886	81.16
2885	81.47
2884	81.72
2883	81.91
2882	82.03
2881	82.09
2880	82.07
2879	81.97
2878	81.8
2877	81.55
2876	81.23
2875	80.89
2874	80.54
2873	80.23
2872	80
2871	79.84
2870	79.74
2869	79.7
2868	79.66
2867	79.61
2866	79.51
2865	79.31
2864	79
2863	78.57
2862	78.03
2861	77.4
2860	76.68
2859	75.91
2858	75.12
2857	74.36

2856	73.7
2855	73.18
2854	72.87
2853	72.79
2852	72.96
2851	73.39
2850	74.03
2849	74.86
2848	75.83
2847	76.87
2846	77.96
2845	79.04
2844	80.1
2843	81.1
2842	82.06
2841	82.97
2840	83.82
2839	84.61
2838	85.34
2837	86
2836	86.59
2835	87.1
2834	87.55
2833	87.95
2832	88.3
2831	88.62
2830	88.91
2829	89.16
2828	89.38
2827	89.58
2826	89.76
2825	89.92
2824	90.07
2823	90.2
2822	90.32
2821	90.42
2820	90.52
2819	90.61
2818	90.7
2817	90.79
2816	90.89

2815	90.98
2814	91.06
2813	91.15
2812	91.22
2811	91.3
2810	91.37
2809	91.43
2808	91.49
2807	91.55
2806	91.6
2805	91.65
2804	91.71
2803	91.76
2802	91.81
2801	91.85
2800	91.9
2799	91.93
2798	91.97
2797	92.01
2796	92.05
2795	92.11
2794	92.16
2793	92.2
2792	92.24
2791	92.28
2790	92.33
2789	92.38
2788	92.41
2787	92.44
2786	92.46
2785	92.5
2784	92.54
2783	92.58
2782	92.61
2781	92.64
2780	92.65
2779	92.66
2778	92.67
2777	92.69
2776	92.72
2775	92.76

2774	92.8
2773	92.83
2772	92.87
2771	92.9
2770	92.93
2769	92.95
2768	92.97
2767	92.99
2766	93
2765	93.02
2764	93.03
2763	93.05
2762	93.07
2761	93.08
2760	93.08
2759	93.08
2758	93.08
2757	93.09
2756	93.1
2755	93.12
2754	93.14
2753	93.15
2752	93.17
2751	93.19
2750	93.22
2749	93.23
2748	93.23
2747	93.23
2746	93.23
2745	93.25
2744	93.27
2743	93.29
2742	93.31
2741	93.34
2740	93.36
2739	93.37
2738	93.37
2737	93.35
2736	93.34
2735	93.33
2734	93.32

2733	93.32
2732	93.31
2731	93.31
2730	93.32
2729	93.32
2728	93.32
2727	93.33
2726	93.34
2725	93.36
2724	93.38
2723	93.41
2722	93.43
2721	93.44
2720	93.45
2719	93.46
2718	93.47
2717	93.48
2716	93.5
2715	93.53
2714	93.55
2713	93.58
2712	93.59
2711	93.61
2710	93.64
2709	93.66
2708	93.67
2707	93.68
2706	93.68
2705	93.69
2704	93.7
2703	93.71
2702	93.72
2701	93.73
2700	93.74
2699	93.75
2698	93.76
2697	93.77
2696	93.78
2695	93.79
2694	93.8
2693	93.8

2692	93.8
2691	93.8
2690	93.79
2689	93.78
2688	93.79
2687	93.8
2686	93.81
2685	93.82
2684	93.83
2683	93.83
2682	93.84
2681	93.86
2680	93.86
2679	93.87
2678	93.86
2677	93.86
2676	93.86
2675	93.86
2674	93.86
2673	93.86
2672	93.87
2671	93.88
2670	93.88
2669	93.89
2668	93.9
2667	93.92
2666	93.93
2665	93.94
2664	93.94
2663	93.93
2662	93.93
2661	93.93
2660	93.92
2659	93.93
2658	93.95
2657	93.97
2656	93.99
2655	94.01
2654	94.02
2653	94.03
2652	94.03

2651	94.04
2650	94.05
2649	94.06
2648	94.07
2647	94.08
2646	94.08
2645	94.09
2644	94.11
2643	94.13
2642	94.16
2641	94.17
2640	94.16
2639	94.15
2638	94.13
2637	94.13
2636	94.13
2635	94.14
2634	94.17
2633	94.19
2632	94.21
2631	94.22
2630	94.23
2629	94.23
2628	94.24
2627	94.25
2626	94.26
2625	94.29
2624	94.32
2623	94.33
2622	94.33
2621	94.31
2620	94.31
2619	94.32
2618	94.34
2617	94.36
2616	94.39
2615	94.41
2614	94.43
2613	94.44
2612	94.44
2611	94.44

2610	94.43
2609	94.43
2608	94.42
2607	94.41
2606	94.4
2605	94.39
2604	94.39
2603	94.39
2602	94.38
2601	94.39
2600	94.4
2599	94.43
2598	94.45
2597	94.47
2596	94.48
2595	94.48
2594	94.48
2593	94.48
2592	94.48
2591	94.47
2590	94.47
2589	94.48
2588	94.51
2587	94.54
2586	94.57
2585	94.58
2584	94.58
2583	94.58
2582	94.59
2581	94.62
2580	94.64
2579	94.66
2578	94.67
2577	94.67
2576	94.68
2575	94.69
2574	94.69
2573	94.69
2572	94.69
2571	94.69
2570	94.7

2569	94.71
2568	94.71
2567	94.71
2566	94.72
2565	94.72
2564	94.74
2563	94.75
2562	94.76
2561	94.76
2560	94.76
2559	94.76
2558	94.78
2557	94.79
2556	94.8
2555	94.8
2554	94.8
2553	94.82
2552	94.82
2551	94.81
2550	94.79
2549	94.77
2548	94.78
2547	94.79
2546	94.81
2545	94.81
2544	94.79
2543	94.77
2542	94.76
2541	94.77
2540	94.79
2539	94.8
2538	94.8
2537	94.79
2536	94.78
2535	94.78
2534	94.78
2533	94.78
2532	94.78
2531	94.78
2530	94.79
2529	94.81

2528	94.84
2527	94.87
2526	94.88
2525	94.87
2524	94.87
2523	94.87
2522	94.87
2521	94.86
2520	94.85
2519	94.84
2518	94.85
2517	94.86
2516	94.89
2515	94.91
2514	94.91
2513	94.9
2512	94.9
2511	94.92
2510	94.93
2509	94.94
2508	94.94
2507	94.93
2506	94.93
2505	94.95
2504	94.96
2503	94.96
2502	94.94
2501	94.94
2500	94.95
2499	94.98
2498	95.01
2497	95.04
2496	95.06
2495	95.05
2494	95.04
2493	95.02
2492	95.02
2491	95.03
2490	95.03
2489	95.01
2488	95

2487	95
2486	95.02
2485	95.02
2484	95.01
2483	94.99
2482	94.98
2481	94.99
2480	95.01
2479	95.03
2478	95.03
2477	95.01
2476	95
2475	95
2474	95.03
2473	95.05
2472	95.07
2471	95.08
2470	95.08
2469	95.09
2468	95.1
2467	95.11
2466	95.12
2465	95.13
2464	95.15
2463	95.16
2462	95.14
2461	95.1
2460	95.06
2459	95.05
2458	95.05
2457	95.07
2456	95.08
2455	95.08
2454	95.08
2453	95.07
2452	95.06
2451	95.06
2450	95.08
2449	95.09
2448	95.09
2447	95.08

2446	95.06
2445	95.05
2444	95.05
2443	95.06
2442	95.08
2441	95.11
2440	95.14
2439	95.16
2438	95.17
2437	95.15
2436	95.14
2435	95.13
2434	95.13
2433	95.13
2432	95.13
2431	95.13
2430	95.13
2429	95.14
2428	95.15
2427	95.17
2426	95.19
2425	95.19
2424	95.18
2423	95.15
2422	95.13
2421	95.13
2420	95.14
2419	95.16
2418	95.19
2417	95.22
2416	95.22
2415	95.22
2414	95.22
2413	95.22
2412	95.22
2411	95.23
2410	95.24
2409	95.25
2408	95.24
2407	95.23
2406	95.22

2405	95.21
2404	95.2
2403	95.18
2402	95.16
2401	95.14
2400	95.14
2399	95.17
2398	95.21
2397	95.24
2396	95.26
2395	95.26
2394	95.25
2393	95.24
2392	95.23
2391	95.21
2390	95.2
2389	95.19
2388	95.18
2387	95.18
2386	95.2
2385	95.22
2384	95.26
2383	95.28
2382	95.31
2381	95.32
2380	95.32
2379	95.32
2378	95.31
2377	95.32
2376	95.32
2375	95.33
2374	95.33
2373	95.34
2372	95.35
2371	95.35
2370	95.34
2369	95.35
2368	95.38
2367	95.42
2366	95.46
2365	95.46

2364	95.43
2363	95.41
2362	95.38
2361	95.36
2360	95.35
2359	95.34
2358	95.36
2357	95.37
2356	95.37
2355	95.36
2354	95.34
2353	95.34
2352	95.35
2351	95.37
2350	95.38
2349	95.38
2348	95.37
2347	95.34
2346	95.32
2345	95.31
2344	95.32
2343	95.33
2342	95.33
2341	95.33
2340	95.33
2339	95.34
2338	95.34
2337	95.35
2336	95.34
2335	95.32
2334	95.29
2333	95.26
2332	95.26
2331	95.28
2330	95.31
2329	95.32
2328	95.3
2327	95.25
2326	95.18
2325	95.11
2324	95.07

2323	95.07
2322	95.1
2321	95.15
2320	95.2
2319	95.21
2318	95.21
2317	95.21
2316	95.21
2315	95.22
2314	95.25
2313	95.27
2312	95.29
2311	95.29
2310	95.27
2309	95.24
2308	95.22
2307	95.21
2306	95.23
2305	95.26
2304	95.28
2303	95.29
2302	95.27
2301	95.26
2300	95.25
2299	95.26
2298	95.25
2297	95.23
2296	95.19
2295	95.15
2294	95.14
2293	95.14
2292	95.15
2291	95.16
2290	95.17
2289	95.18
2288	95.18
2287	95.18
2286	95.17
2285	95.17
2284	95.17
2283	95.18

2282	95.18
2281	95.18
2280	95.18
2279	95.18
2278	95.2
2277	95.2
2276	95.18
2275	95.13
2274	95.1
2273	95.08
2272	95.11
2271	95.16
2270	95.24
2269	95.32
2268	95.38
2267	95.41
2266	95.4
2265	95.39
2264	95.4
2263	95.42
2262	95.45
2261	95.46
2260	95.47
2259	95.49
2258	95.55
2257	95.6
2256	95.61
2255	95.56
2254	95.48
2253	95.42
2252	95.4
2251	95.41
2250	95.42
2249	95.4
2248	95.38
2247	95.38
2246	95.39
2245	95.42
2244	95.45
2243	95.48
2242	95.49

2241	95.49
2240	95.48
2239	95.46
2238	95.44
2237	95.42
2236	95.41
2235	95.41
2234	95.43
2233	95.44
2232	95.45
2231	95.46
2230	95.47
2229	95.49
2228	95.53
2227	95.59
2226	95.63
2225	95.62
2224	95.57
2223	95.53
2222	95.51
2221	95.52
2220	95.51
2219	95.49
2218	95.47
2217	95.49
2216	95.51
2215	95.54
2214	95.55
2213	95.58
2212	95.62
2211	95.66
2210	95.68
2209	95.66
2208	95.64
2207	95.65
2206	95.66
2205	95.67
2204	95.69
2203	95.75
2202	95.84
2201	95.95

2200	96.01
2199	96
2198	95.91
2197	95.8
2196	95.73
2195	95.75
2194	95.83
2193	95.94
2192	96.04
2191	96.11
2190	96.15
2189	96.14
2188	96.08
2187	96
2186	95.96
2185	95.96
2184	95.98
2183	95.99
2182	96.01
2181	96.04
2180	96.06
2179	96.05
2178	96.02
2177	96
2176	96.04
2175	96.13
2174	96.17
2173	96.13
2172	96.02
2171	95.92
2170	95.84
2169	95.78
2168	95.77
2167	95.83
2166	95.99
2165	96.14
2164	96.21
2163	96.19
2162	96.18
2161	96.28
2160	96.48

2159	96.69
2158	96.8
2157	96.78
2156	96.68
2155	96.55
2154	96.42
2153	96.31
2152	96.23
2151	96.22
2150	96.24
2149	96.26
2148	96.26
2147	96.26
2146	96.28
2145	96.27
2144	96.21
2143	96.11
2142	96.01
2141	95.97
2140	95.99
2139	96.04
2138	96.08
2137	96.08
2136	96.04
2135	95.97
2134	95.91
2133	95.89
2132	95.91
2131	95.94
2130	95.92
2129	95.85
2128	95.77
2127	95.73
2126	95.75
2125	95.81
2124	95.84
2123	95.81
2122	95.74
2121	95.68
2120	95.66
2119	95.66

2118	95.65
2117	95.61
2116	95.56
2115	95.53
2114	95.53
2113	95.56
2112	95.59
2111	95.59
2110	95.57
2109	95.53
2108	95.48
2107	95.44
2106	95.43
2105	95.48
2104	95.56
2103	95.65
2102	95.67
2101	95.64
2100	95.62
2099	95.64
2098	95.68
2097	95.72
2096	95.72
2095	95.72
2094	95.72
2093	95.72
2092	95.72
2091	95.73
2090	95.73
2089	95.73
2088	95.72
2087	95.71
2086	95.71
2085	95.7
2084	95.7
2083	95.71
2082	95.73
2081	95.75
2080	95.76
2079	95.77
2078	95.79

2077	95.8
2076	95.82
2075	95.83
2074	95.81
2073	95.77
2072	95.74
2071	95.76
2070	95.81
2069	95.85
2068	95.86
2067	95.85
2066	95.83
2065	95.79
2064	95.76
2063	95.77
2062	95.82
2061	95.91
2060	95.99
2059	96.06
2058	96.09
2057	96.07
2056	96.02
2055	95.99
2054	95.96
2053	95.93
2052	95.91
2051	95.93
2050	96.01
2049	96.09
2048	96.13
2047	96.13
2046	96.13
2045	96.12
2044	96.11
2043	96.12
2042	96.13
2041	96.12
2040	96.1
2039	96.08
2038	96.1
2037	96.14

2036	96.22
2035	96.33
2034	96.44
2033	96.53
2032	96.59
2031	96.62
2030	96.65
2029	96.69
2028	96.74
2027	96.86
2026	97.01
2025	97.14
2024	97.17
2023	97.11
2022	96.98
2021	96.83
2020	96.69
2019	96.59
2018	96.52
2017	96.49
2016	96.48
2015	96.51
2014	96.54
2013	96.54
2012	96.55
2011	96.59
2010	96.68
2009	96.74
2008	96.77
2007	96.76
2006	96.72
2005	96.63
2004	96.52
2003	96.42
2002	96.35
2001	96.3
2000	96.28
1999	96.28
1998	96.3
1997	96.31
1996	96.29

1995	96.25
1994	96.21
1993	96.19
1992	96.22
1991	96.3
1990	96.43
1989	96.55
1988	96.63
1987	96.63
1986	96.56
1985	96.44
1984	96.35
1983	96.29
1982	96.23
1981	96.17
1980	96.14
1979	96.2
1978	96.33
1977	96.46
1976	96.55
1975	96.6
1974	96.6
1973	96.57
1972	96.54
1971	96.51
1970	96.5
1969	96.48
1968	96.47
1967	96.48
1966	96.45
1965	96.36
1964	96.26
1963	96.22
1962	96.24
1961	96.27
1960	96.29
1959	96.29
1958	96.25
1957	96.18
1956	96.11
1955	96.1

1954	96.12
1953	96.15
1952	96.14
1951	96.08
1950	96
1949	95.92
1948	95.87
1947	95.85
1946	95.85
1945	95.84
1944	95.86
1943	95.92
1942	96
1941	96.05
1940	96.07
1939	96.06
1938	96.06
1937	96.06
1936	96.05
1935	96.05
1934	96.02
1933	95.95
1932	95.86
1931	95.79
1930	95.76
1929	95.74
1928	95.74
1927	95.76
1926	95.8
1925	95.83
1924	95.84
1923	95.85
1922	95.85
1921	95.83
1920	95.78
1919	95.74
1918	95.74
1917	95.75
1916	95.75
1915	95.74
1914	95.74

1913	95.74
1912	95.73
1911	95.72
1910	95.71
1909	95.71
1908	95.71
1907	95.72
1906	95.73
1905	95.72
1904	95.7
1903	95.68
1902	95.68
1901	95.68
1900	95.67
1899	95.67
1898	95.65
1897	95.61
1896	95.57
1895	95.55
1894	95.54
1893	95.52
1892	95.48
1891	95.44
1890	95.42
1889	95.43
1888	95.45
1887	95.46
1886	95.46
1885	95.45
1884	95.44
1883	95.44
1882	95.46
1881	95.49
1880	95.51
1879	95.51
1878	95.49
1877	95.47
1876	95.45
1875	95.44
1874	95.45
1873	95.45

1872	95.44
1871	95.43
1870	95.43
1869	95.41
1868	95.38
1867	95.37
1866	95.36
1865	95.37
1864	95.38
1863	95.41
1862	95.44
1861	95.47
1860	95.47
1859	95.48
1858	95.47
1857	95.44
1856	95.4
1855	95.37
1854	95.37
1853	95.38
1852	95.39
1851	95.41
1850	95.44
1849	95.48
1848	95.51
1847	95.52
1846	95.52
1845	95.5
1844	95.49
1843	95.49
1842	95.48
1841	95.44
1840	95.39
1839	95.36
1838	95.35
1837	95.36
1836	95.38
1835	95.42
1834	95.45
1833	95.43
1832	95.36

1831	95.29
1830	95.27
1829	95.28
1828	95.28
1827	95.27
1826	95.26
1825	95.28
1824	95.3
1823	95.29
1822	95.27
1821	95.26
1820	95.25
1819	95.26
1818	95.27
1817	95.28
1816	95.28
1815	95.27
1814	95.25
1813	95.23
1812	95.22
1811	95.23
1810	95.24
1809	95.22
1808	95.19
1807	95.15
1806	95.12
1805	95.08
1804	95.04
1803	95.01
1802	94.98
1801	94.97
1800	94.98
1799	94.99
1798	94.99
1797	94.97
1796	94.93
1795	94.88
1794	94.83
1793	94.79
1792	94.79
1791	94.82

1790	94.86
1789	94.87
1788	94.86
1787	94.86
1786	94.86
1785	94.87
1784	94.87
1783	94.86
1782	94.85
1781	94.84
1780	94.84
1779	94.85
1778	94.85
1777	94.84
1776	94.8
1775	94.75
1774	94.69
1773	94.64
1772	94.63
1771	94.67
1770	94.69
1769	94.68
1768	94.65
1767	94.63
1766	94.61
1765	94.56
1764	94.51
1763	94.49
1762	94.49
1761	94.49
1760	94.46
1759	94.4
1758	94.34
1757	94.28
1756	94.23
1755	94.18
1754	94.1
1753	93.99
1752	93.87
1751	93.76
1750	93.67

1749	93.58
1748	93.47
1747	93.35
1746	93.2
1745	93.04
1744	92.86
1743	92.69
1742	92.53
1741	92.36
1740	92.21
1739	92.11
1738	92.05
1737	91.97
1736	91.86
1735	91.75
1734	91.69
1733	91.68
1732	91.67
1731	91.66
1730	91.66
1729	91.67
1728	91.69
1727	91.73
1726	91.78
1725	91.83
1724	91.88
1723	91.92
1722	91.94
1721	91.95
1720	91.92
1719	91.89
1718	91.9
1717	91.93
1716	91.94
1715	91.93
1714	91.9
1713	91.86
1712	91.82
1711	91.78
1710	91.74
1709	91.7

1708	91.64
1707	91.57
1706	91.51
1705	91.45
1704	91.37
1703	91.25
1702	91.12
1701	90.94
1700	90.75
1699	90.63
1698	90.52
1697	90.36
1696	90.17
1695	90
1694	89.89
1693	89.79
1692	89.67
1691	89.54
1690	89.39
1689	89.23
1688	89.07
1687	88.9
1686	88.71
1685	88.45
1684	88.17
1683	87.98
1682	87.83
1681	87.67
1680	87.5
1679	87.33
1678	87.16
1677	86.97
1676	86.73
1675	86.5
1674	86.32
1673	86.16
1672	85.99
1671	85.8
1670	85.58
1669	85.37
1668	85.17

1667	84.99
1666	84.82
1665	84.64
1664	84.43
1663	84.21
1662	83.99
1661	83.8
1660	83.62
1659	83.46
1658	83.32
1657	83.21
1656	83.1
1655	83
1654	82.88
1653	82.72
1652	82.62
1651	82.57
1650	82.54
1649	82.53
1648	82.52
1647	82.49
1646	82.47
1645	82.45
1644	82.44
1643	82.46
1642	82.48
1641	82.5
1640	82.51
1639	82.52
1638	82.55
1637	82.58
1636	82.58
1635	82.57
1634	82.58
1633	82.61
1632	82.65
1631	82.72
1630	82.8
1629	82.89
1628	82.99
1627	83.09

1626	83.18
1625	83.27
1624	83.39
1623	83.54
1622	83.68
1621	83.79
1620	83.88
1619	83.97
1618	84.08
1617	84.21
1616	84.38
1615	84.54
1614	84.66
1613	84.75
1612	84.84
1611	84.93
1610	85.03
1609	85.11
1608	85.18
1607	85.25
1606	85.31
1605	85.36
1604	85.39
1603	85.42
1602	85.45
1601	85.48
1600	85.52
1599	85.57
1598	85.65
1597	85.73
1596	85.82
1595	85.9
1594	85.96
1593	86.01
1592	86.06
1591	86.12
1590	86.17
1589	86.22
1588	86.25
1587	86.28
1586	86.3

1585	86.31
1584	86.32
1583	86.31
1582	86.29
1581	86.27
1580	86.26
1579	86.26
1578	86.27
1577	86.27
1576	86.27
1575	86.27
1574	86.25
1573	86.24
1572	86.24
1571	86.26
1570	86.29
1569	86.32
1568	86.34
1567	86.33
1566	86.3
1565	86.28
1564	86.26
1563	86.24
1562	86.23
1561	86.23
1560	86.22
1559	86.16
1558	86.1
1557	86.04
1556	85.99
1555	85.97
1554	85.97
1553	85.95
1552	85.93
1551	85.91
1550	85.9
1549	85.89
1548	85.86
1547	85.83
1546	85.81
1545	85.8

1544	85.82
1543	85.83
1542	85.85
1541	85.86
1540	85.84
1539	85.83
1538	85.82
1537	85.83
1536	85.86
1535	85.92
1534	85.99
1533	86.04
1532	86.08
1531	86.1
1530	86.12
1529	86.15
1528	86.2
1527	86.24
1526	86.28
1525	86.31
1524	86.33
1523	86.35
1522	86.37
1521	86.38
1520	86.39
1519	86.39
1518	86.39
1517	86.38
1516	86.37
1515	86.36
1514	86.36
1513	86.39
1512	86.43
1511	86.49
1510	86.56
1509	86.63
1508	86.7
1507	86.8
1506	86.89
1505	86.91
1504	86.9

1503	86.91
1502	86.94
1501	86.96
1500	86.95
1499	86.93
1498	86.9
1497	86.86
1496	86.83
1495	86.81
1494	86.81
1493	86.79
1492	86.75
1491	86.71
1490	86.67
1489	86.62
1488	86.58
1487	86.57
1486	86.55
1485	86.5
1484	86.42
1483	86.33
1482	86.21
1481	86.07
1480	85.9
1479	85.73
1478	85.54
1477	85.29
1476	84.99
1475	84.64
1474	84.16
1473	83.44
1472	82.5
1471	81.56
1470	80.7
1469	79.92
1468	79.22
1467	78.64
1466	78.16
1465	77.77
1464	77.48
1463	77.3

1462	77.2
1461	77.15
1460	77.11
1459	77.09
1458	77.04
1457	76.98
1456	77.02
1455	77.16
1454	77.39
1453	77.67
1452	77.98
1451	78.28
1450	78.55
1449	78.78
1448	79
1447	79.21
1446	79.41
1445	79.61
1444	79.81
1443	80.01
1442	80.2
1441	80.37
1440	80.52
1439	80.65
1438	80.78
1437	80.92
1436	81.08
1435	81.23
1434	81.37
1433	81.51
1432	81.67
1431	81.82
1430	81.95
1429	82.05
1428	82.14
1427	82.2
1426	82.25
1425	82.3
1424	82.34
1423	82.37
1422	82.37

1421	82.38
1420	82.38
1419	82.39
1418	82.4
1417	82.39
1416	82.38
1415	82.38
1414	82.39
1413	82.41
1412	82.44
1411	82.47
1410	82.51
1409	82.56
1408	82.65
1407	82.76
1406	82.91
1405	83.08
1404	83.24
1403	83.37
1402	83.48
1401	83.57
1400	83.68
1399	83.79
1398	83.89
1397	83.97
1396	84.06
1395	84.15
1394	84.23
1393	84.31
1392	84.36
1391	84.39
1390	84.4
1389	84.39
1388	84.36
1387	84.29
1386	84.17
1385	84.03
1384	83.84
1383	83.6
1382	83.29
1381	82.92

1380	82.52
1379	82.16
1378	81.94
1377	81.9
1376	82.07
1375	82.43
1374	82.9
1373	83.38
1372	83.77
1371	84.06
1370	84.27
1369	84.42
1368	84.53
1367	84.62
1366	84.73
1365	84.88
1364	85.09
1363	85.33
1362	85.56
1361	85.76
1360	85.92
1359	86.06
1358	86.18
1357	86.29
1356	86.37
1355	86.44
1354	86.49
1353	86.54
1352	86.59
1351	86.65
1350	86.72
1349	86.79
1348	86.87
1347	86.95
1346	87.02
1345	87.08
1344	87.14
1343	87.21
1342	87.26
1341	87.32
1340	87.38

1339	87.42
1338	87.45
1337	87.49
1336	87.53
1335	87.58
1334	87.64
1333	87.69
1332	87.73
1331	87.75
1330	87.76
1329	87.78
1328	87.82
1327	87.85
1326	87.87
1325	87.89
1324	87.91
1323	87.91
1322	87.92
1321	87.91
1320	87.89
1319	87.87
1318	87.84
1317	87.81
1316	87.79
1315	87.77
1314	87.76
1313	87.76
1312	87.75
1311	87.74
1310	87.73
1309	87.71
1308	87.69
1307	87.68
1306	87.66
1305	87.65
1304	87.64
1303	87.62
1302	87.6
1301	87.57
1300	87.55
1299	87.52

1298	87.5
1297	87.48
1296	87.45
1295	87.43
1294	87.39
1293	87.36
1292	87.32
1291	87.27
1290	87.22
1289	87.17
1288	87.14
1287	87.13
1286	87.1
1285	87.08
1284	87.05
1283	87.02
1282	87.01
1281	86.99
1280	86.98
1279	86.95
1278	86.92
1277	86.88
1276	86.82
1275	86.77
1274	86.71
1273	86.65
1272	86.57
1271	86.47
1270	86.33
1269	86.18
1268	86
1267	85.8
1266	85.55
1265	85.26
1264	84.96
1263	84.68
1262	84.46
1261	84.32
1260	84.27
1259	84.29
1258	84.37

1257	84.51
1256	84.67
1255	84.82
1254	84.95
1253	85.04
1252	85.1
1251	85.14
1250	85.16
1249	85.18
1248	85.19
1247	85.19
1246	85.18
1245	85.15
1244	85.1
1243	85.06
1242	85.02
1241	84.97
1240	84.92
1239	84.86
1238	84.79
1237	84.73
1236	84.66
1235	84.6
1234	84.52
1233	84.44
1232	84.34
1231	84.25
1230	84.16
1229	84.07
1228	83.97
1227	83.86
1226	83.76
1225	83.64
1224	83.53
1223	83.43
1222	83.33
1221	83.21
1220	83.08
1219	82.96
1218	82.84
1217	82.72

1216	82.61
1215	82.5
1214	82.4
1213	82.3
1212	82.19
1211	82.08
1210	81.98
1209	81.88
1208	81.78
1207	81.67
1206	81.55
1205	81.42
1204	81.29
1203	81.17
1202	81.06
1201	80.95
1200	80.82
1199	80.68
1198	80.52
1197	80.34
1196	80.16
1195	79.97
1194	79.79
1193	79.61
1192	79.41
1191	79.21
1190	79.01
1189	78.82
1188	78.63
1187	78.43
1186	78.22
1185	78
1184	77.78
1183	77.56
1182	77.33
1181	77.1
1180	76.87
1179	76.65
1178	76.44
1177	76.24
1176	76.05

1175	75.86
1174	75.67
1173	75.49
1172	75.31
1171	75.15
1170	74.98
1169	74.79
1168	74.6
1167	74.42
1166	74.26
1165	74.12
1164	74.01
1163	73.94
1162	73.93
1161	73.98
1160	74.09
1159	74.21
1158	74.3
1157	74.33
1156	74.3
1155	74.23
1154	74.14
1153	74.03
1152	73.91
1151	73.79
1150	73.67
1149	73.54
1148	73.42
1147	73.28
1146	73.12
1145	72.93
1144	72.74
1143	72.54
1142	72.35
1141	72.14
1140	71.91
1139	71.67
1138	71.43
1137	71.17
1136	70.87
1135	70.55

1134	70.2
1133	69.82
1132	69.43
1131	69.03
1130	68.62
1129	68.2
1128	67.78
1127	67.37
1126	66.97
1125	66.59
1124	66.22
1123	65.85
1122	65.48
1121	65.09
1120	64.66
1119	64.19
1118	63.7
1117	63.21
1116	62.73
1115	62.28
1114	61.87
1113	61.5
1112	61.16
1111	60.84
1110	60.54
1109	60.22
1108	59.87
1107	59.53
1106	59.2
1105	58.88
1104	58.55
1103	58.23
1102	57.92
1101	57.59
1100	57.23
1099	56.89
1098	56.57
1097	56.28
1096	56
1095	55.74
1094	55.46

1093	55.17
1092	54.89
1091	54.63
1090	54.4
1089	54.17
1088	53.95
1087	53.76
1086	53.58
1085	53.41
1084	53.23
1083	53.05
1082	52.86
1081	52.67
1080	52.48
1079	52.3
1078	52.15
1077	52.02
1076	51.89
1075	51.78
1074	51.67
1073	51.54
1072	51.4
1071	51.26
1070	51.12
1069	50.96
1068	50.79
1067	50.6
1066	50.4
1065	50.18
1064	49.93
1063	49.68
1062	49.43
1061	49.16
1060	48.88
1059	48.59
1058	48.3
1057	47.98
1056	47.64
1055	47.27
1054	46.88
1053	46.46

1052	46.02
1051	45.57
1050	45.13
1049	44.65
1048	44.12
1047	43.57
1046	43.02
1045	42.43
1044	41.82
1043	41.2
1042	40.54
1041	39.82
1040	39.05
1039	38.27
1038	37.5
1037	36.73
1036	35.98
1035	35.26
1034	34.6
1033	33.97
1032	33.38
1031	32.88
1030	32.47
1029	32.14
1028	31.89
1027	31.75
1026	31.7
1025	31.68
1024	31.67
1023	31.67
1022	31.67
1021	31.66
1020	31.62
1019	31.56
1018	31.48
1017	31.34
1016	31.15
1015	30.95
1014	30.71
1013	30.38
1012	29.93

1011	29.43
1010	28.92
1009	28.4
1008	27.91
1007	27.5
1006	27.2
1005	26.99
1004	26.84
1003	26.77
1002	26.76
1001	26.79
1000	26.83
999	26.91
998	27.03
997	27.14
996	27.25
995	27.39
994	27.55
993	27.72
992	27.87
991	28.01
990	28.14
989	28.26
988	28.37
987	28.51
986	28.69
985	28.87
984	29.02
983	29.17
982	29.34
981	29.53
980	29.74
979	29.97
978	30.24
977	30.5
976	30.78
975	31.08
974	31.43
973	31.79
972	32.15
971	32.53

970	32.93
969	33.33
968	33.72
967	34.13
966	34.57
965	35.01
964	35.47
963	35.94
962	36.41
961	36.85
960	37.27
959	37.69
958	38.13
957	38.56
956	38.96
955	39.34
954	39.73
953	40.09
952	40.44
951	40.77
950	41.07
949	41.34
948	41.58
947	41.8
946	42
945	42.17
944	42.3
943	42.41
942	42.52
941	42.61
940	42.7
939	42.8
938	42.93
937	43.06
936	43.18
935	43.31
934	43.46
933	43.61
932	43.75
931	43.89
930	44.06

929	44.23
928	44.38
927	44.51
926	44.6
925	44.66
924	44.68
923	44.67
922	44.64
921	44.56
920	44.43
919	44.27
918	44.08
917	43.85
916	43.61
915	43.39
914	43.19
913	43.03
912	42.93
911	42.96
910	43.13
909	43.41
908	43.74
907	44.11
906	44.53
905	44.99
904	45.48
903	46
902	46.54
901	47.09
900	47.64
899	48.2
898	48.77
897	49.31
896	49.81
895	50.29
894	50.76
893	51.22
892	51.68
891	52.12
890	52.54
889	52.91

888	53.23
887	53.54
886	53.81
885	54.04
884	54.21
883	54.35
882	54.49
881	54.6
880	54.68
879	54.73
878	54.74
877	54.72
876	54.69
875	54.67
874	54.73
873	54.86
872	55.11
871	55.49
870	56
869	56.58
868	57.15
867	57.66
866	58.09
865	58.45
864	58.78
863	59.11
862	59.47
861	59.85
860	60.25
859	60.64
858	61.01
857	61.33
856	61.62
855	61.91
854	62.22
853	62.53
852	62.81
851	63.05
850	63.26
849	63.44
848	63.6

847	63.77
846	63.94
845	64.1
844	64.21
843	64.32
842	64.41
841	64.5
840	64.55
839	64.57
838	64.57
837	64.53
836	64.46
835	64.39
834	64.34
833	64.29
832	64.23
831	64.18
830	64.15
829	64.13
828	64.13
827	64.14
826	64.16
825	64.18
824	64.21
823	64.27
822	64.34
821	64.42
820	64.46
819	64.47
818	64.45
817	64.42
816	64.37
815	64.32
814	64.24
813	64.11
812	63.92
811	63.65
810	63.31
809	62.89
808	62.38
807	61.76

806	61.05
805	60.25
804	59.41
803	58.54
802	57.7
801	56.9
800	56.18
799	55.6
798	55.18
797	54.93
796	54.82
795	54.84
794	54.99
793	55.21
792	55.47
791	55.74
790	56
789	56.22
788	56.39
787	56.53
786	56.63
785	56.66
784	56.58
783	56.42
782	56.22
781	55.98
780	55.73
779	55.51
778	55.38
777	55.35
776	55.42
775	55.58
774	55.81
773	56.08
772	56.36
771	56.64
770	56.9
769	57.14
768	57.32
767	57.47
766	57.58

765	57.64
764	57.66
763	57.65
762	57.64
761	57.63
760	57.6
759	57.56
758	57.5
757	57.43
756	57.35
755	57.31
754	57.31
753	57.33
752	57.32
751	57.29
750	57.25
749	57.23
748	57.23
747	57.24
746	57.25
745	57.27
744	57.28
743	57.32
742	57.4
741	57.54
740	57.71
739	57.88
738	58.04
737	58.17
736	58.3
735	58.42
734	58.52
733	58.59
732	58.62
731	58.61
730	58.58
729	58.54
728	58.5
727	58.46
726	58.42
725	58.36

724	58.3
723	58.24
722	58.22
721	58.24
720	58.3
719	58.4
718	58.52
717	58.62
716	58.64
715	58.57
714	58.45
713	58.33
712	58.26
711	58.24
710	58.21
709	58.11
708	57.94
707	57.74
706	57.53
705	57.27
704	56.95
703	56.57
702	56.17
701	55.73
700	55.25
699	54.73
698	54.17
697	53.58
696	53.02
695	52.57
694	52.28
693	52.13
692	52.08
691	52.08
690	52.1
689	52.11
688	52.12
687	52.15
686	52.21
685	52.26
684	52.27

683	52.28
682	52.33
681	52.4
680	52.49
679	52.6
678	52.69
677	52.72
676	52.71
675	52.68
674	52.68
673	52.72
672	52.79
671	52.87
670	52.95
669	52.98
668	52.94
667	52.92
666	52.99
665	53.12
664	53.23
663	53.3
662	53.35
661	53.39
660	53.44
659	53.48
658	53.51
657	53.49
656	53.43
655	53.35
654	53.26
653	53.17
652	53.08
651	53.02
650	52.97
649	52.9
648	52.81
647	52.72
646	52.66
645	52.61
644	52.57
643	52.57

642	52.59
641	52.61
640	52.58
639	52.55
638	52.56
637	52.61
636	52.69
635	52.78
634	52.85
633	52.9
632	52.91
631	52.92
630	52.95
629	53
628	53.05
627	53.09
626	53.1
625	53.09
624	53.07
623	53.06
622	53.07
621	53.07
620	53.05
619	53.01
618	52.93
617	52.8
616	52.61
615	52.43
614	52.29
613	52.18
612	52.09
611	52.01
610	51.93
609	51.81
608	51.63
607	51.41
606	51.21
605	51.05
604	50.97
603	50.96
602	51

601	51.02
600	50.96
599	50.83
598	50.69
597	50.56
596	50.44
595	50.33
594	50.21
593	50.09
592	49.95
591	49.79
590	49.6
589	49.38
588	49.13
587	48.88
586	48.66
585	48.44
584	48.19
583	47.92
582	47.69
581	47.51
580	47.36
579	47.22
578	47.03
577	46.8
576	46.59
575	46.45
574	46.37
573	46.27
572	46.11
571	45.94
570	45.78
569	45.6
568	45.33
567	45.01
566	44.7
565	44.4
564	44.11
563	43.8
562	43.49
561	43.15

560	42.8
559	42.44
558	42.06
557	41.65
556	41.26
555	40.99
554	40.78
553	40.51
552	40.08
551	39.57
550	39.13
549	38.78
548	38.42
547	38.01
546	37.52
545	36.91
544	36.19
543	35.45
542	34.77
541	34.18
540	33.65
539	33.18
538	32.75
537	32.28
536	31.76
535	31.28
534	30.89
533	30.53
532	30.17
531	29.86
530	29.66
529	29.56
528	29.5
527	29.46
526	29.42
525	29.34
524	29.22
523	29.16
522	29.23
521	29.38
520	29.51

519	29.62
518	29.69
517	29.69
516	29.64
515	29.63
514	29.72
513	29.85
512	29.95
511	30.04
510	30.14
509	30.21
508	30.25
507	30.33
506	30.49
505	30.62
504	30.67
503	30.71
502	30.78
501	30.89
500	31
499	31.17
498	31.38
497	31.53
496	31.59
495	31.69
494	31.89
493	32.1
492	32.17
491	32.11
490	32.04
489	31.95
488	31.82
487	31.64
486	31.39
485	31
484	30.48
483	29.97
482	29.53
481	29.07
480	28.51
479	27.9

478	27.3
477	26.64
476	25.9
475	25.15
474	24.41
473	23.54
472	22.53
471	21.62
470	21.03
469	20.61
468	20.14
467	19.58
466	18.99
465	18.4
464	17.87
463	17.53
462	17.4
461	17.3
460	17.09
459	16.91
458	16.85
457	16.76
456	16.57
455	16.46
454	16.52
453	16.6
452	16.56
451	16.59
450	16.83
449	17.11
448	17.16
447	17.02
446	16.89
445	16.83
444	16.8
443	16.92
442	17.21
441	17.47
440	17.52
439	17.46
438	17.41

437	17.31
436	17.11
435	16.92
434	16.81
433	16.66
432	16.39
431	16.2
430	16.21
429	16.22
428	16.06
427	15.88
426	15.9
425	15.95
424	15.81
423	15.6
422	15.47
421	15.27
420	14.89
419	14.8
418	15.17
417	15.18
416	14.57
415	14.02
414	14.09
413	14.55
412	14.85
411	14.91
410	15.08
409	15.37
408	15.58
407	15.8
406	16.25
405	16.65
404	16.87
403	17.28
402	18.23
401	18.91
400	18.39

Appendix B:

Sample Calculations

Appendix B: Sample Calculations

Coagulation Removal Efficiencies

All calculations are based on the 100 mg/L (average) PAC Dosage.

COD

$$COD\ \%\ removal = \frac{COD_i - COD_t}{COD_i}\ x\ 100$$

$$COD\ \%\ removal = \frac{1220 - 385}{1220}\ x\ 100$$

$$COD\ \%\ removal = 68.44\ \%$$

Turbidity

$$Turbidity\ \%\ removal = \frac{T_i - T_t}{T_i}$$

$$Turbidity\ \%\ removal = \frac{99.4 - 4.275}{99.4}$$

$$Turbidity\ \%\ removal = 95.70\ \%$$

FOG

$$FOG\ \%\ removal = \frac{FOG_i - FOG_t}{FOG_i}\ x\ 100$$

$$FOG\ \%\ removal = \frac{48.2 - 1}{48.2}\ x\ 100$$

$$FOG\ \%\ removal = 97.93\ \%$$

Anionic Surfactants

$$Anionic\ Surfactant\ \%\ removal = \frac{AS_i - AS_t}{AS_i}\ x\ 100$$

$$Anionic\ Surfactant\ \%\ removal = \frac{25.9 - 20.75}{25.9}\ x\ 100$$

$$Anionic\ Surfactant\ \%\ removal = 19.88\ \%$$

Electrochemical Oxidation Calculations

Determining Current Density

Example: 10 mA/cm^2

$$Current\ Density\ \left(\frac{mA}{cm^2}\right) = \frac{Applied\ Current}{Electrode\ \ Area\ (Both\ sides)}$$

$$Current\ Density\ \left(\frac{mA}{cm^2}\right) = \frac{2A\ x\ 1000}{(10\ cm\ x\ 10\ cm) + (10\ cm\ x\ 10\ cm)}$$

$$Current\ Density\ \left(\frac{mA}{cm^2}\right) = \ 10\ mA/cm^2$$

Example: 5.5 mA/cm^2

$$Current\ Density\ \left(\frac{mA}{cm^2}\right) = \frac{Applied\ Current}{Electrode\ \ Area\ (Both\ sides)}$$

$$Current\ Density\ \left(\frac{mA}{cm^2}\right) = \frac{1.1A\ x\ 1000}{(10\ cm\ x\ 10\ cm) + (10\ cm\ x\ 10\ cm)}$$

$$Current\ Density\ \left(\frac{mA}{cm^2}\right) = \ 5.5\ mA/cm^2$$

Example: 1 mA/cm^2

$$Current\ Density\ \left(\frac{mA}{cm^2}\right) = \frac{Applied\ Current}{Electrode\ \ Area\ (Both\ sides)}$$

$$Current\ Density\ \left(\frac{mA}{cm^2}\right) = \frac{0.2A\ x\ 1000}{(10\ cm\ x\ 10\ cm) + (10\ cm\ x\ 10\ cm)}$$

$$Current\ Density\ \left(\frac{mA}{cm^2}\right) = \ 1\ mA/cm^2$$

Electrochemical Oxidation Removal Efficiencies

All Calculations are based on Run 10 (average)

COD

$$COD\ \%\ removal = \frac{COD_i - COD_t}{COD_i}\ x\ 100$$

$$COD\ \%\ removal = \frac{1220 - 290}{1220}\ x\ 100$$

$$COD\ \%\ removal = 76.23\ \%$$

Turbidity

$$Turbidity\ \%\ removal = \frac{T_i - T_t}{T_i}$$

$$Turbidity\ \%\ removal = \frac{99.4 - 0.25}{99.4}$$

$$Turbidity\ \%\ removal = 99.75\ \%$$

FOG

$$FOG\ \%\ removal = \frac{FOG_i - FOG_t}{FOG_i}\ x\ 100$$

$$FOG\ \%\ removal = \frac{48.2 - 0}{48.2}\ x\ 100$$

$$FOG\ \%\ removal = 100\ \%$$

Anionic Surfactants

$$Anionic\ Surfactant\ \%\ removal = \frac{AS_i - AS_t}{AS_i}\ x\ 100$$

$$Anionic\ Surfactant\ \%\ removal = \frac{25.9 - 6.495}{25.9}\ x\ 100$$

$$Anionic\ Surfactant\ \%\ removal = 74.92\ \%$$

Specific Energy Consumption

Table B- 1: Specific Energy Consumption Data

Ucell (Voltage)	Current Density (mA/cm^2)	Current (A)	Ec (kWh m^{-3})	Current Density(mA/cm^2)	Time(s)
1.45	1	0.2	6.96	1	86400
7.4	5.5	1.1	195.36	5.5	
14.6	10	2	700.8	10	

Volume (V) = 1 dm^3

$$E_c = \frac{U_{cell}.I.t}{V.3600}$$

Sample Calculation: 1 mA/cm^2

$$E_c = \frac{(1.45)(0.2)(86400)}{(1).3600}$$

$$E_c = 6.96\ kWh\ m^{-3}$$

Instantaneous Current Efficiency (ICE)

$$\%ICE = FV\left(\frac{[COD]_0 - [COD]_t}{8I\Delta t}\right) x\ 100$$

Where: COD0 & CODt initial & final COD values (g.O_2/L), F the Faraday constant (96,487 C/mol),V the volume treated (dm^3), I the Applied Current (A), 8 is the oxygen equivalent mass (g $eq.^{-1}$) and Δt is the time is seconds.

The calculations are based on the COD after 100 mg/L PAC coagulation (385 mg/L)

Sample Calculation: Based on Run 1 (1 mA/cm^2)

$$\%ICE = (96487)(1)\left(\frac{[0.385]_0 - [0.29]_t}{8(0.2)(86400)}\right) x\ 100$$

$$\%ICE = 6.63\ \%$$

Sample Calculation: Based on Run 2 (5.5 mA/cm^2)

$$\%ICE = (96487)(1)\left(\frac{[0.385]_0 - [0.145]_t}{8(1.1)(86400)}\right) x\ 100$$

$$\%ICE = 3.05\ \%$$

Sample Calculation: Based on Run 6 (10 mA/cm^2)

$$\%ICE = (96487)(1)\left(\frac{[0.385]_0 - [0.065]_t}{8(2)(86400)}\right) x\ 100$$

$$\%ICE = 2.23\ \%$$

Table B- 2: ICE % Data

Run	Current Density (mA/cm^2)	ICE %
1	1	6.630689381
2	5.5	3.045675505
3	5.5	3.680191235
4	5.5	3.807094381
5	1	8.375607639
6	10	2.23349537
7	1	2.268393736
8	5.5	4.251255392
9	10	2.442885561
10	5	1.205579887
11	1	1.744918258
12	10	2.09390191
13	10	2.16369864

Appendix C:

Analytical Procedure

Appendix C: Analytical Procedure

Chemical Oxygen Demand High Range

Measurement Procedure

Reagent Blank Correction: This method requires a reagent blank correction. A single blank vial may be used more than once. The blank vial is stable for several months at room temperature. For improved accuracy, a new blank was used each time a set was measurements were taken.

- The Hanna Reactor (HI839800) was pre-heated to 150 °C.
- The caps of two COD high range vials were removed.
- 0.2 mL deionized water was added to the first vial and 0.2 mL of sample was added to the second vial, while keeping a 45 ° angle. The caps were replaced, and the vials were inverted several times.
- The vials were then inserted into the Hanna Reactor at 150 °C for a period of two hours.
- At the end of the digestion period the reactor was switched off. It was then left to cool for 20 minutes, until the vials reached approximately 120 °C.
- Each vial was then inverted several times while still warm, and then it was placed in the test tube rack.
- The vials were then left to cool until it reached room temperature.
- Once cooled to room temperature, the blank vial was inserted into the Hanna Photometer and the zero key was pressed, once “0.00’’ was displayed, the meter is ready for measurement.
- The second vial was then inserted into the Hanna Photometer, then “Read” was selected. The instrument then displays the COD in the sample in the units mg/L.